# Field Relations, Structural Geology, and Geochemistry of the Jonestown Volcanic Field, Lebanon County, Southeastern Pennsylvania

Abstract of

a thesis presented to the Faculty

of the University at Albany, State University of New York

in partial fulfillment of the requirements

for the degree of

Master of Sciences

College of Arts & Sciences

Department of Earth and Atmospheric Sciences

Tristan J Ashcroft
2002

**Abstract**

The Jonestown Volcanic Field is a five kilometer by fifteen kilometer area of volcanic and hypabyssal rocks, basalt and diabase, located in southeastern Pennsylvania. These igneous rocks presently occur within an allochthonous belt of Ordovician deep water sedimentary rocks and Taconic flysch rocks known collectively as the Hamburg Klippe. Detailed field mapping during this project has revealed that the contacts between the igneous rocks and the flysch are not conformable. The volcanic rocks are associated with the Ordovician limestone that is adjacent to these volcanics. This limestone also is not conformable to the Hamburg Klippe sediments, rather it shares outcrop characteristics of some Laurentian platform carbonates in the region. The association between the igneous rocks and the limestone suggests that the igneous rocks were emplaced on a carbonate platform. Trace element data gathered from whole rock geochemical analysis suggests that the volcanic and hypabyssal rocks formed from different melts. They could, however, have formed in the same magmatic province. The volcanic rocks share geochemical characteristics with rocks emplaced on continental forelands, while the hypabyssal rocks show evidence of continental lithospheric influence on the magma, suggesting the Jonestown igneous rocks were emplaced on a carbonate platform on the Laurentian foreland, not a seamount. Their origin may be related to the approach of the Taconic arc. The structural geology indicates the flysch rocks and the igneous rocks were originally deformed and juxtaposed during the Taconic orogeny. Detailed mapping has also shown that a sandstone unit in the Bunker Hills region previously mapped as part of the Hamburg Klippe sequence is more likely an outlier of the Silurian Tuscarora Formation, and it is probably not conformable to any of the other rocks in the field area. The geometry of the deformation of the sandstone in

the Bunker Hills region suggests there was again thrusting in the region during the Alleghanian orogeny.

# Field Relations, Structural Geology, and Geochemistry of the Jonestown Volcanic Field, Lebanon County, Southeastern Pennsylvania

A thesis presented to the Faculty

of the University at Albany, State University of New York

in partial fulfillment of the requirements

for the degree of

Master of Sciences

College of Arts & Sciences

Department of Earth and Atmospheric Sciences

Tristan J Ashcroft
2002

**Acknowledgements**

Foremost, I must thank Bill Kidd for encouraging me to return to graduate school, then for putting up with me once I did. His ability to see important field relations and desire to see me finish has been invaluable during this project. Greg Harper introduced me to basalt geochemistry, and helped me make sense of my data in the project. John Arnason helped me understand the igneous petrology that continued to vex me. All three provided invaluable reviews of the content of my thesis and patiently continued to correct my consistently inconsistent spelling. Dave Lehmann first suggested I consider a project in the Hamburg Klippe, providing the impetus for this project. Gary Lash answered every question I asked, which was especially important in the early phases of the project. Jamie MacDonald taught me everything I understand about basalt geochemistry that I did not learn from Greg, and was able to give short answers to an uncountable number of questions. I thank long time friends Ryan Mathur, Kevin Eastham and Chris Thomas for being great role models and reminding me that there are rewards to continuing education. I thank all my friends, fellow students, and my parents and Grandmother Crowningshield for all their support and encouragement over the years I have been in Albany. And thanks must go to Diana Paton who took care of all the little things, and was responsible in one way or another for providing a significant amount of the food I have eaten while in Albany.

## Table of Contents


Abstract……..……..……...……...…i
Acknowledgements……...……..……..v
Table of Contents…... ……..……...……vi
List of Figures……..……..……viii
List of Tables. ……ix

Chapter 1: Introduction……...……..……....……1
Jonestown Volcanic Field….. ……..……...…..4
The Purpose of the Project…..……..……...…5

Chapter 2: Field Work of this Study. ……...…..……..7
The Field Area……... ……..…...……..7
The Map……..……..……..7
Comparisons of the Field Mapping to Other Data Sources... ……..…...…..9
Soil Map……..…....9
Aeromagnetic Map….……...……....10
Results of the Mapping in This Study…….... …...……..12
Sedimentary Rocks… …..……...……...……..12
Igneous Rocks……..……...……15
Limestones…..……...……...18
Contact Relations…...……..……...……18
1) Bridge at Swatara Creek…..……...……20
2) Railroad Cut in Bunker Hill……...……..……...……25
3) Road Cut on PA Route 72. ……..……...……..…….26
4) Road Cut on PA Route 343…….... ……..……...…...……..29
Structure……..……...……30

Chapter 3: Whole Rock Geochemistry……. ……..…...……...……..35
Jonestown Volcanic Field….. ……..……...……35
Herting and Wright's Rocks.. ……..……....36
Herting and Wright's Data…. ……..……...36
Lash's Rocks..……...……..……37
Lash's Data… ……...……..……37
Smith and Barnes' Rocks…... ……...……....38
Smith and Barnes' Data……. ……...……..38
The Samples From This Study……...…...……...……....39
Geochemical Analysis……... ……..……...……..43
Discrimination Diagrams…... ……...……...……....43
Nb/Y-Zr/$TiO_2$ (Winchester and Floyd, 1976) ……....……46
Ti-Zr-Y (Pearce and Cann, 1973)….. ……....……...46
Ti-V (Shervais, 1982) ……....……49
Zr-$TiO_2$ (Pearce, 1980 ……....……49
Hf-Th-Ta (Wood, 1980)……. ……....……...52
Nb-Zr-Y (Meschede, 1986)... ……....……52

Spider Diagram……..……...……....55
Rare Earth Element Diagram.……....……55

Chapter 4: Stark's Knob……..…...……59
Summary of Discrimination Diagram Results…….... ……61

Chapter 5: Possible Analogues……. ……...……...……...…..63
Karacalidag Setting…….63
Karacalidag Geochemistry…….66
Penghu Islands Setting……..……66
Penghu Islands Geochemistry……72
Belcher Islands Setting…….. ……72
Belcher Islands Geochemistry…….... ……73

Chapter 6: Discussion…….... ……...…..……80
Structure and Deformation…….81
Importance of the Bunker Hill Fault.……82
Note on the Origin of the Igneous Rocks…...…….……83
The Limestone…….... ……..…83
Whole Rock Geochemistry… ……..…85
Karacalidag… ……..…86
Penghu Islands…….... ……86
Belcher Islands……..…….……87

Chapter 7: Synthesis and Conclusions……..……...……...…..……..89

References Cited…… ……...…….…….93

Appendix A: Whole Rock Geochemical Data From Other
Studies of the Jonestown Volcanic Field….. ……....…99

Appendix B: Thin Section Descriptions of Selected Rocks. ……...……....103

Appendix C: Analyses of Standards and Calculations of
Accuracy for the Washington State University ICP-MS….. ……...…109

## List of Figures


Figure 1. Regional Map of Hamburg Klippe……..……...2
Figure 2. Sketch of Taconic Collision…… ……...3
Figure 3. Sketch Map of Jonestown Volcanic Field…….... ……..……..3
Figure 4. Location Map of Field area……. ……...…8
Figure 5. Soil Map and Aeromagnetic Map……....11
Figure 6. Thin Section of HK-16… ……14
Figure 7. Thin Section of HK-26… ……14
Figure 8. Graptolite Zones and the Hamburg Klippe……. ……..……16
Figure 9. Graptolite Zones and Ages…….. ……17
Figure 10. Thin-Bedded Limestone Outcrop……19
Figure 11. Massive Limestone Outcrop……20
Figure 12. Sketch Map of Swatara Creek Bridge Area…… ……21
Figure 13. Limestone in Basalt Pillows…… ……22
Figure 14. Formation of Cavities in Basalt Pillows..……24
Figure 15. Contact in Bunker Hills, Pennsylvania……27
Figure 16. Regional Cross Section……33
Figure 17. Thin Section of HK-11b2 ……40
Figure 18. Thin Section of HK-31… ……40
Figure 19. Thin Section of HK-23… ……42
Figure 20. Thin Section of HK-43… ……42
Figure 21. Nb/Y-Zr/$TiO_2$….. ……47
Figure 22. Ti-Zr-Y… ……48
Figure 23. Ti-V……. ……50
Figure 24. Zr-$TiO_2$… ……51
Figure 25. Hf-Th-Ta..……53
Figure 26. Nb-Zr-Y... ……54
Figure 27. MORB Normalized Spider Diagram…... ……56
Figure 28. C1 Chondrite Normalized REE Diagram……57
Figure 29. Thin Section of SN-4…..……60
Figure 30. Thin Section of SN-4 Xenolith……60
Figure 31. Orogen-Normal Rifting... ……64
Figure 32. Karacalidag Setting……. ……65
Figure 33. Karacalidag and Penghu Hf-Th-Ta……. ……67
Figure 34. Karacalidag and Penghu MORB Normalized Spider Diagram..……68
Figure 35. Karacalidag and Penghu C1 Chondrite Normalized REE Diagram…… ….69
Figure 36. Penghu Setting……70
Figure 37. Flaherty Formation Hf-Th-Ta…. ……74
Figure 38. Flaherty Formation C1 Chondrite Normalized REE Diagram… ……75
Figure 39. Flaherty Formation MORB Normalized Spider Diagram……..……76
Figure 40. Eskimo Formation Hf-Th-Ta…..……78
Figure 41. Eskimo Formation MORB Normalized Spider Diagram……79
Figure 42. Emplacement and Juxtaposition of Jonestown Igneous Rocks..……91
Figure 43. Volcanics as Erosional Remant... ……92

## List of Tables


Table I: Data From This Study……...……..44
Table II: Data From Herting and Wright…….. ……...……100
Table III: Data From Lash……..……...101
Table IV: Data From Smith and Barnes ……...……102
Table V: Estimates of Accuracy…….. ……...110
Table VI: ICP-MS Precision….. ……...…111
Table VII: ICP-MS Detection Limits….. ……...111


## List of Plates


Plate I: Geologic Map of the Jonestown Volcanics, Lebanon County, Southeastern Pennsylvania ……...……..in pocket

# Chapter 1 Introduction

The Hamburg Klippe, or Allochthon, is a belt of rocks in the Great Valley of Pennsylvania that occupies the same physiographic position between the Valley and Ridge and the Piedmont as the Martinsburg Formation shales (Fig. 1). It is differentiated from the Martinsburg on the basis of fossil ages and lithological differences, and thought to be a Taconic allochthon (Stose, 1946).

The late Ordovician Taconic Orogeny was the result of a collision between the Laurentian passive margin and a subduction complex and associated island arc(s) or microcontinent (Chapple, 1973; Rowley and Kidd, 1981; Stanley and Ratcliffe, 1985; Bradley, 1989). This arc complex or microcontinent is known collectively as the Taconic "arc". While the exact nature of what comprised the "arc" is not entirely understood, the geometry, timing, and nature of the collision and the effects of the collision on Laurentia are well understood. This collision (Fig. 2) closed the ocean separating the Taconic "arc" and the Laurentian margin, drowned the Laurentian carbonate shelf, and thrust flysch and other trench-related and older passive margin-related deepwater rocks onto Laurentia, forming the Taconic allochthons that presently occur in a belt from Pennsylvania to Canada.

The Hamburg Klippe, the southernmost allochthon along that belt, extends from an area west of Harrisburg to an area northeast of Reading, a distance of approximately 100 km, and has a variable width, up to 30 km in some areas. The main lithologies of the Hamburg Klippe are tan to olive drab mudstones and turbidite sandstones (greywackes), which comprise approximately 85 percent of the klippe (Lash and Drake, 1984). Numerous studies by Lash (1986a, 1986b, 1986c) have provided a significant amount of evidence suggesting that these rocks were deposited in a trench.

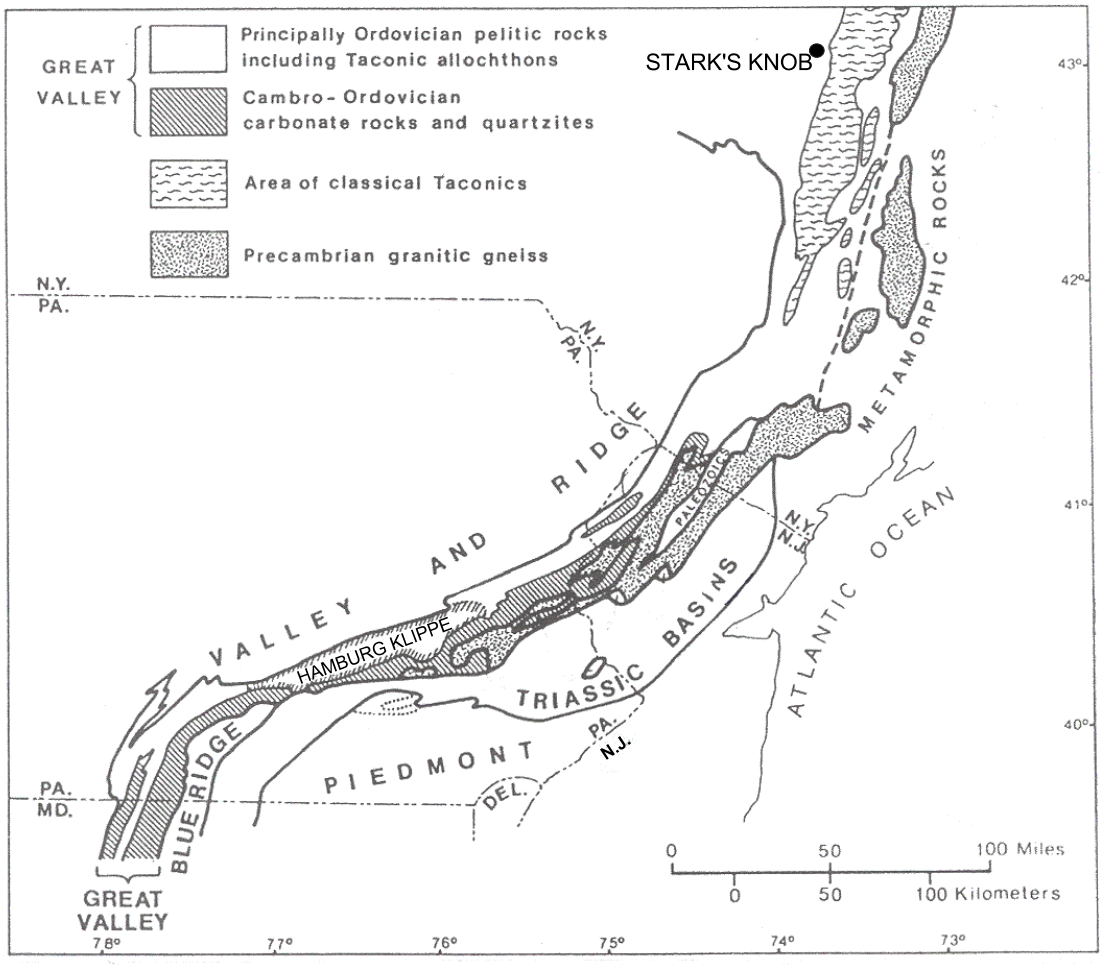


Fig. 1. Generalized location map showing the jaxtapostion of the Hamburg Klippe between the Valley and Ridge and Piedmont. Position of the type Taconic allochthon and Stark's Knob also shown. Slightly modified from Root and MacLachlan, 1978.

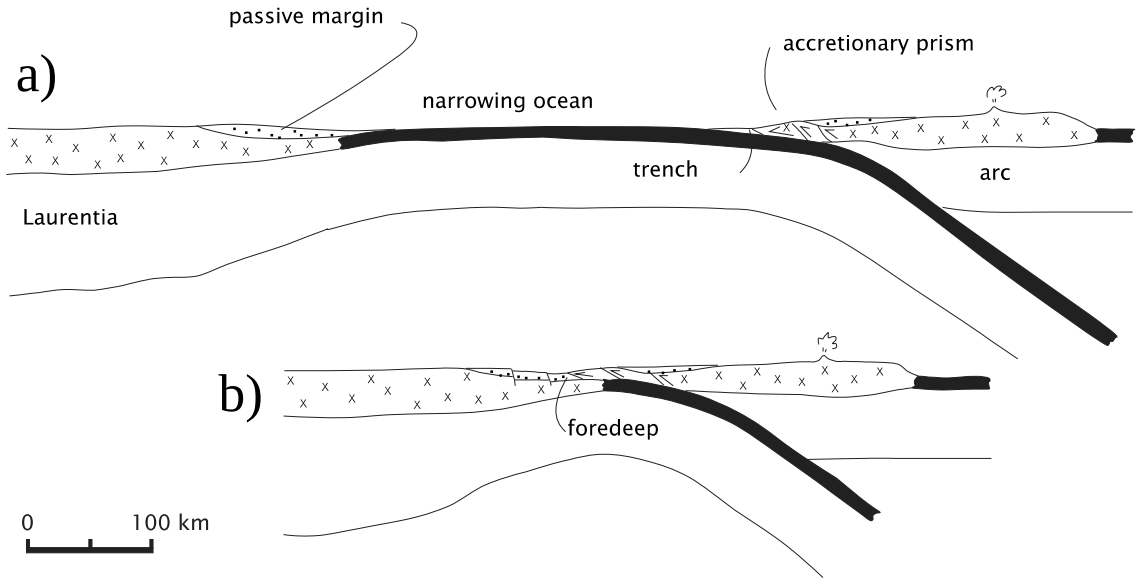


Figure 2. Sketch diagram showing the closing of the Ordovician ocean (Iapetus) between Laurentia and the Taconic Arc. Figure 2a shows before collision, figure 2b shows during collision. Note the location of the Laurentian passive margin and the direction of subduction. From Bradley and Kidd (1991).

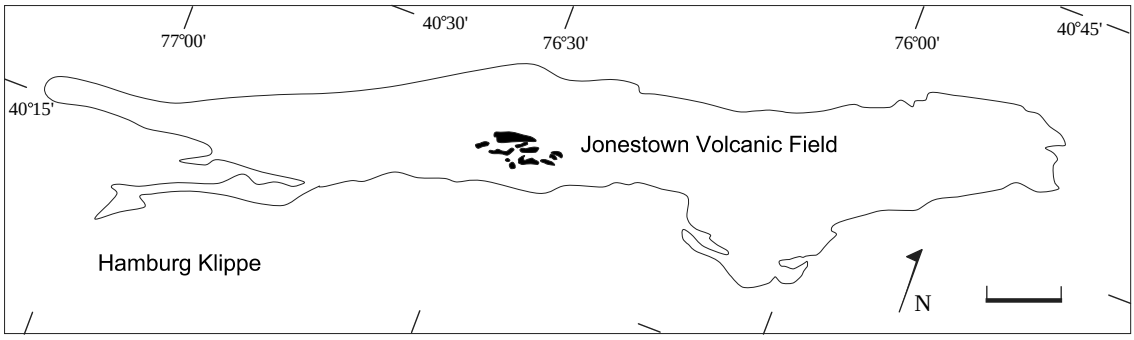


Fig. 3. Sketch map typical of previous maps of the Jonestown Volcanic Field. Simplified from Root and MacLachlan, 1978.

Approximately 14 percent of the Klippe consists of red and light green pelagic mudstone, and deep water facies limestone and chert. These rocks have been interpreted as abyssal plain or continental rise rocks deposited in a deep ocean basin far from both land and a trench (Lash and Drake, 1984). The Klippe also has minor quartz arenites, conglomerates, pebbly mudstones, and an area of mafic igneous rocks (Lash 1986b), known as the Jonestown volcanic field.

## Jonestown Volcanic Field

The Jonestown volcanic field is a small area of volcanic and hypabyssal mafic rocks in the central area of the Hamburg Klippe. It is unfortunately named in the sense that the hypabyssal rocks outcrop in a greater area of the field area than do the truly volcanic rocks, but rather than rename the area, that name is kept for this study. The Jonestown volcanic field extends from an area west of Mt. Ararat, Pennsylvania, near Swatara Creek, to an area east of Mt. Zion, Pennsylvania, near Little Swatara Creek, a distance of approximately 15 kilometers. Its northern boundary closely mimics Little Swatara Creek, and the southern boundary, while not due east-west, can be approximated by the southern boundary of the USGS 7.5 minute Fredericksburg quadrangle. Its maximum width is approximately four kilometers. It was first recognized as Ordovician by Gordon (1920). Since then, numerous articles and field guides (Stose and Jonas, 1927; Urry, 1936; Bricker, 1960; Zen, 1974; Herting and Wright, 1977; Lash, 1986a; Smith and Barnes, 1994) have discussed various aspects of the Jonestown volcanic field. While significant findings have been reported, understanding of the genesis of the igneous rocks and the reason for their present occurrence in the Hamburg Klippe is limited. Detailed maps of the eastern and western areas of the Hamburg Klippe have been published, but only sketch maps of the

Jonestown volcanic field have been published (Fig. 3). They are all small scale, and do not show the exact locations of the volcanics. Contact relations between the volcanics and the clastic sedimentary trench rocks are not well known. The consensus of previous workers has been to assume the igneous rocks are conformable to the trench sediments (i.e. Ganis, 1997). Given this assumption, theories concerning the origin of the Jonestown volcanics places their environment of formation in the basin where the flysch was being deposited, usually thought to be the trench. Strong evidence that previously reported contacts between the igneous rocks and the flysch rocks are conformable is lacking, however. Previous work in the area has demonstrated that the reason for magma generation and the location where the Jonestown igneous rocks were emplaced is not entirely clear. While other workers (Herting and Wright, 1977; Lash, 1986a) assumed the volcanism occurred in the trench, there is little reason to think that the volcanism could not have occurred in the Laurentian foreland. Evidence for this idea is considered in this study.

## The Purpose of the Project

Mindful of the lack of a detailed map, I undertook a project to make a detailed map of the area on the USGS 7.5 minute Fredericksburg quadrangle. My goal was to delineate the extent of the volcanic rocks, to establish what the relationships are between the volcanic rocks and associated sedimentary rocks, and to confirm or refute previous reports of conformable contacts between the volcanics and the sedimentary rocks. I also took advantage of the mapping project to sample the igneous rocks for whole rock geochemical analysis. Previous studies of whole rock geochemistry either did not report findings on significant trace elements such as Th, Ta, and Hf (Herting and Wright, 1977; Lash, 1986a), or are quite limited in their scope (Smith and Barnes, 1994). I thought it

would be valuable to compare new trace element data with the existing published data on rocks from the area, and to synthesize this new geochemical data with the new data of field relations in order to better understand the origin and history of the volcanic rocks. Since a detailed study of field relations can provide a much fuller picture of the history of a rock than just a geochemical analysis, the geochemical data is meant to be viewed in the context of the established field relations, not vice versa.

## Chapter 2 Field Work of this Study

### The Field Area

The field area for this study includes the southern portion of the US Geological Survey 7.5 minute Fredericksburg, Pennsylvania quadrangle (Fig 4). The northern boundary of mapping was approximately US route 22. Besides US route 22, major roads include PA route 72, PA route 343, and an abandoned railroad grade (Reading Railroad), which all cross the field area on a generally north-south trend. The major drainages in the area are Swatara Creek and Little Swatara Creek. The field area is in the Great Valley physiographic province of the Appalachians, and relief is low, approximately 100 meters from Swatara Creek to the ridge tops. The major land use in the area is farmland, wooded areas are also common, and there are small areas of residential development. Outcrop is uncommon, and the creeks and roads provide the main source of outcrop in the field area in cutbanks and road cuts. Rare occurrences of outcrop can be found on ridge tops. Float, while not common, is more common than outcrops, and can be expected on ridge tops. Plowed fields can provide some sense of lithology, based on the color of the soil. Red soil implies red shale, tan soil implies tan shales and sandstone, and reddish-purple soil implies igneous rocks. The southern limit of glaciation is north of the Great Valley of Pennsylvania, (Hack, 1989), so float rocks and soil colors are useful indicators of underlying lithology.

### The Map

Field mapping was conducted in the summer of 2001, and the data collected was compiled to produce a detailed geologic map (Plate 1). Both outcrop and float were mapped, and are differentiated on the map. Soil color is distinctive in some areas, and was used to help interpret field relations. The field area includes clastic sedimentary

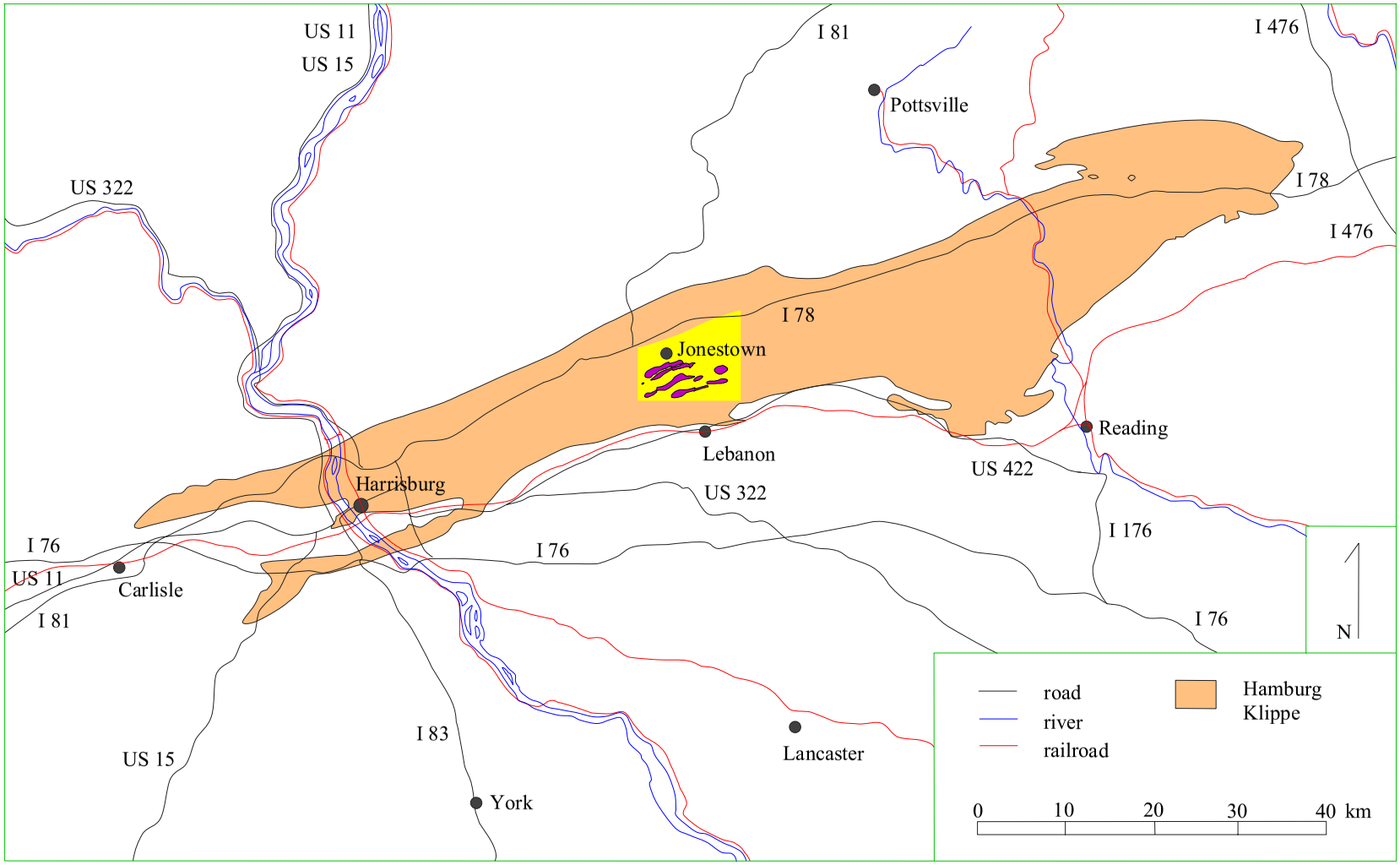


Fig 4. Map of the Hamburg Klippe (undifferentiated) showing overall extent. The field area mapped in this project is highlighted in yellow.

rocks, mafic igneous rocks, and minor carbonate sedimentary rocks. Regional strike in the area is approximately N70E, roughly parallel to the overall strike of the Great Valley.

Particular attention was paid to the igneous rocks, and their contacts with the sedimentary rocks. Consideration of the extent of float and topography shows that the volcanic rocks occur in belts. Mapping also shows that the igneous rocks mainly occur south of the Swatara and Little Swatara Creek. There is one occurrence of igneous float on the northern bank, but it is not extensive. Due to the focus on the igneous rocks in this study, unless stated otherwise, discussion will focus on the southern area, south of Little Swatara Creek.

Mapping shows that sedimentary rock units, however, can not be traced in detail from outcrop to outcrop. Because of this, no attempt was made to extrapolate sedimentary lithology across areas of no outcrop or float, and a large portion of the area underlain by sedimentary rocks is shown as undifferentiated. Many areas in the undifferentiated portions of the map are underlain by brown to tan soil similar in color to the brown and tan shales, mudstones, and sandstones. The tan soil color is not unique to areas underlain by the tan rocks, though, so those soil color areas are not included on the map.

## Comparisons of the Field Mapping to other Data Sources

### Soil Map

Due to the paucity of outcrop, and the recognition that soil type is influenced by underlying lithology, results of the field work were compared to a soil map of Lebanon County (Holzer, 1977). A particular soil group, the Neshaminy, is described as derived from igneous soil. The extent of that soil can be compared to the extent of igneous rocks. It is important to note that soil maps are not maps of bedrock geology, and that

there will be discrepancies, especially in valleys, where soils eroded from many lithologies have been deposited. A comparison of the soil map to the geologic map (Fig. 5) shows that the main discrepancy lies in the extent of soil in streambeds and their floodplains underlain by the sedimentary rocks. The volcanic rocks are associated with topographic highs, and eroded soil can only wash downhill. This likely shows the extent of sediment derived from the igneous rocks rather than the extent of the igneous rocks and float themselves. Allowing for this fact, there is a strong correlation between the belts of rocks mapped in this survey and the belts of soil derived from igneous rocks shown on the soil map.

## Aeromagnetic Map

The mafic igneous rocks and clastic sedimentary rocks in this field area might be thought have different aeromagnetic signatures. The igneous rocks are a significant lithology in the Hamburg Klippe, and their magnetic intensity could vary considerably from that of the sedimentary rocks, if so causing noticeable deflections of the contours on the aeromagnetic map. The largest scale map of the region available is the open file contoured map GJM-231, associated with the open file report GJBX-033 (1978), a result of flight NUR6028A. The aircraft was flown at approximately 79 mph at an altitude of 400 feet above the ground. Flight lines were flown approximately north to south, and spacing between lines was approximately three miles. Data was collected with a ASQ-10 modified fluxgate magnetometer. Study of the JGM-231 map reveals that the contours over the Jonestown Volcanic field have consistent geometries with the contours in rest of the map. In the Jonestown area, they parallel regional strike (Fig. 5), and show only minor deflection, if any, by the igneous rocks. This minor detectable variation in

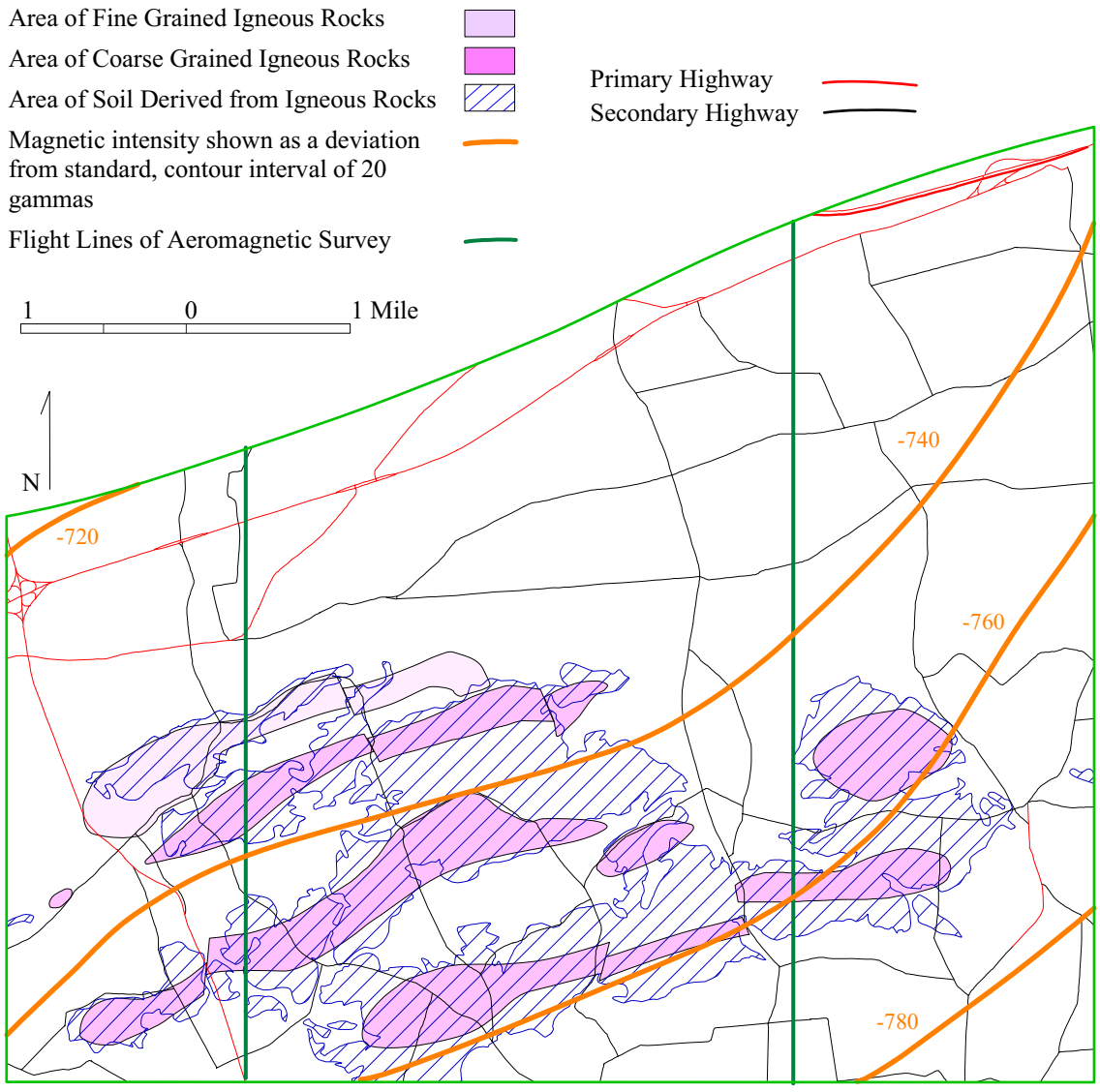


Figure 5. Map showing the favorable comparison between the extent of volcanic belts and the extent of soil mapped as derived from volcanic rocks by Holzer (1977). Also showing the aeromagnetic data from NURE map JGM-261. The value of the International Geomagnetic Reference Field for this latitude and longitude in 1978, calculated by the NASA National Space Scientific Data Center website (http://nssdc.gsfc.nasa.gov/space/model/models/igrf.html) was approximately 56,325 nanoTeslas, or gammas.

the magnetic intensity caused by the existence of the volcanic rocks could be due to alteration of the magnetic minerals in those rocks, so that the igneous rocks do not now have a significantly different aeromagnetic signal than the surrounding sedimentary rocks. This alteration of the magnetic minerals is evident in thin section. The aeromagnetic map does not allow individual belts of igneous rocks to be distinguished.

## Results of Mapping in This Study

### Sedimentary Rocks

South of Little Swatara Creek the predominant sedimentary lithologies are olive drab tan mudstone, siltstone, and sandstone, much of it wacke. More quartz-rich sandstones and fine conglomerates are also common. Minor amounts of red shale are found throughout the area, and there is one occurrence of black shale south of Swatara Creek. A belt of unusually pure quartz sandstone occurs on the Bunker Hills ridge, parallel to Little Swatara Creek. Massive limestone outcrops near the confluence of Swatara and Little Swatara Creeks, and occurs as float in two other localities. This limestone only occurs adjacent to igneous rocks. The lack of continuous outcrop does not allow the determination of stratigraphic thicknesses of the sedimentary units.

One occurrence of quartz sandstone, the quartzarenite on Bunker Hill, is distinct in that it can be mapped continously for over two kilometers. It is the most prominent ridge forming rock type in the area. Bedding in the rocks is parallel to regional strike, as is the belt of rock as a whole aside from an offset at a low point in the ridge. The lower contacts of this quartz arenite are not exposed, and the top of the sandstone is eroded. This quartz arenite is estimated to be at least ten meters thick. The Bunker Hills sandstone is separated from the other sedimentary rocks of the klippe by the belt of fine grained igneous rocks. Thin section analysis shows that while other quartz sandstones in

the klippe (Fig. 6) also contain feldspar and lithic fragments, and the grains are often mud supported or have significant mud matrix, the Bunker Hill sandstone (Fig. 7) is almost pure quartz. The quartz grains are more rounded than the grains of other sandstones, and there is no mud matrix. Geomorphologically, the sandstone is distinct from all other sandstone in the klippe. Since no other sandstone is a good ridge former, the other sandstones must occur in much thinner units, be not as well cemented, or be structurally much more complicated. Either scenario suggests differences that can not easily be explained if all the sandstones share the same origin. This, plus the fact that the Bunker Hills sandstone is separated from the rest of the klippe by volcanic rocks, suggests that the quartzarenite of Bunker Hills is separate from other sandstones in the field area. The fact that the Bunker Hills sandstone is almost pure quartz, the grains are rounded, and that it is a good ridge-former suggest that it is actually quart arenite of the Silurian Tuscarora formation, a fluvial quartz arenite. The Tuscarora is the main ridge forming unit in central Pennsylvania. It outcrops on top of Blue Mountain, the first major ridge to the north of the field area (Cotter, 1983).

The outcrops along the north bank of Little Swatara Creek are predominantly black shale, along with some red and green shale along Little Swatara Creek east of Jonestown. North of the creek bank, outcrop is rare, but tan soil or red soil is common, suggesting the tan and red shales or mudstones are the dominant lithology. Some quartzarenite float is present in Jonestown, and black, red, and green shale is exposed in a small quarry southeast of Fredericksburg. Thin units (less than two meters) of thin bedded limestone occur sporadically, interbedded with the tan shale or mudstone.

The lithological units and sedimentology of the eastern Hamburg klippe have been well documented in other studies (Lash, 1986b; Lash, 1986c; Lash and Drake,

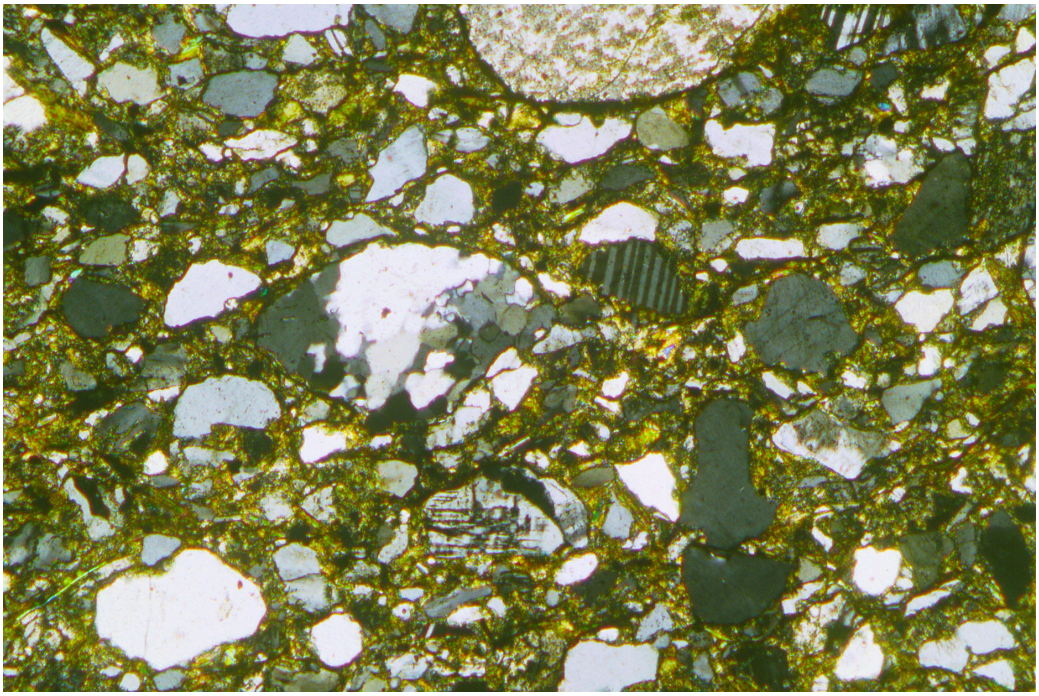

Figure 6. Thin section of HK-16, a sample of Hamburg Klippe flysch, viewed under crossed polars. Note the grains of plagioclase, microcline, and polycrystalline quartz, the lithic fragment, and the significant mud matrix. Field of view is 2.12 mm by 1.38 mm.

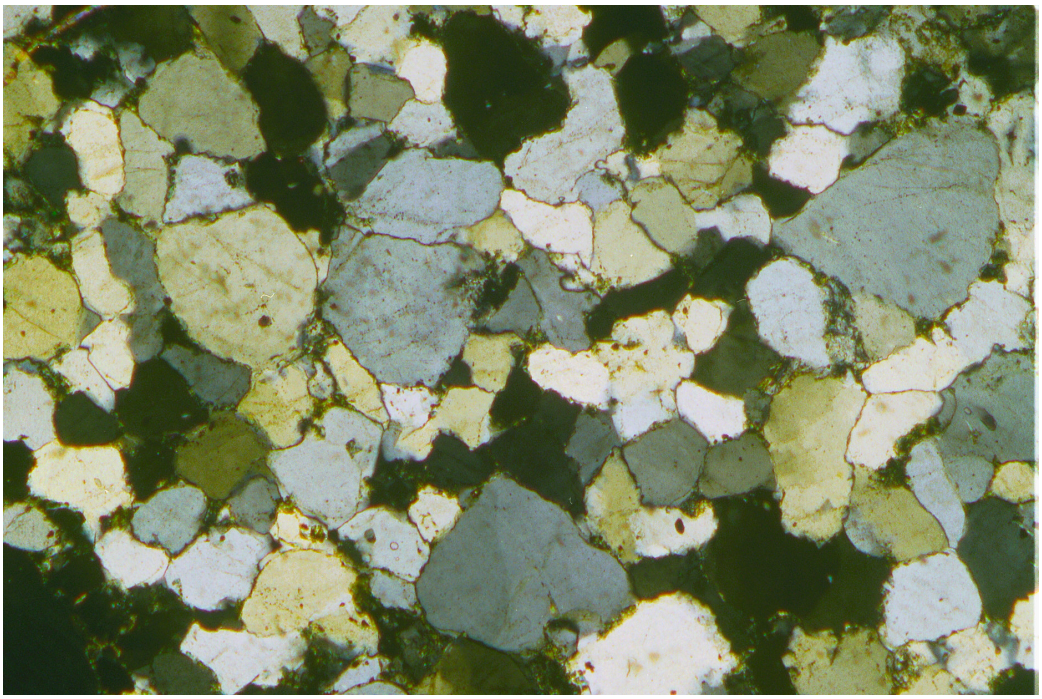

Figure 7. Thin section of HK-26, a sample of Bunker Hill sandstone, viewed under crossed polars. The sample consists almost entirely of monocrystalline quartz, with little matrix. Field of view is 2.12 mm by 1.38 mm.

1984). These authors proposed that most clastic rocks were deposited in a trench or basin in front of an approaching Taconic allochthon. Studies of the klippe to the east (Lash, 1985) and to the west (Ganis, et al, 2001) of the field area have constrained the age of the coarse clastic sedimentation to the N. Gracilis graptolite zone (Fig 8), which ranges from upper Llandeilo to lower Caradoc (see timescale compilation in Fig 9). The thin limestones, according to Lash (1985) and Gannis, et al. (2001), are part of the Hamburg Klippe sequence. The red shales represent an older pelagic sequence, and are a basal unit where stratigraphic sections can be measured. Observations made in this study did not contradict observations of previous work.

## Igneous Rocks

The field area contains both hypabyssal and volcanic mafic igneous rocks. The igneous rocks occur mainly as float, and they are associated with soil of a characteristic purplish-red color. Mapping reveals that the igneous rocks can be grouped into three parallel discontinuous belts, all tending along a strike of roughly N70E, parallel to the overall regional strike. A positive correlation was noticed between higher elevations and the occurrence of igneous rocks. All rocks are weathered and altered to varying degrees, and are often fractured.

The northern belt can be subdivided into northern and southern sub-belts. The northern sub-belt consists of fine grained rocks, a basal unit of pillow basalts, and an overlying sequence of pillow breccia. This belt also includes massive basalts. Massive limestone is found associated with the pillows. The thickness of the sequence of unbroken pillows, estimated by taking into account patterns of float and known strike and dip, is approximately five to ten meters, and the sequence of pillow breccia is approximately 20 to 30 meters thick. The thickness of neither the massive basalt nor the

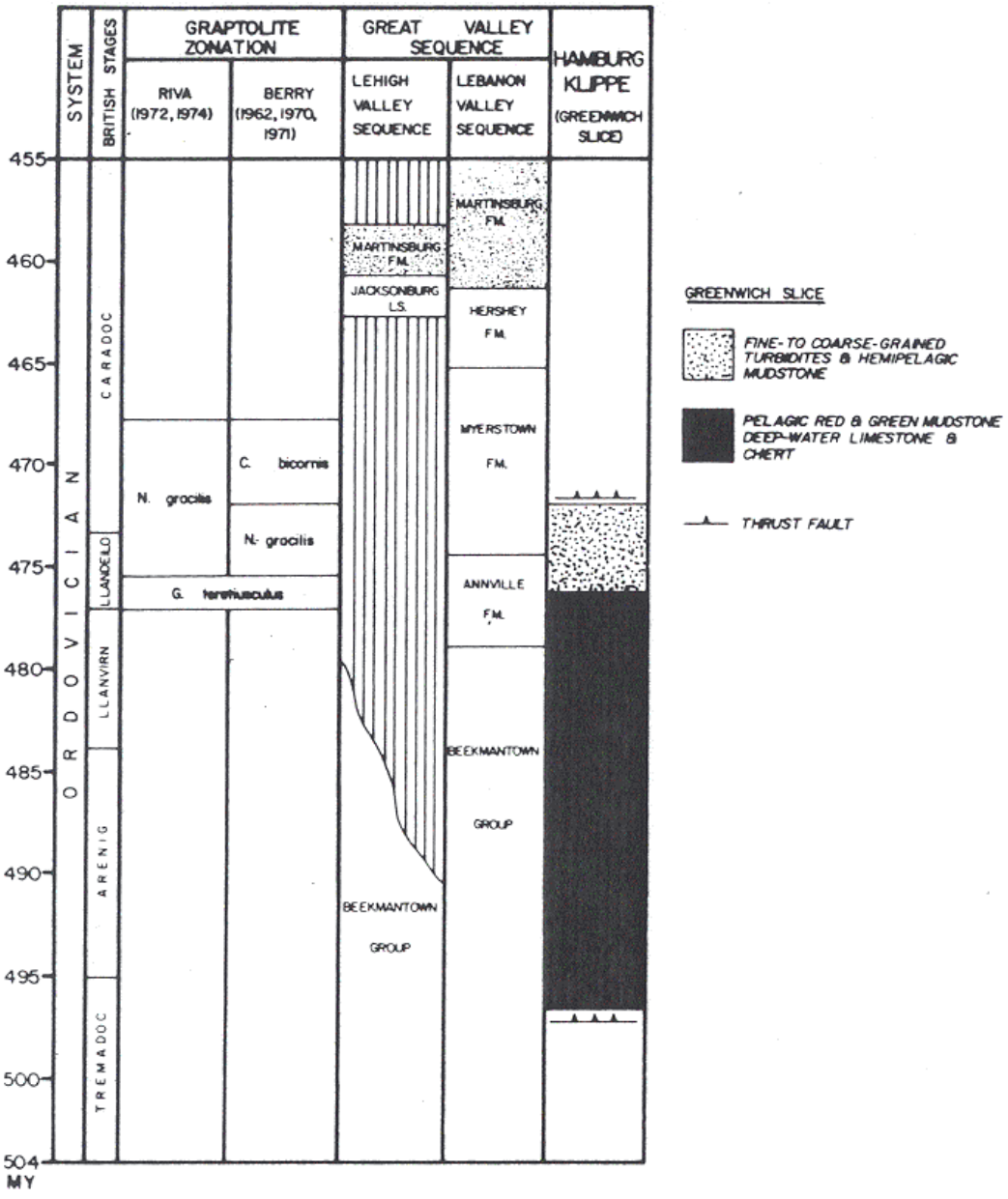


Figure 8. Middle Ordovician graptolite zones, shown in relation to rocks of the Hamburg Klippe, and regional autochthonous units. Note the similar ages between the trench sediments and the Annville Formation and that while the pelagic mudstone and deepwater limestone and chert were deposited for a longer period of time, the flysch sequence is far thicker due to voluminous sedimentation. From Lash, (1986c).

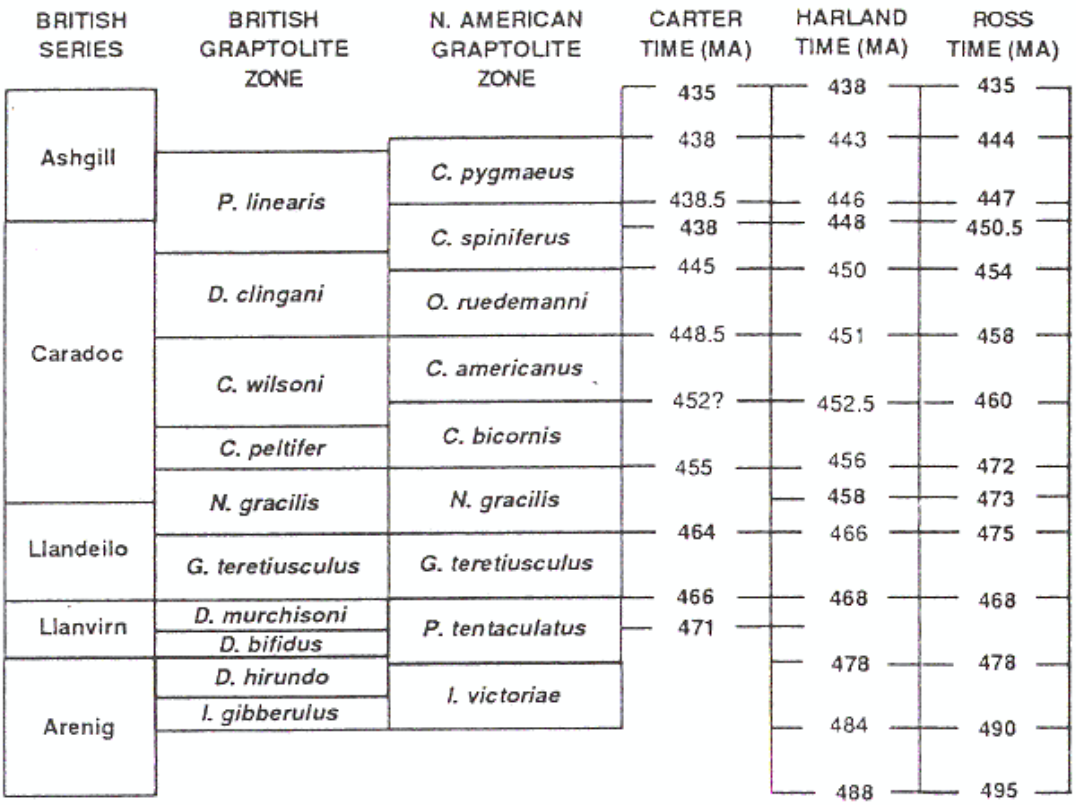


Figure 9. Graptolite zones and ages showing the upper Llandeilo and lower Caradoc ages of N. Gracilus. From Bradley (1989). See Bradley (1989) for discussion of references on the various time scales.

massive limestone is determined. The southern sub-belt consists of the hypabyssal igneous rocks. The other two belts of igneous rocks, further south, are also comprised of hypabyssal rocks. Thicknesses of these hypabyssal sequences are not determined.

## Limestones

Limestone is present in a few localities in the field area. South of Swatara Creek, it is associated with igneous rocks. Unlike the limestone beds north of Swatara Creek, which are interbedded with the other sedimentary rocks, conformable, and visibly part of the klippe, the limestone south of Little Swatara Creek has not been shown to be conformable to those sedimentary rocks. The two groups of limestone, aside from different associations, are visibly different. The limestone north of Swatara Creek (Fig. 10) is gray to black and micritic. It occurs in thin (one centimeter or less) beds. These beds are interbedded with dark gray to black limey shale beds of similar thickness. These intervals of interbedded limestone and shale are not more than two meters thick. The limestone south of Little Swatara Creek (Fig. 11) is gray, massive, calcite pure and crystalline. It weathers to a gray to blue-gray color, and has smooth to fluted surfaces. Bedding is not obvious in the five to ten meter wide outcrops. The evidence suggests that the two limestones are not the same, and there is no evidence that the limestone south of Little Swatara Creek is part of the sedimentary sequence of the Hamburg Klippe. Its association with the igneous rocks is significant.

## Contact Relations

An understanding of the nature of the contacts between the igneous and the sedimentary rocks in the Hamburg Klippe is vital to an interpretation of the origin of the igneous rocks. Previous workers have suggested that the two groups of rocks formed in the same environment (Lash, 1986a, Ganis, 1997), but conclusive evidence for this

Figure 10. A photograph of the thin bedded limestone exposed in the cut on the east side of PA rt 343, just south of the intersection with Shirksville Road. Sledge for Scale. Although the contacts are obscured in this photo, excavation revealed that the limestone is conformable to the flysch stratigraphically above and below it. The readily discernable bedding and association with flysch rocks highlight the differences between this limestone and the limestone exposed beneath the pillows along Swatara Creek.

Figure 11. Photograph of the massive limestone outcropping below the southern end of the abandoned railroad bridge over Swatara Creek. Hammer and clipboard for scale. The same limestone is visible in the near background above the clipboard. While bedding is not distinct, it can be approximated and strike is northeast to southwest, and dip is approximately 30 degrees to the south, roughly equivalent to the pillow basalt exposed in the woods above to the right, (to the south), stratigraphically above the limestone. View is looking east upstream on Swatara Creek. The confluence between Swatara Creek and Little Swatara Creek is out of the picture upstream.

important interpretation is lacking, largely due to inadequate data. Therefore, close attention was paid to those contacts in this study. Four locations were found during mapping where the suggestions of conformability could be tested. They are: 1) the vicinity of the south end of the abandoned Reading Railroad bridge over Swatara Creek; 2) a cut on the abandoned Reading Railroad in Bunker Hill; 3) a cut on PA route 72 south of Bunker hill; and 4) a cut on PA route 343 south of Freeport Mills.

1) Bridge at Swatara Creek

The area south of Swatara Creek near the abandoned Reading Railroad bridge, shown in the sketch map on Figure 12, exposes a variety of rock types, including pillow basalt, massive basalt, massive limestone, and black shale. The pillow basalt is weathered, fractured, and some is vesicular. Exposure is limited, but a small outcrop of pillow basalt east of the railroad grade, approximately 30 meters south of the bridge, exposes a significant relationship. Some of the exposed pillows are intact, while others are broken up. The vesicular pillows often contain concentric rings of amygdaloidal calcite. In the outcrop there are also small (two to four cm) angular pieces of limestone between the pillows, and in rare cases, small pieces of angular limestone can be found encased in the intact pillows (Fig. 13). These pieces are not secondary calcite, rather they are sedimentary limestone.

There are two separate exposures of massive limestone. The main exposure is under the southern end of the bridge, and continues along the west side of the railroad grade and west into the abandoned Union Canal bed. A second smaller exposure can be found west of the unnamed creek, south of the Union Canal bed. The two outcrops are separated by outcrop of massive basalt in the unnamed creek. Neither exposure can be traced in any direction beyond the outcrop. The exposures occur as individual blocks.

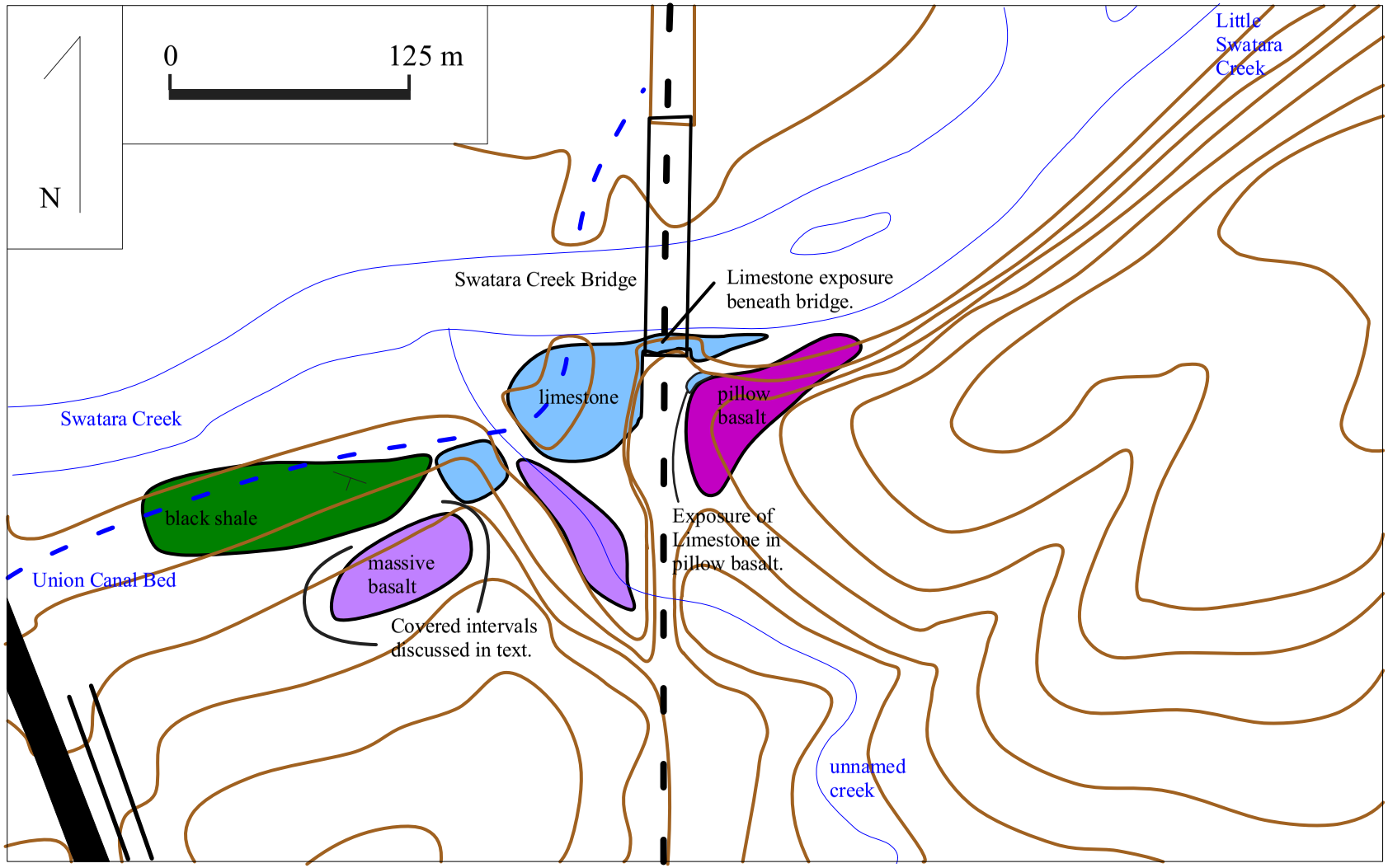


Figure 12. Sketch map of the vicinity of the abandoned Reading Railroad bridge over Swatara Creek. The locality of the pillows containing limestone is shown, as are the locations of rock types mentioned in the text. Scale about 1 to 300. Contour interval 20 feet.

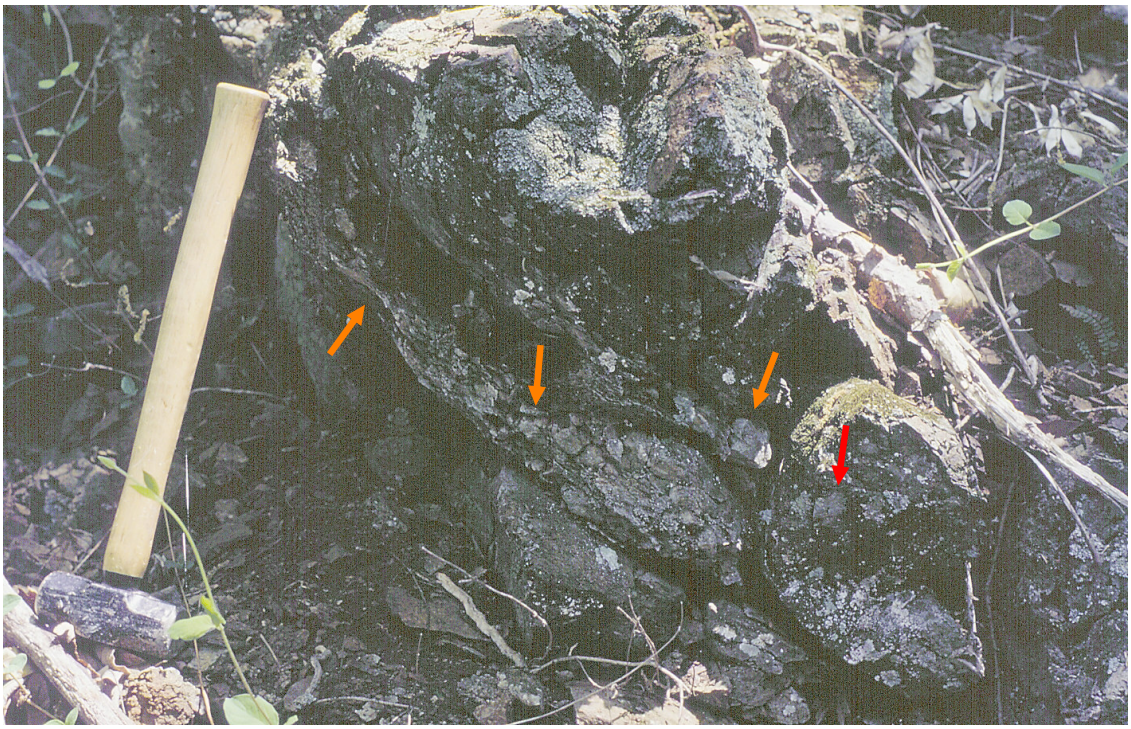

Figure 13. Photograph of outcrop showing limestone in in the pillow basalt. Sledge for scale. The handle is approximately four centimeters in width. Pillows can be made out in the lower right hand corner of the outcrop. The matrix of the outcrop is basalt, and the white areas, some up to two or three centimeters in diameter, are the micritic limestone. This limestone is visibly indistinguishable from the massive limestone outcrop under the nearby bridge. The orange arrows point to angular limestone clasts that occur between the pilllows, and the red arrow points to a piece of limestone encased in a basalt pillow.

Black shale can be found south and mainly west of the smaller block of limestone, along the Union Canal bed and tow path. Bedding in the shale can not be traced for more than five to ten meters in any location.

The observation of the angular limestone in and between the pillows is significant. There are two possible mechanisms for occurrences of limestone in basalt in this manner. One mechanism (Fig. 14) requires basalt that originally contained cavities (Ballard and Moore, 1977; Francheteau, et al., 1980). These cavities can form shortly after eruption, when the rim of a pillow or lava tube has cooled and is solid, but the inside is still molten. If the supply is cut off, the magma can drain out of the basalt leaving a cavity. These cavities can be quite large, especially in lava tubes, but they can be smaller. In a carbonate sedimentary environment, these cavities can fill with lime mud, which becomes limestone. This could explain the occurrence of the limestone pieces in the pillows at Swatara Creek bridge. The other mechanism explains the juxtaposition of breccia. The limestone breccia and the pillow breccia simply accumulated together at the base of a slope. This mechanism requires that the two rocks be present in the source area for that slope. Both mechanisms require that the basalt be erupted into an environment where limestone is forming so which mechanism predominates in this case is not important. The field observations, viewed in light of these mechanisms, strongly suggest that this limestone was present when the basalt was erupted. These limestone pieces are visually indistinguishable from limestone in the outcrop beneath the bridge. These observations suggest that the pillow basalts at Swatara Creek bridge are conformable to the massive limestone exposed there.

While these observations imply that the massive limestone and the pillow basalts were originally conformable, the nature of contacts between these rocks and the other

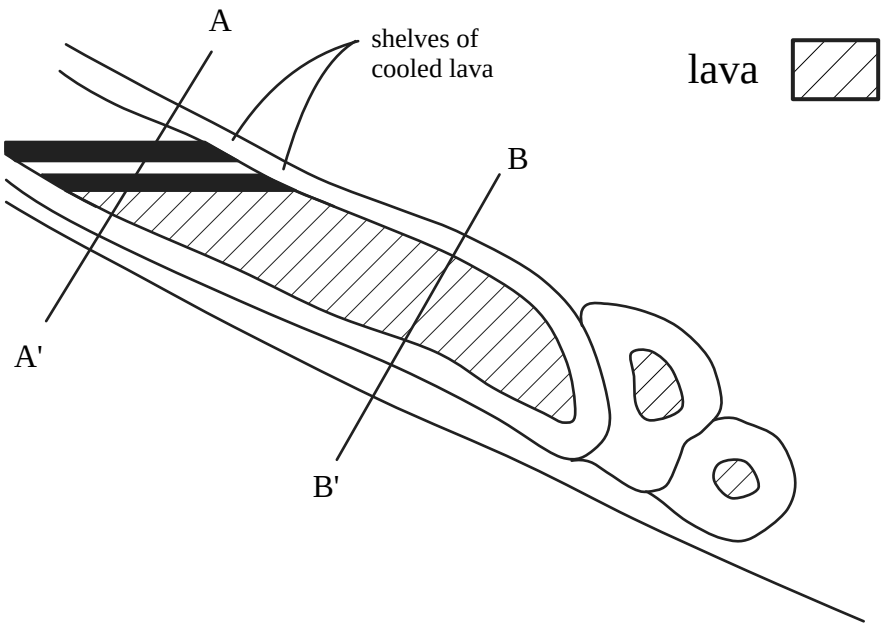


Figure 14. Sketchs showing how cavities can form in basalt flows. The lava tube (generally a string of interconected pillows) leads to pillows. The lava source has been cut off. While the lava is static, the top of the lava cools and solidifies. When another pillow forms, the lava that forms that pillow drains and lowers the lava level in the tube, leaving behind a shelf of rock and a cavity. The shelves of cooled rock correlate to formation of the pillows. Presumably, in the case shown in this sketch, pillows could continue forming, draining the tube of lava. If the basalt was emplaced in a carbonate sedimentary environment, the cavities can then fill with limestone. If very little magma leaves in each successive event, a cross section of the tube would show limestone fragments in several areas (line A-A'). If a large amount of lava leaves at once and a large cavity forms, a cross section across the magma tube could show basalt ringing a center of limestone (line B-B', assumes the rest of the lava drains in one event).

nearby sedimentary rock unit, the black shale, is not as clear. Outcrop of the black shale shows that it is highly fractured. The contact between the black shale and the smaller block of limestone is obscured by a thin (less than two meter) covered interval, comprised mainly of fractured black shale float. Extrapolation across this interval shows that bedding in the shale is truncated by the contact with that block of limestone.

Similarly, the contact between the black shale and the basalt is obscured by a narrow covered interval of fractured shale and basalt. Extrapolation across that interval shows that the contact between those two units also truncates the bedding of the black shale. The outcropping shale and basalt on each side of the covered interval are highly fractured and exhibit slickenlines. Study of the two rock types reveals that both the amount of fracture and the occurrence of slickenlines significantly decreases further away from the contact. In the exposed basalt near the contact, there is no evidence of smaller crystal sizes, suggesting it is not a chilled margin. The exposed shale near the contact shows no evidence of contact metamorphism.

While it is apparent that the pillow basalts and the limestone are conformable at this locality, the same can not be said for those two rock types and the clastic sedimentary rocks in the area. I found no evidence here for the conformability of either the limestone or the igneous rocks to the clastic sedimentary rocks in this locality, and have instead observed evidence that the clastic sedimentary rocks are truncated at their contacts with the igneous rocks and with the limestone, and that there is faulting at those contacts.

### 2) Railroad Cut in Bunker Hill

The abandoned Reading Railroad cut near the settlement of Bunker Hill, Pennsylvania (note that this settlement is distinct from the topographic expression

named the Bunker Hills, in the settlement of Beverly Hights), parallel to an unnamed secondary road, cuts approximately perpendicular to strike, and exposes both sedimentary and igneous rocks. Dip is moderately steep (approximately 50 degrees) to the southeast. Igneous rocks outcrop in an approximately ten meter wide interval, mainly on the west side of the cut. The igneous rocks on the east side of the cut are mainly covered. On the west side, the south contact is also covered. The north contact on the west side, however, is not covered by much overburden, and was dug out for this study (Fig. 15). The igneous rocks, coarse grained hypabyssal rocks, are a bit more weathered than usual for Jonestown igneous rocks. Enough is present, however, to show that crystal size does not decrease closer to the contact, indicating that there is no chilled margin. The sandstones are friable, and exhibit no evidence of contact metamorphism. Rocks on both sides of the contact are fractured, and fracture surfaces exhibit slickenlines. The amount of fracture in the igneous rocks near contacts causes them to be recessed in the outcrop. This in large part causes the covered interval directly at the contact. The fracture in the sandstones does not cause them to be recessed, but it does tend to strongly parallel the contact. This tendency does not exist a few meters or further from the contact. Excavation, therefore, revealed that the contact is bordered by a fractured zone one to two meters wide that truncates the bedding of the sandstone. The surfaces of rocks in this zone are rife with slickenlines. In this locality, there is no evidence that the igneous rocks intruded the sedimentary rocks, and there is instead evidence that the contact is a fault.

### 3) Road Cut on PA Route 72

This outcrop is located on the east side of PA route 72, south of Bunker Hill, in a road cut just north of an auto dealership. It has previously been referred to (Ganis,

Figure 15. Photograph of the contact zone between the trench sedimentary rocks of the Hamburg Klippe and of coarse grained igneous rocks of the Jonestown volcanic field, with a sledge placed on the contact for scale. The ignous rocks, highly fractured and exhibiting slickenlines, visible in the left (south) side of the picture. Near the contact, they are recessed and covered in dirt and yard waste*. The sedimentary rocks (mainly sandstone) on the right (north) of the picture exhibit the strike and dip of the surrounding sedimentary rocks. The sedimentary rocks near the contact exhibit a strong fracture plane that is parallel to the contact. All sandstones in the picture show a high amount of fracture. The density of fracture decreaseses further away from the contact. The photograph was taken in an abandoned railroad cut just east of the settlement of Bunker Hill. View is of the west side of the cut.

*Of all the places the adjacent property owner could have decided to deposit a few year's worth of grass clippings, leaves, and other yard waste, said individual decided to do so on the contact between the igneous and sedimentary rocks. I do not applaud that choice.

1997) as an example of a conformable contact between the hypabyssal igneous rocks and the quartz sandstone exposed there. Much of the cut is actually covered by fractured, weathered rock and soil. Both the sandstone and the igneous rock that do outcrop are significantly weathered. By my observation, the contact is not exposed, but rather there is a small covered interval, approximately one-third of a meter wide near the base of the outcrop, between the igneous rocks and the sedimentary rocks. The covered interval made determination of the strike and dip of the contact impossible. Furthermore, the cut on the west side of the highway is covered, so strike and dip could not be determined by extrapolating across the highway.

The igneous rocks outcrop in the northern third of the outcrop. I saw no planes in the igneous rocks I could determine to be significant, so I did not measure strike and dip. The rocks are extensively weathered, and usually have soft, light colored rinds of altered minerals. They are significantly fractured in a zone from the contact to 10 to 20 meters away, and many fracture surfaces exhibit slickenlines. Fracture intensity and the occurrence of slickenlines decreases away from the contact. There is no evidence for a chilled margin in the rocks.

The sandstones are massive, and I could not determine bedding. This lack of measurable orientation in either unit means I can not prove or disprove whether either of the units truncates the other. However, the occurrence of the igneous rocks at the northern end of the outcrop and the sedimentary rocks at the southern end of the outcrop both at road grade suggests the contact has a moderate to high angle. The sandstones are highly fractured within a zone five to ten meters from the contact. Those fracture surfaces often exhibit slickenlines. Fracture density and the amount of surfaces with slickenlines decreases away from the contact. There is no evidence for a baked zone in

the sedimentary rocks. In my opinion, there is no evidence for a conformable contact at this locality, but there is evidence for faulting.

4) Road Cut on PA Route 343

The fourth locality is a cut along the western side of PA route 343, south of Freeport Mills, and north of the intersection with Heffelfinger Rd. Hypabyssal rocks are exposed at the north end of the cut. They are fractured, highly altered, and some surfaces exhibit slickenlines. The density of fractures and degree of alteration increases towards the contact, but there was not enough exposure of slickenlines to determine if they increase towards the contact. It can be said that they do not occur away from the contact. The flysch rocks outcrop in the south end of the cut. They do not crop out well, but outcrop of the flysch is better on the east side of the highway, and the occurrence of sedimentary rocks on the west side of the highway can be extrapolated. The igneous rocks at the north end of the outcrop and the sedimentary rocks at the south end of the outcrop occur at approximately the same elevation, suggesting that the contact is steep. Due to poor exposure, the amount of fracture, intensity of slickenlines, and effects of alteration on the sedimentary rocks were not determined. The contact between the igneous and sedimentary rocks is covered by vegetation, soil, and in small areas, fractured float. The covered interval is a few meters wide, and outcrop on both sides is sparse, so it is not possible to determine if the igneous rocks exhibit a chilled margin, or if the sedimentary rocks are baked at the contact.

On the eastern side of the highway, approximately two meters into the woods, is the sample locality HK-11b, in the midst of a large, approximately one or two acre, area of igneous float. No sedimentary rocks can be found in the immediate vicinity. The outcrop and blocks of float there are not strongly fractured. The rocks also have not

undergone significant alteration, unlike the rocks near the contact. The indication of structural complexity and weathering near the contact and the absence of such complexity away from the contact indicates that the contact itself is the reason for the structural complication, and is probably a fault.

## Structure

Due to the poor outcrop, study of the overall structural geology of the field area is limited. Structural studies in the eastern and western klippe (Alterman, 1972; Root and MacLachlan, 1978, Lash and Drake, 1984) have shown that the sediments of the klippe have a complicated deformation history. Lash and Drake (1984) suggested there are mappable internal units, and proposed that the deformation is complex, and can be understood as a series of stacked thrusts.

In the Jonestown volcanic field, the sedimentary rocks exhibit a strong tendency to strike N70E, and dip south. This tendency is not as pronounced near contacts with igneous rocks. The contacts between sedimentary rocks and igneous rocks, as previously discussed, are structurally complex. The three belts of igneous rocks, when treated as a whole, also trend N70E, although individual strikes at contacts vary. The igneous rocks cap low ridges that do not always parallel the regional strike, but the ridges are often offset by stream valleys, and the resulting belt is overall roughly strike parallel. In some locations in the northernmost belt, strike and dip could be measured or at least estimated. Strike in pillows was estimated by using shape of pillows to determine original horizontality and in the pillow brecchia by assuming that elongate clasts had settled parallel to horizontal. Both the sequence of pillows and the sequence of pillow breccia trend N70E, and dip to the south.

Some structure can be inferred by map patterns in the vicinity of the Bunker Hills. In the northernmost belt of volcanic rocks, the pillows and pillow breccias outcrop mainly on the northern edge of the belt. Intact pillows and blocks of limestone lie at the structural base of the belt. Strike of the basalts along Little Swatara Creek in Beverly Heights is N70E and dip is to the south. However, near the western extent of the belt, the strike begins to curve to the south and dip rotates to the east. Intact pillow float and limestone float can be found at the western extremity and along the nearby part of the southern margin of the belt. The existence of this basal unit of limestone on both sides and western margin of the belt suggests that the belt is folded into a syncline, and that the end of the belt is due to the fold axis plunging to the east. The east end is covered, but by analogy if it is assumed that the syncline runs the length of the belt, then the end of the eastern end is due to the fold axis plunging to the west in that area. If the belt were cross-faulted, it would be expected to continue elsewhere in the field area, which it does not.

The Bunker Hill sandstone lies structurally on top of the northernmost belt of volcanics. Field observations showed that the sandstone has a consistent shallow dip to the south, and no dips to the north were observed. Since the sandstone is a prominent ridge former, it is reasonable to expect that if it were folded like the volcanics below it, it would then cross a fold axis and part would dip to the north, or there would then be a second ridge to the south. No such second ridge exists. The sandstone, therefore, is inferred to be unfolded, and to truncate the inferred fold of the volcanics. The contact along which this truncation occurs is covered, so until data can be gathered that suggests there has been motion along this contact, I will consider it an unconformity. The Bunker Hill sandstone is itself truncated on the southern margin. Study of the outcrop

pattern on the map and on the cross section, when taken into account with the shallow dip, suggests that if the sandstone were to maintain its shallow dip, it would outcrop south of Moore Rd. It does not, and with no data suggesting the sandstone is folded, I interpret this map pattern to be the result of a fault. The ridge forming Bunker Hill also exhibits a right lateral offset near the eastern end of Moore Rd. This offset is quite likely due to an offset of the ridge forming sandstone that comprises Bunker Hill, and indicates the presence of cross faulting in the field area.

The hypabyssal rocks occur in three different belts, and there is positive correlation between the hypabyssal rocks and higher elevations in the field area. The contacts along PA route 72 (contact 3) and PA route 341 (contact 4) Two possibilities involving thrusting, can explain the repetition of the volcanic units. One possibility is that the hypabyssal rocks occur in three separate thrust sheets, and are repeated by relatively high angle faults. This would be unusual in the Great Valley, where rocks on opposite sides of high angle faults are thought to not be greatly offset (Fig. 16). The other possibility is that the rocks were emplaced in one thrust sheet along a shallow angle thrust fault, then later offset slightly by high angle thrusts. This would require that the rocks were part of a thrust sheet dipping slightly south, which is consistent with other thrust sheets in the great valley, have steep southern fault contacts, which does not contradict the field relations at the outcrops discussed in detail, and have shallow south dipping northern fault contacts. These contacts are not exposed, so their angles can only be inferred. The northern contact in the Bunker Hill railroad cut is steep (contact 2), but that could be due to a second high angle fault also truncating the northern end of the rocks.

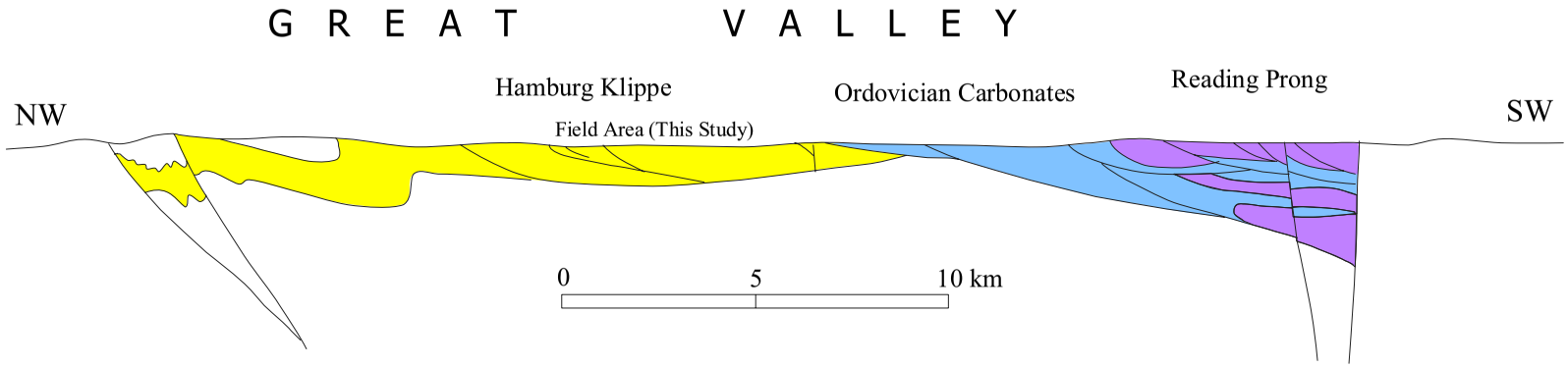


Figure 16. Generalized cross section (from Berg, 1980) of the Great Valley- Hamburg Klippe (in Yellow), Ordovician carbonates (in Blue) and Reading Prong (in purple). Major thrust faults are shown, minor faults are omitted. The thrusting in the area has inverted the section on a regional scale, with the pre-Cambrian rocks of the Reading Prong sitting on the early to middle Ordovician carbonates, and those carbonates sitting on the late Ordovician rocks of the Hamburg Klippe. Note the low angle faults cut by later high angle faults. Scale is 1:187,500. No vertical exageration.

Discussion of the structure of the trench sedimentary rocks must be more general. Most sedimentary rocks dip to the south, suggesting that the rocks are either isoclinally folded, rest in thrust sheets, or both. Sixteen of seventeen structural measurements of sedimentary rocks in the field area found the rocks to be dipping to the southeast. Only one bed was shown to be overturned. Evidence for large fold hinges have not been found. This suggests that folding does not play a large role in the area . Neither individual beds nor units of rock can be traced from outcrop to outcrop. Observed truncation of beds suggests faulting. Small quantities of red shale are present throughout the field area, appearing to be interbedded variously with the shales, mudstones, and sandstones. In the eastern area of the klippe, where stratigraphic sections can be measured, the red shale is described only in the base of the Hamburg Klippe sequence (Lash, 1984). It is interpreted by Lash (1984) as a pelagic mud that underlies the trench sediments and was not originally interbedded with trench rocks. The red shale in the klippe is highly cleaved, suggesting it has been strongly deformed. The widespread occurrence of red shale in the field area means it is repeated, and the apparent lack of folds perhaps means it was faulted. Because it is only the basal stratigraphic unit, but now occurs throughout the sedimentary sequence with the flysch, the red shale in the field area could define a thrust horizon. This interpretation leads to the conclusion that the sedimentary rocks in the field area are imbricately thrust, and the red shale is the basal horizon of many of those thrusts sheets. Mapping each individual thrust is not possible with the current level of outcrop.

## Chapter 3 Whole Rock Geochemistry

Field relations along the Taconic Belt are well constrained. Mapping in the type Taconic allochthons in New York and Vermont has shown that these allochthons preserve only older slope and rise sediments and late Ordovician flysch. These rocks were deposited on Laurentian foreland or in the Taconic trench, and thrust onto Laurentia during the Taconic orogeny. Little to no evidence of the arc itself or the volcanism in this arc is preserved in these allochthons, located near the western (northwestern in Pennsylvania) limit of Taconic deformation. The Hamburg Klippe is lithologically quite similar to the type Taconic allochthons (Lash and Drake, 1984). It too, preserves slope and rise Laurentian foreland deposits and Taconic flysch. The Jonestown igneous rocks presently occur within this belt, suggesting they were formed somewhere between Laurentian foreland and the Taconic trench. The geochemistry of Jonestown Volcanic Field basalt and diabase was investigated with the intention to help constrain where these rocks were emplaced.

### Jonestown Volcanic Field

The geochemistry in this paper builds on previous studies conducted by Herting and Wright (1977), Lash (1986a), and considers the limited data collected by Smith and Barnes (1994) All three studies considered only bulk rock geochemistry. The studies done by Herting and Wright (1977) and Lash (1986a) only considered data collected from x-ray fluorescence analysis, which limited their analyses to major elements and some trace elements. The analytical methods available to Smith and Barnes (1994) were not significantly improved over those available to Lash, so they only supplemented his data with analysis for a few additional trace elements, notably, Th, Ta, and Hf. They used various methods of analysis depending on the element, including ICP, x-ray

fluorescence, instrumental neutron activation analysis, and atomic absorption (personal communication, R. Smith, 2001).

## Herting and Wright's Rocks

Herting and Wright (1977) published the first geochemical analysis of the Jonestown igneous rocks (Appendix A). As part of their study, they conducted thin section analysis and reported relict primary mineralogies in the hypabyssal rocks including euhedral augite, sub-ophitic pigeonite, slightly zoned plagioclase ($An_{54}$-$An_{62}$), quartz, opaque oxides, and secondary biotite and chlorite. They classified the hypabyssal rocks as medium grained quartz diabase. In the volcanic rocks, they reported plagioclase phenocrysts ($An_{30}$), extensively chloritized pyroxene phenocrysts, and an aphanitic matrix, along with opaque oxides, quartz, and secondary metamorphic minerals. After thin section analysis, they picked fourteen samples, twelve coarse grained and two fine grained rocks, to analyze.

## Herting and Wright's Data

Herting and Wright (1977) noted similarities between elemental abundance in the hypabyssal and volcanic rocks, but described the volcanic rocks as more altered than the hypabyssal rocks. In the volcanic rocks, they found statistically lower concentrations of calcium, aluminum, and potassium, and statistically higher concentrations of silicon and sodium relative to the hypabyssal rocks, and concluded the volcanic rocks had been spilitized. Spilitization is a typically low grade hydrothermal alteration process during which primary plagioclase is replaced with albite. This secondary albite is difficult to distinguish from the primary plagioclase (Yardley, 1989), but has lower extinction angles. However, they noted that comparisons between the hypabyssal and volcanic rocks showed "remarkable homogeneity" (p. 150) with respect to all other elements, and

concluded that the hypabyssal and volcanic rocks shared the same parental magma. They found their samples plotted mainly in ocean-floor tholeiite fields, while some also plotted in the island-arc tholeiite field. Based on this, they described the igneous rocks as back-arc marginal basin rocks, and proposed they were erupted in a back-arc spreading center.

## Lash's Rocks

Lash (1986a) also reported X-ray Fluorescence data (Appendix A). He sampled hypabyssal float from ridge tops, and sampled unweathered pillow fragments from the pillow breccia sequence. He conducted thin section analysis and in the hypabyssal rocks he reported subhedral to anhedral clinopyroxene, which he assumed to be augite and pigeonite, laths of subhedral to anhedral plagioclase, minor quartz, and skeletal opaque grains. In the volcanic rocks, he reported fine grained plagioclase laths, with lesser subhedral to anhedral pyroxene. He reported alteration in all rocks he studied, and reported some plagioclase partially altered to epidote and sericite. While he did not report on spilitization, he did report significant alteration in all rocks, confirmed Zen's (1974) observations of prehnite and pumpellyite, and suggested that they had undergone zeolite to low-greenschist facies metamorphism. The work of Zen (1974) shows that meta-igneous rocks in the Taconic belt from Pennsylvania to Newfoundland have undergone similar metamorphism. The rocks in the northern part of this belt are unaffected by Alleghanian metamorphism, suggesting that this metamorphism in Pennsylvania is Taconic.

## Lash's Data

Lash chose seventeen samples for analysis, thirteen hypabyssal and four volcanic rocks. Lash (1986a) published data on more trace elements than Herting and Wright

(1977) did. Lash (1986a) found that his samples plotted in tholeiite fields, but generally did not plot in island arc tholeiite fields. His samples plotted in either mid-ocean ridge basalt or within-plate basalt fields on most diagrams, and often plotted in areas where these fields overlap. However, based on Ti-V (Shervais, 1982), he classified the rocks as mid-ocean ridge basalt. Because of the assumption that the volcanic rocks were erupted onto and intruded into the trench sediments in which they are now found, Lash (1986a) suggested these rocks were formed during subduction of either a spreading center or a fracture zone. He plotted data on basalts from modern fracture zones, and that data fell within the mid-ocean ridge basalt fields on the diagrams he used, so he could not distinguish between the two scenarios.

### Smith and Barnes' Rocks

Smith and Barnes (1994) sampled three rocks, one hypabyssal rock and two pillow breccia fragments, for the purpose of including data in a field guide. They provided the only published analyses of Ta and Th, among other trace elements. The hypabyssal rock was collected from a cut along Pennsylvania state highway 72. Based on the paucity of outcrop on highway 72, it is likely from the cut discussed in detail in the field relations section of this paper. One of the pillow breccia fragments is described as a hexagonal column. No petrography is discussed in the field guide.

### Smith and Barnes' Data

Smith and Barnes (1994) conducted a very small study, intended as an addendum to Lash's previous work. Because of this, they only analyzed the rocks for a few elements (Appendix A). Discussion was limited, but they suggested that their samples were enriched or plume ocean-floor basalts (essentially P-MORB or E-MORB). In spite of the fact Lash (1986a) discounted the possibility these rocks formed in a back-arc

basin, Smith and Barnes, on the basis of the Th-Ta-Hf diagram (Wood, 1980), suggested there was some back arc component.

## The Samples from This Study.

Overall, the igneous rocks in the Jonestown Volcanic field are significantly weathered and are fractured. Most of these rocks are best left in the field, but some localities do contain rocks that have not been weathered and deformed beyond recognition. Thin section analysis revealed rocks are indeed altered throughout the field area. Rock descriptions do not significantly vary from descriptions from the previous work. The four samples from the Jonestown volcanic complex discussed in this paper were relatively fresh samples, and were carefully selected for whole rock geochemical analysis on that basis. All four rocks were relatively unfractured.

Two hypabyssal rocks, HK-11b2 and HK-31 were selected, one from each end of the southern igneous belt. HK-11b2 was sampled from a large fresh block of float, found approximately three meters downhill from an actual outcrop in a wooded area along Pennsylvania state highway 343. In thin section (Fig. 17) (see Appendix B for detailed rock descriptions), the rock contains a phase replaced mainly by serpentine, plagioclase ($An_{55}$ to $An_{60}$), clinopyroxene, quartz and untwinned feldspar intergrown in a graphitic texture, and primary opaque grains that have been significantly altered (to leucoxene). The serpentine progenitor occurred as small to moderate sized phenocrysts of modest abundance. Secondary minerals include chlorite, amphiboles, pumpellyite, and magnetite. HK-31 is medium grained and has an intergranular texture. Based on primary mineralogy, texture, and grain size, it is a diabase.

HK-31 was collected from a large surprisingly fresh block of float in an otherwise manicured lawn along Pennsylvania state road 1003 in the hamlet of

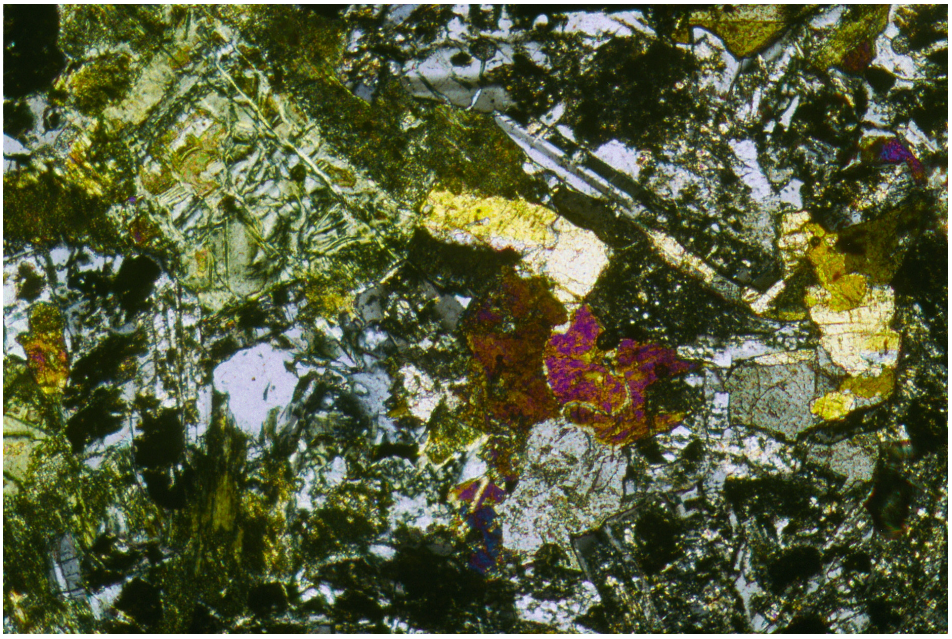

Figure 17. Thin section of HK-11b2, a diabase, viewed under crossed polars. Note the twinned albite, the red and yellow birefringent clinopyroxene, and the serpentine replacing the larger phenocryst in the upper lefthand corner. Field of view is 2.12 mm by 1.38 mm.

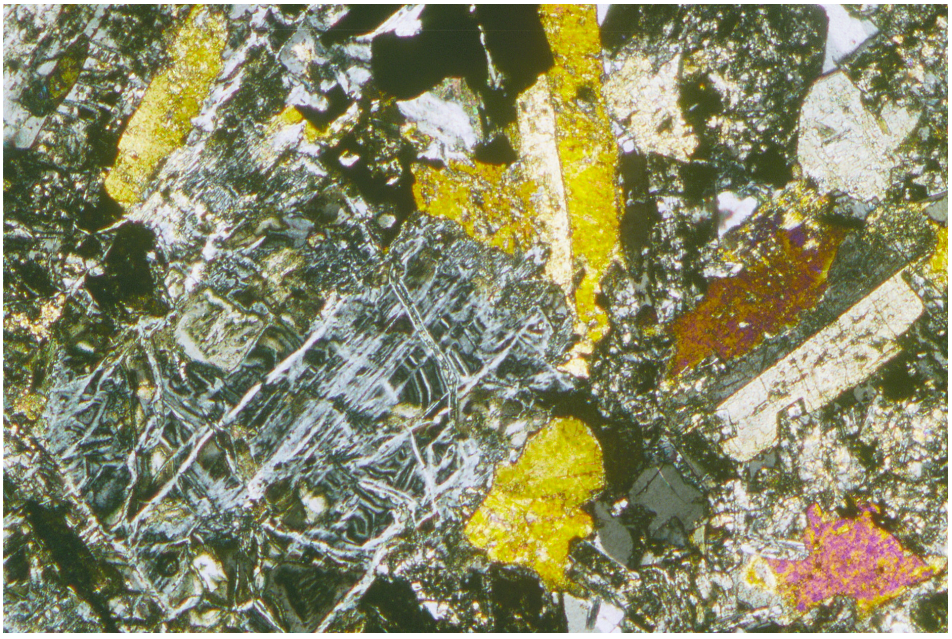

Figure 18. Thin section of HK-31, a diabase, viewed under crossed polars. Note the larger phenocryst replaced with serpentine, the twinned clinopyroxene, and minor quartz in this picture. Field of view is 2.12 mm by 1.38 mm.

Rockwood. In thin section (Fig. 18) (see Appendix B for detailed rock descriptions), the rock contains a phase replaced by serpentine, clinopyroxene, plagioclase, quartz and untwinned feldspar intergrown in a graphitic texture, and primary opaque grains that have been significantly altered (to leucoxene). The serpentine progenitor occurred as small to moderate sized phenocrysts of modest abundance. The rock also contains amphiboles and chlorite, and secondary magnetite and pumpellyite in the groundmass. The rock is fine to medium grained, and has an intergranular texture. The original fresh igneous rock is classified as a diabase.

Two volcanic rocks, actual basalt pillows, rather than pillow breccia, were collected, HK-23 and HK-43. HK-23 was collected from float in a cut on a local road near Little Swatara Creek. It was free of vesicles or amygdules, and was unfractured. There was also massive limestone float present in the cut. In thin section, (Fig. 19) (see Appendix B for detailed rock descriptions), the rock contains plagioclase ($An_{30}$), clinopyroxene, and fine to medium grained phenocrysts replaced with serpentine. HK-23 also contains pumpellyite and prehnite. The groundmass is fine grained, and the rock exhibits a sub-ophitic texture. The rock is a basalt.

HK-43 was collected in an excavated area next to Quarry Road, east of Beverly Hights along Little Swatara Creek. The land owner was excavating a small area before building a garage into the hillside (the garage is now built, and it covers the outcrop). HK-43 came from an area of fresh bedrock in the southeast corner that could not have been dug out and instead had been blasted before excavation, and is therefore the freshest sample collected during the project. The pillow consists of aphanitic basalt along with concentric rings of amygdules of calcite. The occurrence of calcite in basalt in the Jonestown Volcanic field is similar to the occurrence of calcite in the basalt of

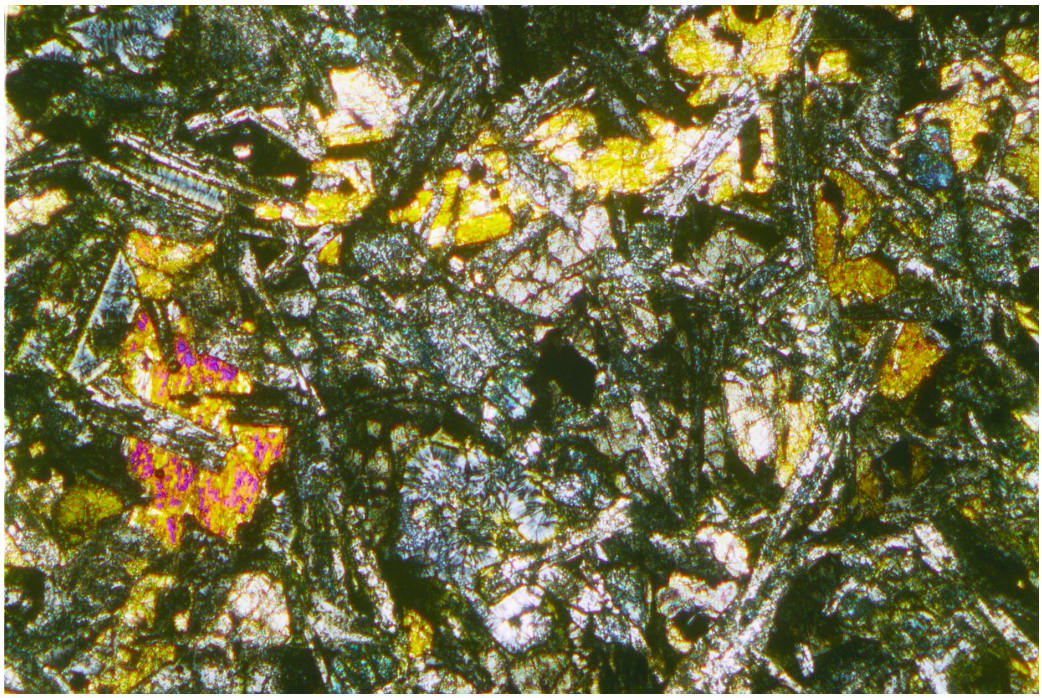

Figure 19. Thin section of HK-23, a basalt, viewed under crossed polars. Note the elongate plagioclases and the clinopyroxenes around them. Field of view is 2.12 mm by 1.38 mm.

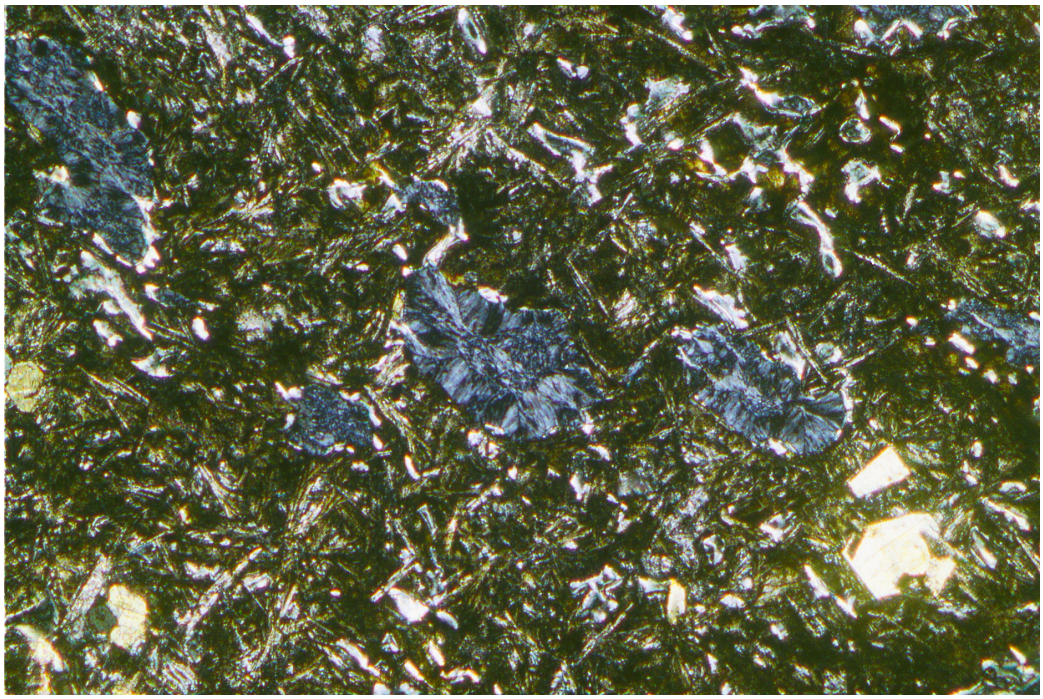

Figure 20. Thin section of HK-43 viewed under crossed polars. Note the fine plagioclase crystals in the groundmass. The anomalous blue mineral is a filling in vesicles. Field of view is 2.12 mm by 1.38 mm.

Stark's Knob, NY, an other Ordovician basalt. Thin section analysis (Fig. 20) (see Appendix B for detailed rock descriptions) shows that HK-43 contains a groundmass of fine grained plagioclase, amygdaloidal calcite, and vesicles filled with an anomalous blue mineral. The groundmass is aphanitic, and the rock has an ophitic texture. The fresh rock classified as a basalt.

## Geochemical Analysis

The samples selected for this study were broken manually with a sledge hammer. Chips were then gathered and carefully selected to avoid obvious chlorite alteration, then sent to the geoanalytical laboratory at Washington State University for analysis. Ten major elements plus seventeen trace elements were analyzed on a Rigaku automated wavelength X-ray fluorescence spectrometer (XRF). Samples were ground to powder in a swing mill with tungsten carbide surfaces. The major and trace elements were both determined on a single low dilution (2:1) Li-tetraborate fused bead for each sample as per the procedure of Johnson, et al. (1999).

Twenty-six trace elements, including all fourteen naturally occurring rare earth elements, were analyzed on a Sciex Elan model 250 inductively coupled plasma mass spectrometer (ICP-MS). Samples were first ground to powder in an iron bowl in a shatterbox swing mill. Three in-house and seventeen international standards are used for calibration (Appendix C).

## Discrimination Diagrams

The data collected in this study (Table I) were plotted on numerous discrimination diagrams to better understand the geochemistry of the Jonestown volcanic rocks. Data from other studies (Herting and Wright, 1977, Lash, 1986a, and Smith and Barnes, 1994) were also plotted to compare with the data from this study.

# Table I

## X-Ray Fluorescence Data From This Study

| | HK-43 | HK-31 | HK-23 | HK-11b2 | SN 4 |
|---|---|---|---|---|---|
| | all samples analyzed 12 Feb 01 | | | | |
| Normalized Results (Weight %): | | | | | |
| $SiO_2$ | 45.96 | 52.71 | 49.05 | 51.92 | 49.26 |
| $Al_2O_3$ | 14.81 | 14.14 | 16.42 | 15.12 | 19.46 |
| $TiO_2$ | 1.927 | 1.140 | 1.494 | 1.020 | 0.993 |
| FeO* | 10.12 | 10.90 | 10.17 | 9.98 | 10.45 |
| MnO | 0.164 | 0.196 | 0.163 | 0.187 | 0.118 |
| CaO | 17.21 | 11.08 | 10.05 | 11.62 | 7.03 |
| MgO | 4.53 | 7.05 | 8.77 | 7.47 | 6.28 |
| $K_2O$ | 1.20 | 0.55 | 0.09 | 0.53 | 1.57 |
| $Na_2O$ | 3.72 | 2.11 | 3.62 | 2.05 | 4.76 |
| $P_2O_5$ | 0.365 | 0.112 | 0.166 | 0.094 | 0.084 |
| LOI | 9.64 | | | | 9.31 |
| Trace Elements (ppm): | | | | | |
| Ni | 87 | 73 | 154 | 88 | 141 |
| Cr | 172 | 163 | 341 | 362 | 532 |
| Sc | 21 | 51 | 40 | 46 | 54 |
| V | 290 | 328 | 244 | 294 | 240 |
| Ba | 425 | 175 | 504 | 196 | 1701 |
| Rb | 27 | 15 | 1 | 16 | 31 |
| Sr | 270 | 226 | 348 | 203 | 581 |
| Zr | 34 | 80 | 92 | 69 | 57 |
| Y | 31 | 27 | 27 | 24 | 22 |
| Nb | 20.8 | 4.9 | 8.9 | 3.7 | 2.1 |
| Ga | 18 | 17 | 17 | 17 | 17 |
| Cu | 62 | 155 | 90 | 137 | 75 |
| Zn | 80 | 85 | 79 | 88 | 63 |

## WSU Standards Run Before and After Samples From This Study Were Run

| | GSP1 10 Feb 01 | GSP1 13 Feb 01 | GSP1 accepted value |
|---|---|---|---|
| Normalized Results (Weight %): | | | |
| $SiO_2$ | 68.24 | 68.11 | 68.25 |
| $Al_2O_3$ | 15.34 | 15.41 | 15.33 |
| $TiO_2$ | 0.664 | 0.669 | 0.660 |
| FeO* | 3.87 | 3.88 | 3.92 |
| MnO | 0.039 | 0.038 | 0.041 |
| CaO | 2.05 | 2.05 | 2.10 |
| MgO | 1.09 | 1.09 | 0.97 |
| $K_2O$ | 5.59 | 5.59 | 5.59 |
| $Na_2O$ | 2.83 | 2.86 | 2.84 |
| $P_2O_5$ | 0.292 | 0.294 | 0.284 |
| Trace Elements (ppm): | | | |
| Ni | 14 | 12 | 9 |
| Cr | 11 | 13 | 13 |
| Sc | 3 | 2 | 6 |
| V | 50 | 64 | 53 |
| Ba | 1298 | 1277 | 1310 |
| Rb | 255 | 254 | 254 |
| Sr | 231 | 233 | 234 |
| Zr | 542 | 540 | 530 |
| Y | 25 | 26 | 26 |
| Nb | 26.5 | 25.3 | 28.0 |
| Ga | 22 | 20 | 23 |
| Cu | 33 | 33 | 33 |
| Zn | 106 | 104 | 104 |

Major elements are normalized on a volatile-free basis, with total Fe expressed as FeO*.
LOI = Lost on ignition.

Table Ia. Whole rock geochemical data produced by X-Ray Fluorescence by the analytical lab at Washington State University for this study, shown compared to the standards they ran. Major elements are reported in weight percent, and minor elements are reported in ppm. Data is reported normalized to 100 and iron is reported as FeO*, as per their suggestion. The Jonestown igneous rocks HK-43 and HK-23 are both volcanic pillows, and HK-31 and HK-11b2 are both hypabyssal. The Stark's Knob sample SN-4 is volcanic. The two rocks with high LOI, HK-43 and SN-4 are the rocks that contain calcite.

Table I

Inductively Coupled-Plasma Mass Spectrometer Data

| | HK-43 | HK 31 | HK-23 | HK-11b2 | SN-4 |
|---|---|---|---|---|---|
| La | 13.73 | 6.23 | 6.92 | 5.58 | 1.51 |
| Ce | 28.38 | 14.04 | 15.21 | 12.51 | 4.08 |
| Pr | 3.62 | 1.88 | 2.14 | 1.68 | 0.70 |
| Nd | 16.61 | 9.08 | 10.68 | 8.17 | 4.36 |
| Sm | 4.76 | 3.00 | 3.55 | 2.74 | 1.90 |
| Eu | 1.67 | 1.06 | 1.34 | 0.98 | 0.68 |
| Gd | 5.16 | 3.81 | 4.42 | 3.43 | 2.54 |
| Tb | 0.90 | 0.73 | 0.79 | 0.67 | 0.50 |
| Dy | 5.45 | 4.76 | 4.97 | 4.33 | 3.47 |
| Ho | 1.10 | 1.01 | 1.03 | 0.93 | 0.76 |
| Er | 3.02 | 2.91 | 2.80 | 2.61 | 2.22 |
| Tm | 0.42 | 0.42 | 0.38 | 0.39 | 0.34 |
| Yb | 2.59 | 2.69 | 2.41 | 2.46 | 2.21 |
| Lu | 0.40 | 0.41 | 0.37 | 0.38 | 0.34 |
| Ba | 367 | 162 | 503 | 175 | 1674 |
| Th | 1.47 | 1.29 | 0.64 | 1.10 | 0.10 |
| Nb | 19.14 | 3.56 | 8.24 | 3.09 | 1.12 |
| Y | 29.12 | 26.92 | 27.37 | 24.89 | 20.13 |
| Hf | 3.06 | 2.17 | 2.37 | 1.94 | 1.44 |
| Ta | 1.24 | 0.27 | 0.55 | 0.22 | 0.08 |
| U | 0.28 | 0.31 | 0.17 | 0.26 | 0.10 |
| Pb | 2.31 | 4.76 | 2.52 | 3.56 | 1.40 |
| Rb | 25.7 | 15.9 | 1.1 | 16.2 | 30.8 |
| Cs | 2.75 | 0.60 | 0.84 | 0.56 | 1.43 |
| Sr | 250 | 218 | 351 | 200 | 574 |
| Sc | 33.7 | 52.6 | 41.9 | 54.7 | 51.7 |
| Zr | 120 | 74 | 86 | 65 | 47 |

Table Ib. Whole rock geochemical data produced for this study by ICP-MS analysis at the analytical lab at Washington State University. The Jonestown igneous rocks HK-43 and HK-23 are both volcanic pillows, and HK-31 and HK-11b2 are both hypabyssal. The Stark's Knob sample SN-4 is volcanic. Precision and accuracy of the WSU ICP-MS are listed in Appendix C.

Those previous studies have not been able to precisely categorize magma types of the igneous Jonestown rocks. By itself, the geochemistry in this study may not allow that either, but the added data in this study, especially with respect to trace elements, when taken into account with field relationships discerned in this study, should add to the understanding of the Jonestown volcanic rocks.

## Basalt Discrimination Diagrams

### Nb/Y-Zr/$TiO_2$ (Winchester and Floyd, 1976)

The four Jonestown rocks analyzed in this study plot as basalt on the revised version of Winchester and Floyd's (1976) rock classification diagram (Fig. 21), consistent with the $SiO_2$ values. HK-43 falls near the boundary between basalt and alkali-basalt, but it still lies within the basalt field. Lash's (1986a) data also plots in the basalt field, but approaches the andesite field. This diagram is shows that the rocks are basaltic and nature, and that therefore the use of basalt discrimination diagrams is appropriate.

### Ti-Zr-Y (Pearce and Cann, 1973)

This diagram (Fig. 22) is useful for discriminating within plate basalts. HK-43 plots in the within plate basalt field close to the boundary to the overlap field labeled "B", which includes mid-ocean ridge basalts, island arc tholeiites, and calc-alkali basalts. The other three rocks plot within field "B", along with Smith and Barnes' (1994) data. The four volcanic and three hypabyssal rocks from the Smith and Barnes (1994) and this study cluster in slightly different areas. Data from Lash (1986a) is scattered, and plots either in field "B" or the calc-alkali basalt field. His data does not show any difference between the volcanic and the hypabyssal rocks. The diagram as a whole suggests the presence of transitional magma types.

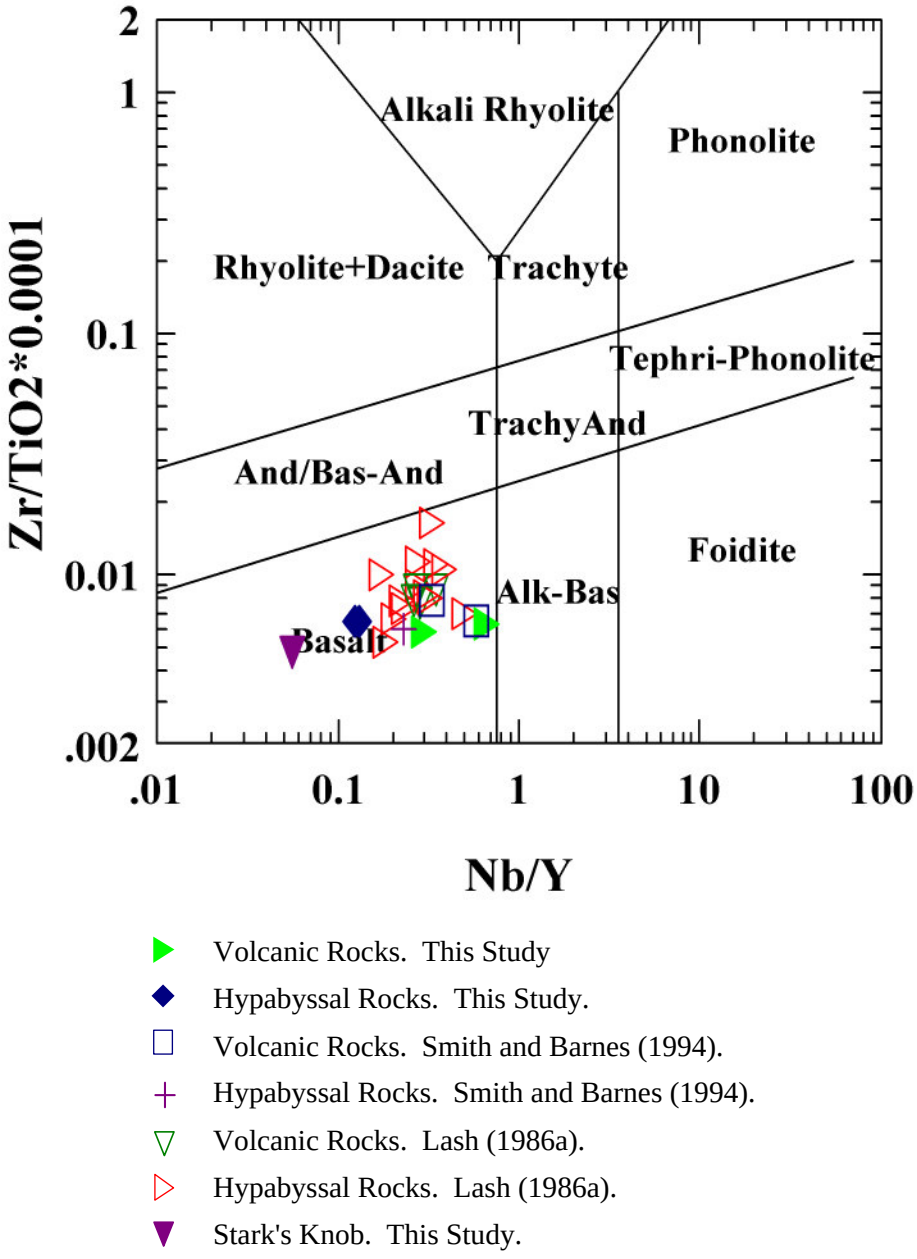


Figure 21. A rock classification diagram based on Winchester and Floyd (1976). The rocks plot in the basalt field, showing that basalt discrimation diagrams will give valid rock types for this suite.

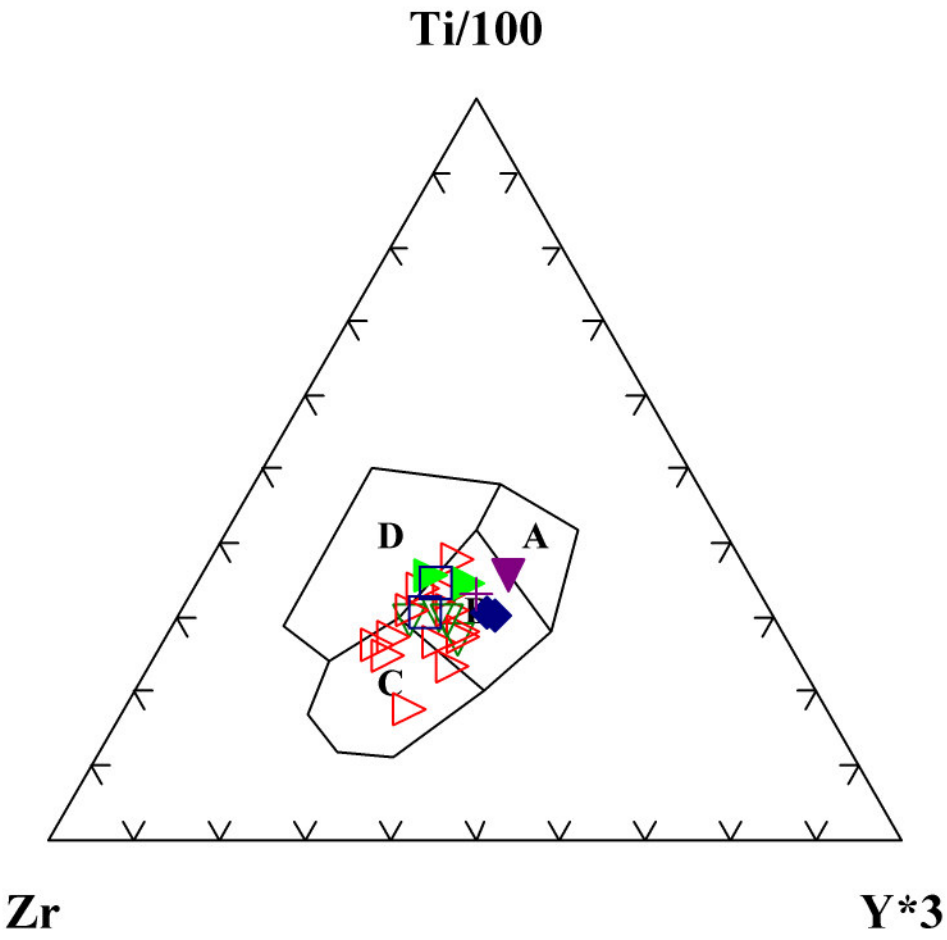


B Mid Ocean Ridge Basalt

B, C Calk-alkaline Basalt

D Within Plate Basalt

- Volcanic Rocks. This Study
- Hypabyssal. This Study.
- Volcanic Rocks. Smith and Barnes (1994).
- Hypabyssal Rocks. Smith and Barnes (1994).
- Volcanic Rocks. Lash (1986a).
- Hypabyssal Rocks. Lash (1986a).
- Stark's Knob. This Study.

Figure 22. Ti-Zr-Y (Pearce and Cann, 1973). Note that while most samples plot in the overlap field between mid-ocean ridge basalt and calc-alkline basalt, four samples from Lash (1986a), GL-9, GL-12, GL-14, and GL-17 plot only in the calc-alkaline field.

Ti-V (Shervais, 1982)

This diagram (Fig. 23) distinguishes between island arc tholeiite, mid-ocean ridge basalt, and within plate basalt. The four Jonestown samples from this study plot in the mid-ocean ridge basalt field. However, both hypabyssal rocks plot along the boundary with the island arc tholeiite field, and the volcanic rocks plot nearer to the boundary with the within plate basalt field. Smith and Barnes's (1994) samples also plot in those areas on the diagram, and again the hypabyssal and the volcanic rocks cluster in different areas. Lash's (1986a) data are scattered and do not show a distinction between volcanic and hypabyssal rocks. The rocks plot mainly in the mid-ocean ridge basalt field and along the boundary between mid-ocean ridge basalt and island arc tholeiite. Herting and Wright's (1977) data , however plot in an area of the Ti-V diagram where basalts do not commonly plot. Typical within-plate basalts have higher Ti values. They sampled rocks from the same area as the other studies, including one sample, HW-1 from the same outcrop as HK-11b2. This leads me to question the accuracy of their data, and in this particular case, to speculate that the V values they determined are significantly low. Overall, the results from the Ti-V diagram suggest the possibility that the rocks from this study are mid-ocean ridge basalt. The hypabyssal rocks could also be transitional between mid-ocean ridge basalt and island arc tholeiite while the volcanic rocks could be transitional between mid-ocean ridge basalt and within plate basalt.

Zr-TiO2 (Pearce, 1980)

This diagram (Fig. 24) discriminates between arc basalt and within plate basalt, but can tell little about mid-ocean ridge basalt, which overlaps both fields. The four Jonestown samples plot in the mid-ocean ridge basalt overlap fields. The hypabyssal rocks plot in the island arc/mid-ocean ridge basalt overlap field, while the volcanic rocks

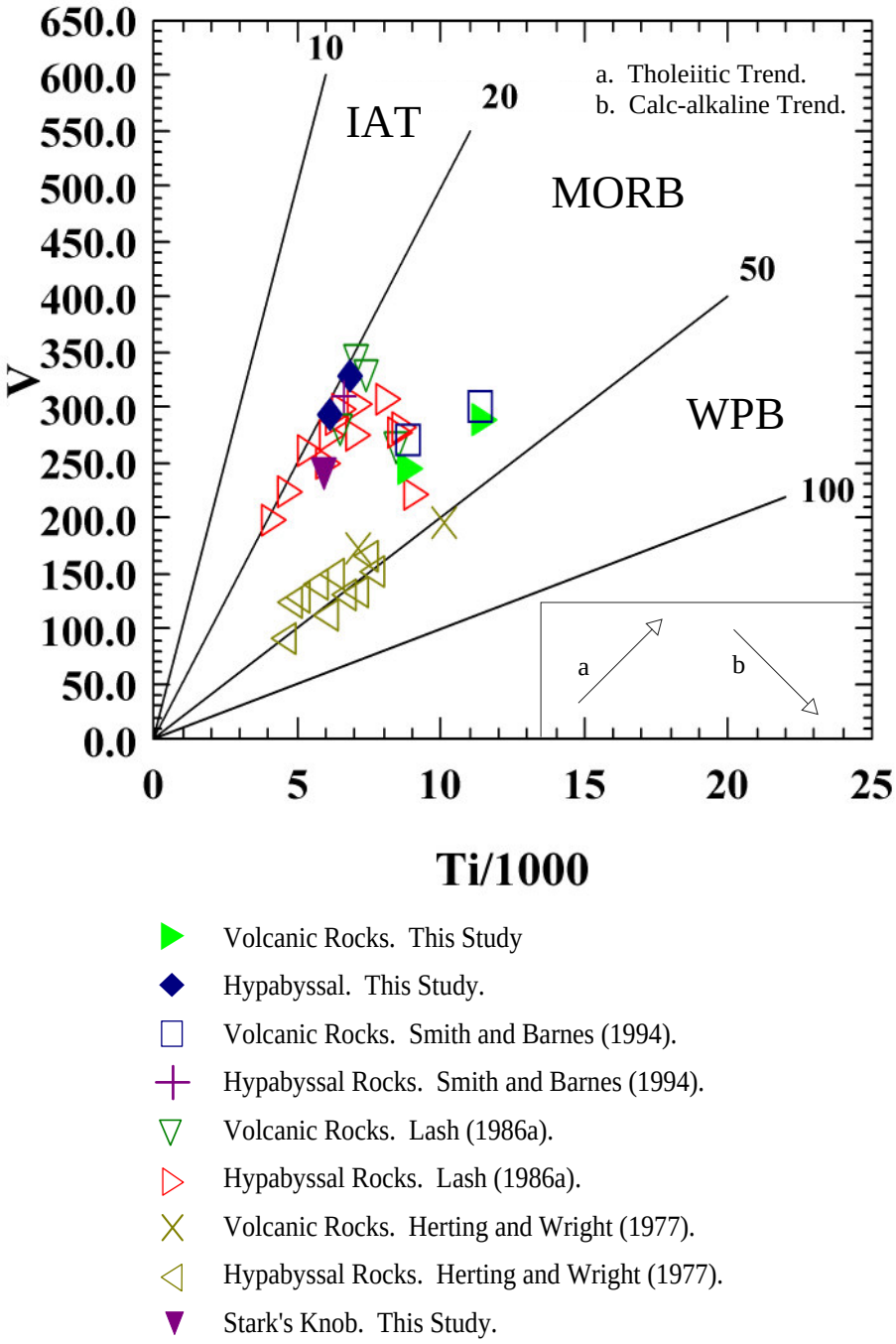


Figure 23. Ti-V (Shervais 1982). Dividing lines are based on Ti/V ratios. Arrows (a) and (b) show tholeiitic and calc-alkaline fractionation trends. The calc-alkaline trend is due largely to fractionation of magnetite. Note that calc-alkaline fractionation can easily cross field boundaries, which is why this diagram is mainly useful for tholeiitic rocks only. Curiously, the four hypabyssal rocks from Lash's (1986a) data that follow the calc-alkaline trend are GL-3, GL-21, GL-23, and GL-40, rocks that do not plot as calc-alkaline on the Ti-Zr-Y diagram. This suggests that the trend is not due to magnetite fractionation, but instead due to variation from MORB to IAT. This variation is not seen in this study or in Smith and Barnes (1994).

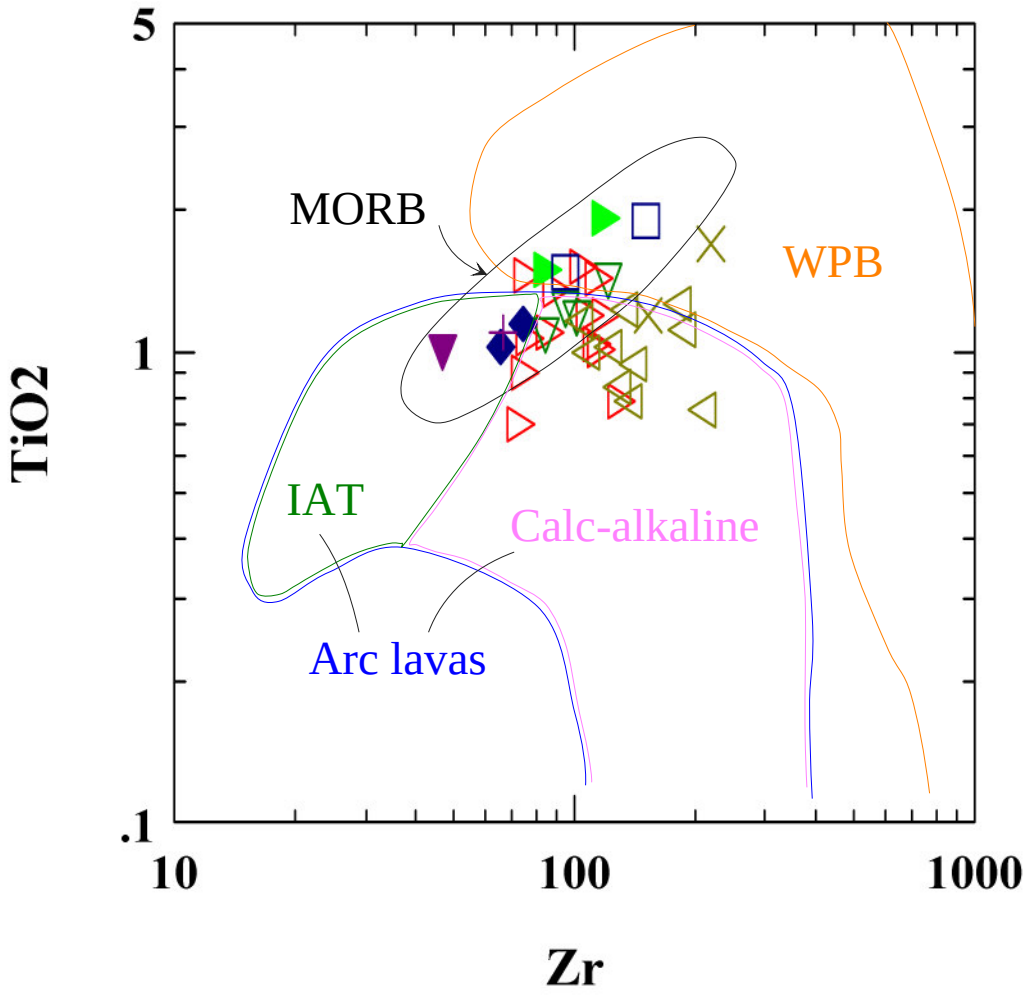


- Volcanic Rocks. This Study
- Hypabyssal Rocks. This Study.
- Volcanic Rocks. Smith and Barnes (1994).
- Hypabyssal Rocks. Smith and Barnes (1994).
- Volcanic Rocks. Lash (1986a).
- Hypabyssal Rocks. Lash (1986a).
- Volcanic Rocks. Herting and Wright (1977).
- Hypabyssal Rocks. Herting and Wright (1977)
- Stark's Knob. This Study.

Figure 24. Zr-$TiO_2$ (Pearce, 1980). Island arc tholeiite field from Pearce and Cann (1973).

plot in the within plate/mid-ocean ridge basalt overlap field. Smith and Barne's (1994) samples shadow the samples from this study. Lash's (1986a) data are scattered, but most plot either in the arc field or in the mid-ocean ridge/island arc basalt overlap field. Four of his samples do plot in the mid-ocean ridge/within plate basalt field. Herting and Wright's (1977) data are also scattered, and plot mainly outside the mid-ocean ridge basalt field, the majority plotting in the arc basalt field. While the data from Herting and Wright (1977) and Lash (1986a) are not diagnostic, the data from Smith and Barnes (1994) show that the hypabyssal rocks plot in the overlap field between island arc tholeiite and mid-ocean ridge basalt and the volcanic rocks plot in the overlap field between within plate basalt and mid-ocean ridge basalt, suggesting the two rock types are dissimilar.

### Hf-Th-Ta (Wood, 1980)

This diagram (Fig. 25) is useful for discriminating between volcanic arc basalt, and normal mid-ocean ridge basalt, while enriched mid-ocean ridge basalt and within plate basalt overap. HK-43 plots in the enriched mid-ocean ridge basalt or tholeiitic within plate basalt field. HK-23 plots on the boundary between that field, and the within plate basalt field. HK-11b2 and HK-31 plot solely in the calc-alkaline basalt field. The two volcanic samples of Smith and Barnes (1994) plot in the within plate basalt or enriched MORB field. The significance of this diagram will be dealt with in the discussion.

### Nb-Zr-Y (Meschede, 1986)

This diagram (Fig. 26) discriminates mainly between mid-ocean ridge basalt and within plate basalt, and can not distinguish volcanic arc basalt. HK-43 plots on the boundary between within plate basalt, and enriched MORB, and HK-23 plots in

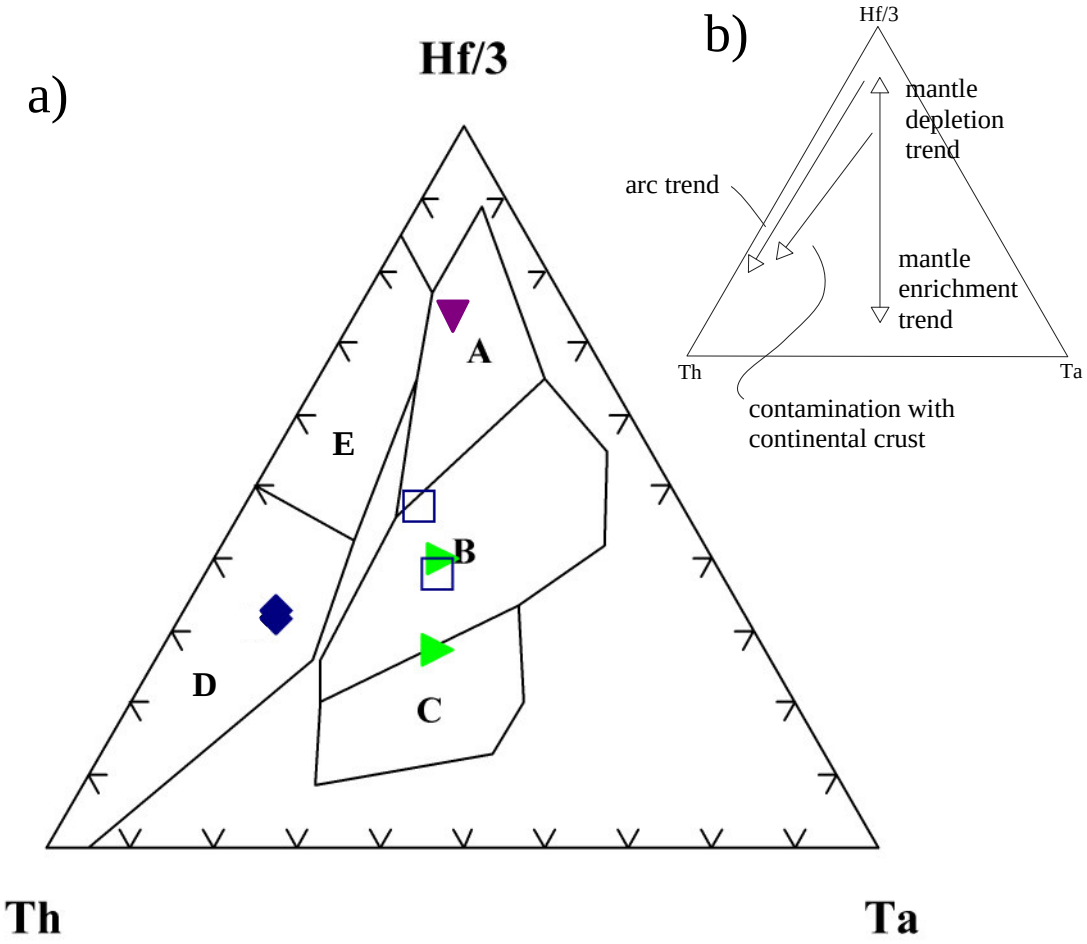


A Normal Mid-Ocean Ridge Basalt

B Enriched Mid Ocean Ridge Basalt and Tholeiitic Within Plate Basalt

C Within Plate Basalt

D Calc-Alkaline Basalt

E Island Arc Tholeiite

- Volcanic Rocks. This Study
- Hypabyssal Rocks. This Study.
- Volcanic Rocks. Smith and Barnes (1994).
- Stark's Knob. This Study.

Figure 25a. Hf-Th-Ta (Wood, 1980). Figure 25b. Schematic showing important trends on the Hf-Th-Ta diagram, from Pearce (1996).

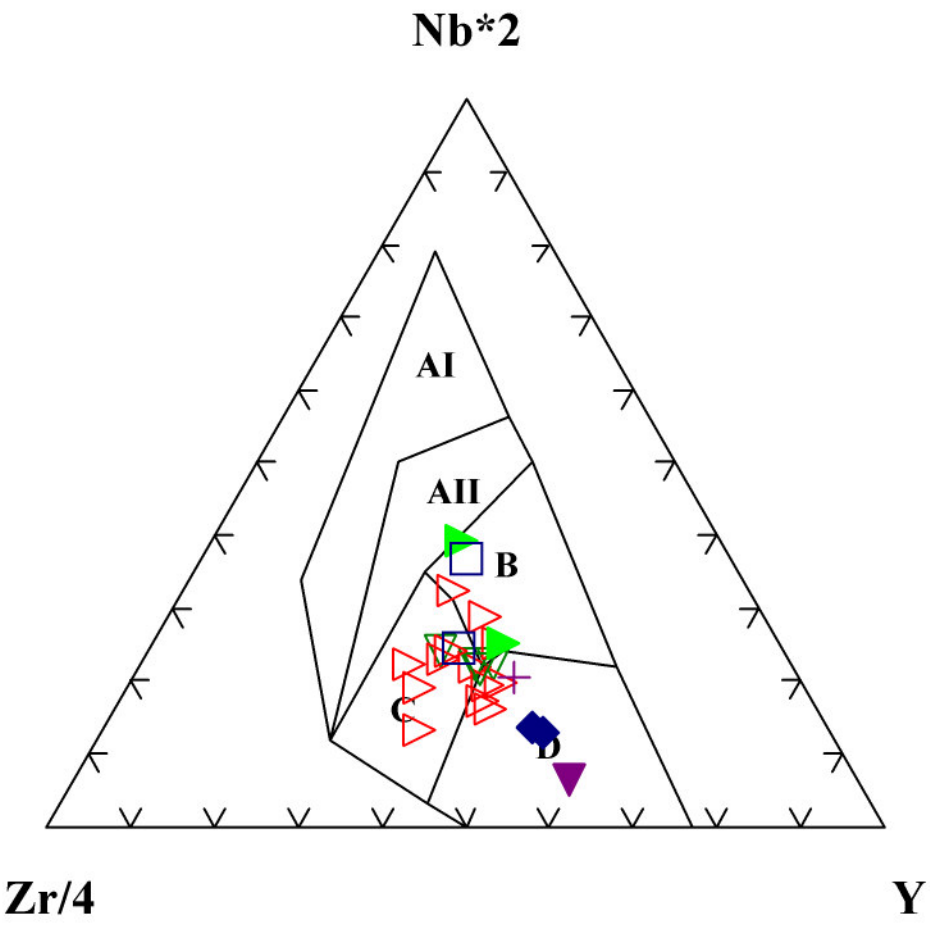


AI, AII Within Plate Alkali Basalt

AII, C Within Plate Tholeiite

B P MORB

D N MORB

C, D Volcanic Arc Basalt

▶ Volcanic Rocks. This Study

◆ Hypabyssal Rocks. This Study.

□ Volcanic Rocks. Smith and Barnes (1994).

+ Hypabyssal Rocks. Smith and Barnes (1994).

▽ Volcanic Rocks. Lash (1986a).

▷ Hypabyssal Rocks. Lash (1986a).

▼ Stark's Knob. This Study

Figure 26. Nb-Zr-Y (Meschede, 1986)

the enriched mid-ocean ridge basalt field. HK-11b2 and HK-31 plot in the mid-ocean ridge basalt or volcanic arc basalt field. As in other diagrams, the data of Smith and Barnes (1994) closely mimics the data produced in this study. Lash's (1986a) data is scattered and plots in three fields, the within plate or volcanic arc basalt field, the mid-ocean ridge or volcanic arc basalt field, and the enriched mid-ocean ridge basalt field. While most samples plot in overlap fields, a few samples plot solely in the enriched mid-ocean ridge basalt field, suggesting that a mantle plume may have played some role in the generation of magmas.

## Spider Diagram

Spider diagrams provide a convenient way to compare data to wide range of rock types on one diagram by comparing a large number of elements to known rock types and their usually distinctive patterns. The Jonestown igneous rocks plotted relative to mid-ocean ridge basalt (Fig. 27) exhibit a pattern similar to that of mantle plume enriched mid-ocean ridge basalt. The hypabyssal rocks are significantly depleted in Ta and Nb relative to enriched mid-ocean ridge basalt. The limited data of Smith and Barnes' (1994) also shows this pattern, but their Nb values are significantly higher relative to the data from this study. Nb/Ta ratios tend to be constant at approximately 17 (Wood, 1980), so it appears that there is some analytical error with Smith and Barne's (1994) Nb and Ta data. The positive Nb anomaly on this diagram suggests the error is with respect to Nb.

## Rare Earth Element Diagram

The four samples plotted relative to C1 chondrite (Fig. 28) have comparable slopes and element abundances relative to each other. This diagram is unusual, for while it shows the hypabyssal rocks and HK-23, a volcanic to be similar suggesting that

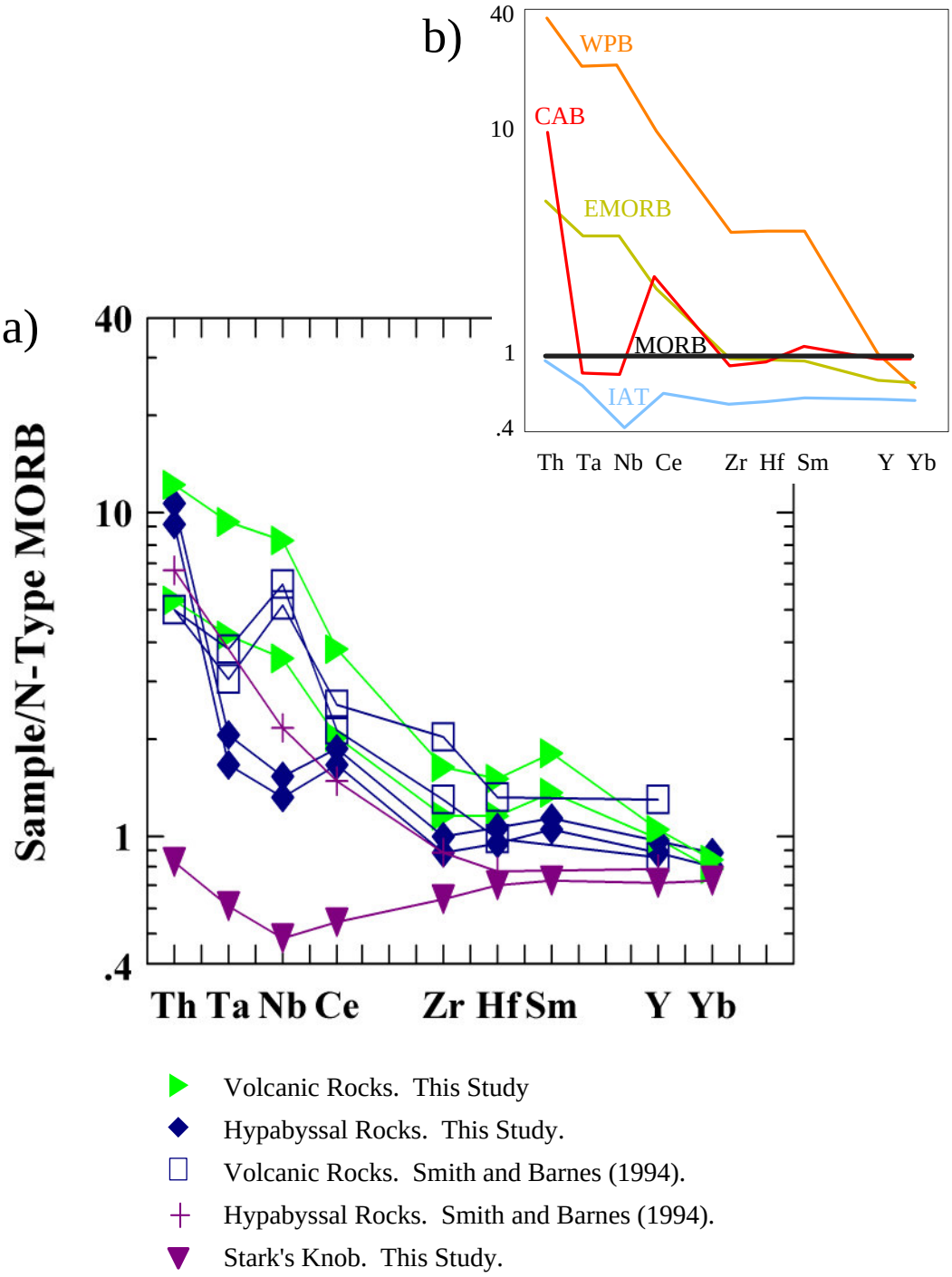


Figure 27a. Mid-ocean ridge basalt normalized spider diagram for the Jonestown igneous rocks, shown along with Stark's Knob. Element order is simplified from Pearce (1982). Figure 27b. Patterns of common basalt types shown for reference. Normalizing values for normal mid-ocean ridge basalt, enriched mid-ocean ridge basalt, and within-plate basalt are from Sun and McDonnough (1989). Normalizing values for calc-alkaline basalt and island arc tholeiite are from Pearce, et al. (1995).

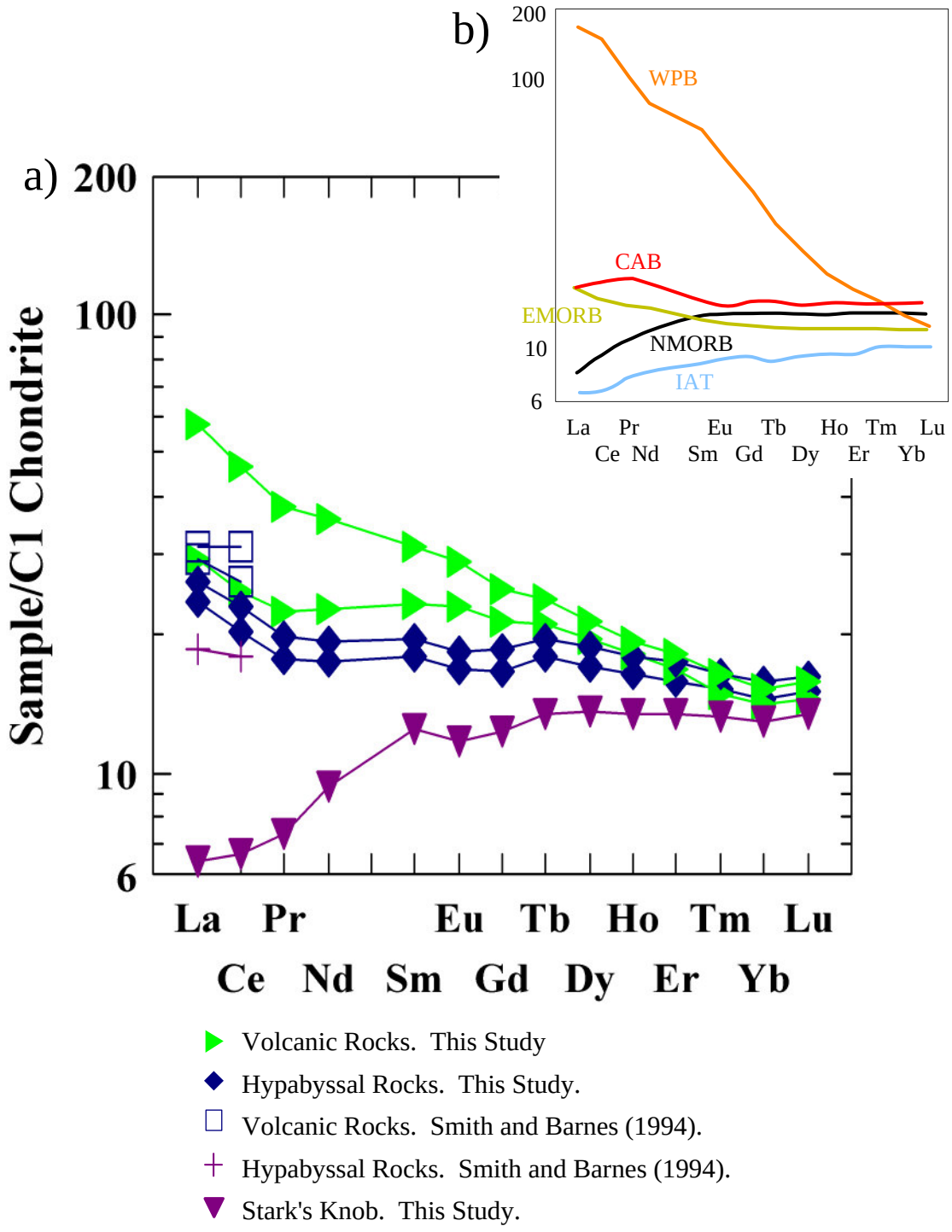


Figure 28a. Rare earth elements normalized relative to C1 Chondrite (values from Sun and McDonough, 1989). Figure 28b. Patterns of common basalt types shown for reference. Normalizing values for normal mid-ocean ridge basalt, enriched mid-ocean ridge basalt, and within-plate basalt are from Sun and McDonnough (1989). Normalizing values for calc-alkaline basalt and island arc tholeiite are from Pearce, et al. (1995).

they could have shared a parental magma, it shows that HK-43 varies from HK-23 in the amount of light rare earth elements, suggesting the two volcanic rocks could have different parental magmas. This is inconsistent with Hf-Th-Ta (Fig. 25) and the mid-ocean ridge basalt normalized spider diagram (Fig. 27). All four rocks show enrichment relative to C1 chondrite, and some enrichment of the light rare earth elements relative to mid-ocean ridge basalt. They do not have the significant enrichment (upwards of 10 times greater than mid-ocean ridge basalt) of within plate basalt, however. The scant data from Smith and Barnes (1994) also shows this intermediate amount of enrichment. The light rare earth enrichment is similar to light rare earth enrichment found in enriched, or plume mid-ocean ridge basalt, found at spreading centers with a hotspot influence. Overall, this diagram suggests that these rocks cooled from magmas formed in similar manner.

## Chapter 4 Stark's Knob

Stark's Knob is a block of pillow basalt, basalt flows, and minor limestone in interstitial cavities located in the melange of the main Taconic thrust zone near Schuylerville, NY (Vollmer and Bosworth, 1984). Along with the limestone, calcite is ubiquitous in the basalt. The origin of Stark's Knob is enigmatic. The association of Ordovician limestone and pillow basalt is similar to the Jonestown volcanic rocks. Like the Jonestown volcanic rocks, the limestone is the only rock that can be confirmed to be associated with the basalt as primary sediment. The location of Stark's Knob relative to the allochthon is also similar to the Pennsylvania rocks. The Jonestown rocks are located about ten to fifteen kilometers from the northeastern (cratonward) boundary of the Hamburg Klippe. Stark's Knob rests in rocks that are traditionally thought to be the western boundary of Taconic rocks, but it is located fifteen to twenty kilometers east of the western limit of Taconic melange and deformation (Kidd, et al., 1995). A difference between Stark's Knob and the Jonestown volcanics may be the nature of the allochthons in which they currently occur, the classic Taconic allochthon of New York incorporates older continental rise rocks, while the allochthon in Pennsylvania is mostly younger flysch.

Since the origin and subsequent history of the Jonestown volcanic rocks is better understood than of the basalt of Stark's Knob, I decided to compare basalt from Stark's Knob with the basalt from the Jonestown volcanic field. One sample from Stark's Knob, SN-4, was included in this study to see if it shared geochemical characteristics with the Jonestown Volcanic rocks. SN-4 is a sample from a flow, and was collected from float. In thin section (Fig. 29) (See Appendix B for detailed rock descriptions), the rock contains small plagioclase lathes, phases that have been replaced by serpentine and

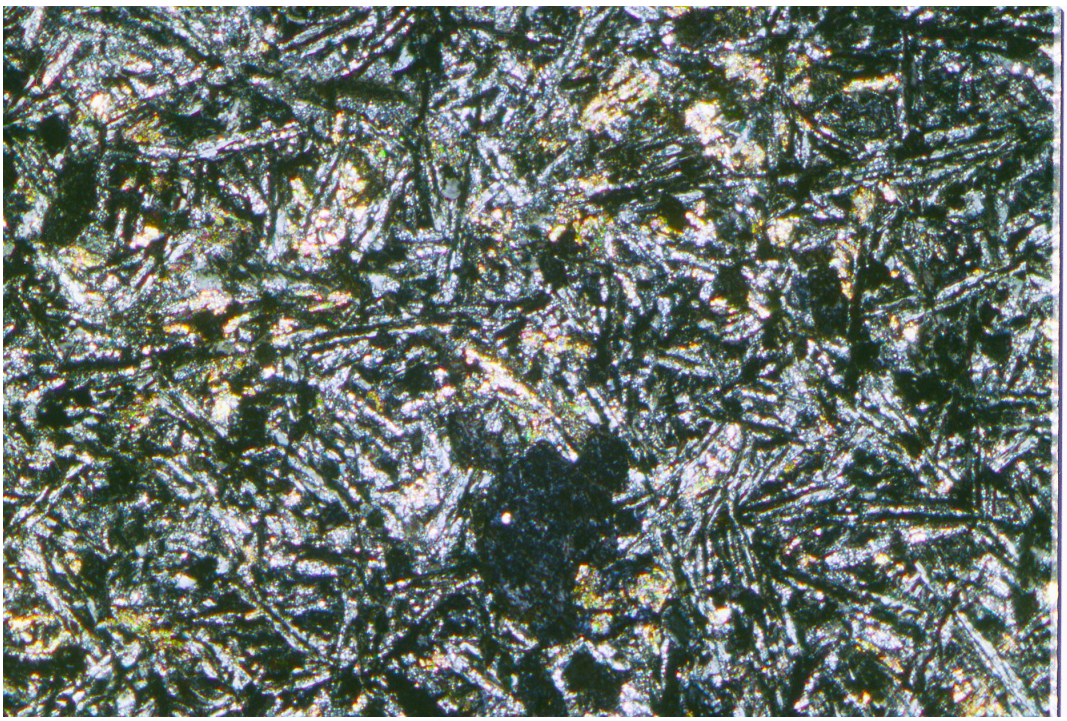

Figure 29. Thin section of SN-4, basalt, viewed under crossed polars. Note the lathes of plagioclase and small altered phenocrysts. Field of view is 2.12 mm by 1.38 mm.

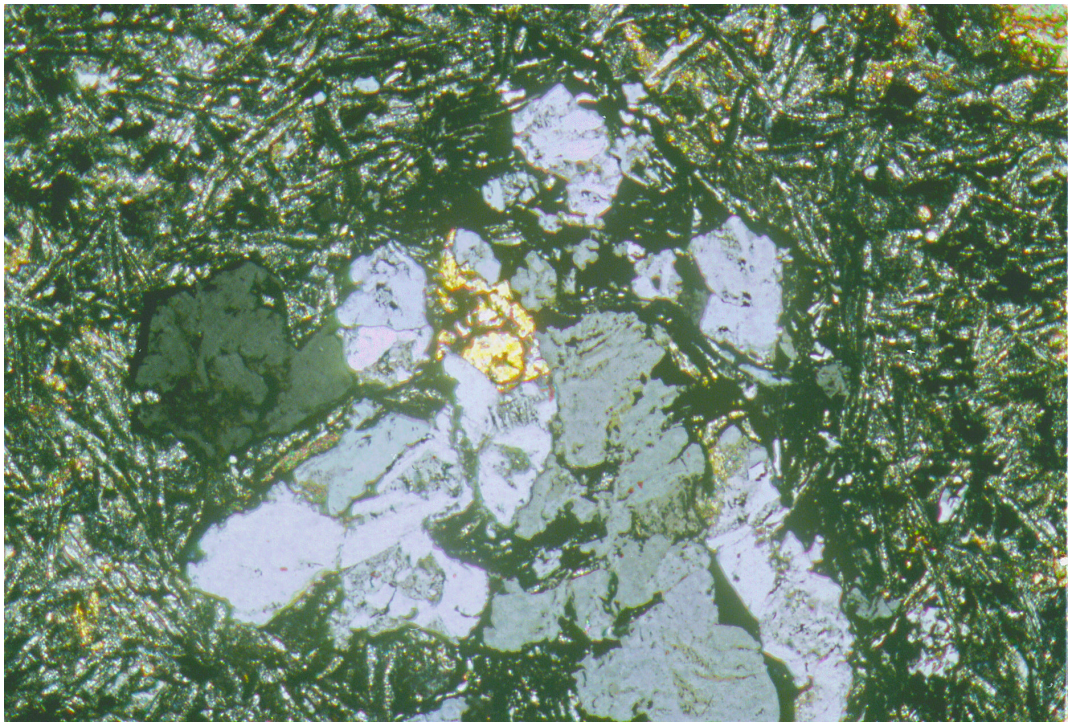

Figure 30. Thin section of SN-4, basalt, showing the microxenolith, composed primarily of quartz along with opaques and altered feldspar. Field of view is 2.12 mm by 1.38 mm.

chlorite, secondary calcite, and minor pumpellyite and prehnite. The serpentine progenitor was likely olivine. The chlorite progenitor could have been pyroxene. The rock also contains a micro-xenolith (Fig. 30) consisting mainly of grains of quartz and untwinned feldspar. Based on the sizes of the crystals and their texture, is likely a piece of continental crust that was entrained in the magma before it was emplaced. This presence of a continental xenolith strongly suggests that the Stark's Knob basalts were erupted in a setting on continental lithosphere.

SN-4 was prepared and analyzed by the same methods that were used to prepare and analyze the four Jonestown volcanic rocks in this study, and is included in Table 1. Care was taken to minimize the amount of calcite present in the sample prepared for analysis, first in selecting a rock with little visible calcite in the field, then by selecting chips with little to no visible calcite in them.

## Summary of Discrimination Diagram Results

SN-4 was plotted on the same set of discrimination diagrams as was used for the Jonestown volcanic rocks (Fig. 21-28). It is a basalt, and on every diagram with a mid-ocean ridge basalt field, it plotted as mid-ocean ridge basalt. It did fall into overlap fields on many diagrams, but on Th-Ta-Hf (Fig. 25) and Ti-V (Fig. 23), it plotted solely in the mid-ocean ridge basalt field. On the mid-ocean ridge basalt spider diagram, its pattern was somewhat similar to that of island arc tholeiite. Its rare earth element pattern relative to chondrite (Fig. 28) suggests it is a primitive mid-ocean ridge basalt, with lower rare earth element abundances than an average mid-ocean ridge basalt.

SN-4 consistently plotted in the same fields as the Jonestown data, suggesting that they did form in similar environments, but based on Th-Ta-Hf (Fig. 25), where the Jonestown rocks plotted as enriched MORB or island arc rocks while SN-4 plotted as

mid-ocean ridge basalt, and a comparison of trace (Fig. 27) and light rare earth (Fig. 28) elements, it is apparent that SN-4 is distinct from the Jonestown rocks, including HK-43.

The difference between SN-4 and HK-43, the two calcite bearing basalts, is significant. The two rocks often plot the furthest apart of the samples of this study, and trace and rare earth element patterns vary significantly between the two. SN-4 has a slight depletion of Ta and Nb relative to mid-ocean ridge basalt, while HK-43 shows no depletion, and the two rocks have different slopes on the spider (Fig. 27) and rare-earth element diagram (Fig. 28). This comparison shows that while the basalt of Stark's Knob may have field relations analogous to the basalts in the Hamburg Klippe, the two groups of basalt were derived from different magmas. The continental xenolith and the depletion of Ta and Nb suggest that the Stark's Knob basalts interacted with continental lithosphere before they were erupted, in this case, likely the Laurentian foreland.

## Chapter 5 Possible Analogues

Magmatic activity on a stable platform in front of an approaching allochthon or trench is not common, but there are a few possible analogues. I have found it useful to compare the Jonestown igneous rocks to three igneous suites: the modern Karacalidag basalt field in eastern Anatolia (Turkey), the Neogene basalt flows of the Penghu Islands in the Taiwan Strait, off the west coast of Taiwan, and the Proterozoic flows of the Flaherty Formation on the Belcher Islands, Hudson, Bay, Canada. While details vary, the three areas represent volcanism in foreland settings on stable or previously stable platforms in front of active thrust systems.

Generation and emplacement of magma is unusual in a compressional foreland setting. However, Sengor, et. al., (1978) point out that rifts can occur in association with orogenic belts, often at high (close to 90 degree) angles to those belts (Fig. 31). These rifts are the result of tensional forces, often seen in underthrusting foreland settings. This rifting or tensional stress could provide a mechanism for the generation of magma from upwelling asthenosphere and melting or at least a conduit for that magma to reach the surface, providing magmatism in a foreland thrust setting.

### Karacalidag Setting

The Karacalidag basalts were erupted out of a series of fissures trending parallel to the current direction of shortening along the east-west collisional zone in eastern Anatolia (Pearce, et al., 1990) (Fig. 32). Magmatism in the area is related to the collision of the Arabian plate and the Eurasian plate to the north. Prior to the start of collision of the two continental lithospheres, there was northward subduction, and the northward underthrusting direction is still present in the active thrust zones, and in many thrust faults in the area. The minimum proposed age of the initiation of the start of

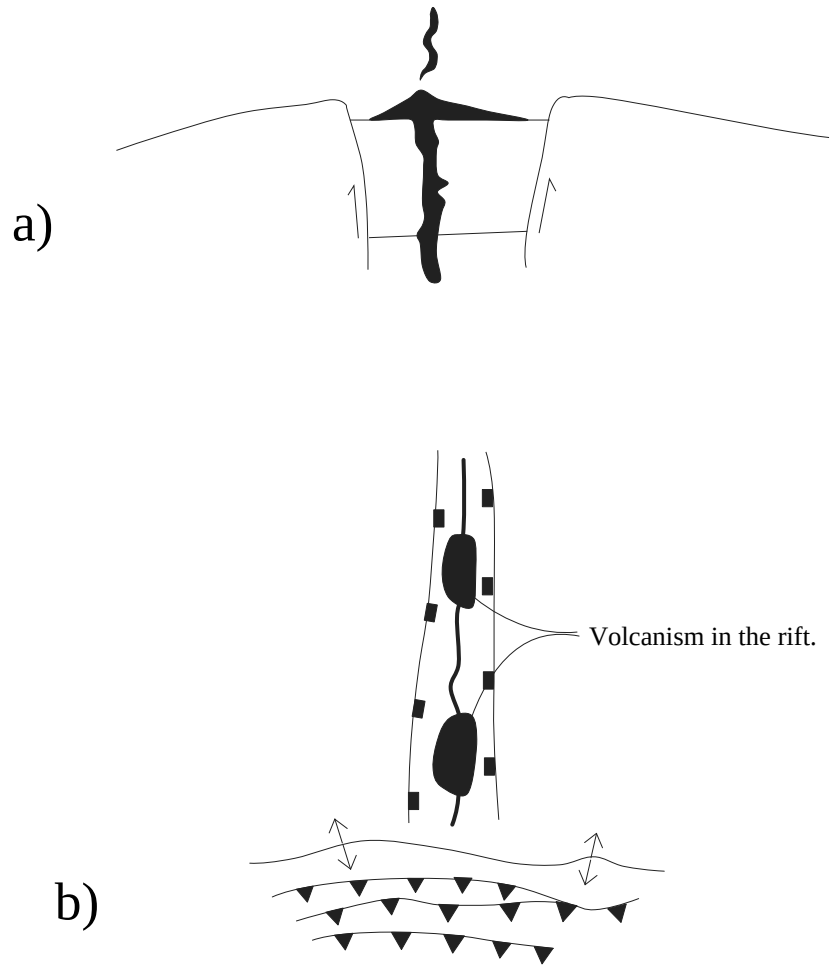


Figure 31. Generalized cartoon drawings from Sengor, et al. (1978) in cross section (a) and map view (b) showing how orogen normal rifting could occur in a foreland setting as a result of collision. The Rhine Graben is an example of this type of rifting.

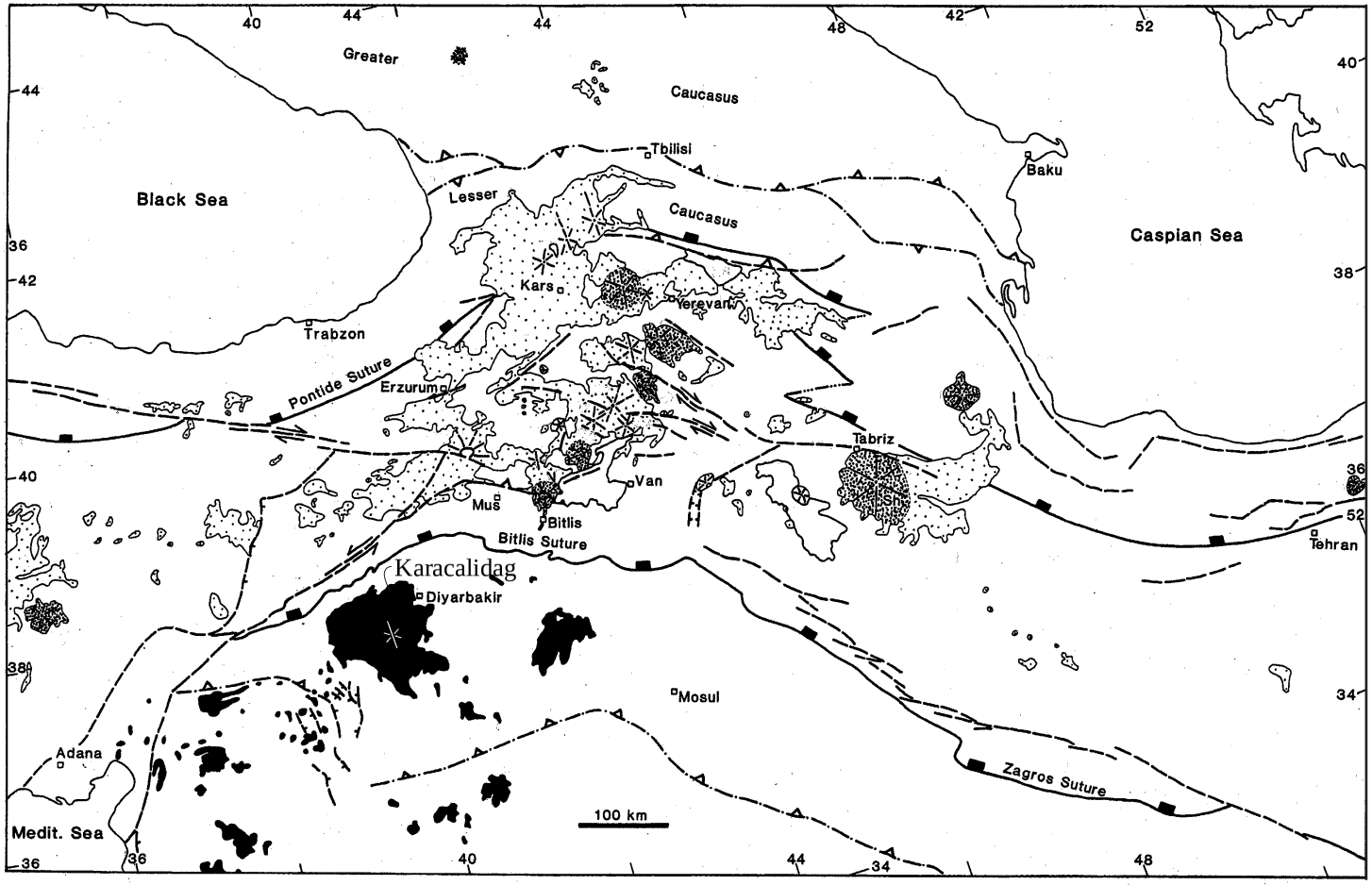


Figure 32. Geologic map of the area containing the Karacalidag basalt flows (from Pearce, et al., 1990). Convergence was accomodated by northward underthrusting, therefore the Karacalidag basalts were erupted on a foreland. Black areas are basalts on the Arabian foreland. Close stipple is young (dormant) volcanoes. Wider Stipple is older (extinct) volcanoes and volcanic strata. Dashed lines: active faults; with vees are limits of folding and thrusting; with ticks are normal faults, with half arrows are strike slip. From Pearce, et al. (1990).

collision is about 12 Ma. Ages of the erupted rocks from the Karacalidag fissures range from 1 Ma to very recent, possibly only a few thousand years ago (Pearce, et al., 1990). Karacalidag, therefore, is located on an active overall compressional system. This suggests, then, that these volcanics are the result of extension normal to the direction of shortening as described in Sengor, et al. (1978), and are possibly analogous to the Jonestown volcanics in a general way.

## Karacalidag Geochemistry

Pearce, et al. (1990) show that the Karacalidag basalts are within-plate basalts. Data published in that paper was plotted on the diagrams used in this paper, to compare with the Jonestown volcanics. The rocks plot consistently in within-plate basalt fields, on both major element diagrams, and trace element diagrams, such as Hf-Th-Ta (Fig. 33). Plots of trace elements on a MORB normalized spider diagram (Fig. 34) and of rare earth elements on a C1 chondrite normalized diagram (Fig. 35) show the distinctive steep negative slope and enrichments of trace and rare earth elements typical of within-plate basalt.

## Penghu Islands Setting

The origin of the Penghu Island basalt magmas is not as well constrained as Karacalidag. The Penghu Islands are located in the Taiwan Strait near the South China sea, on the Asian plate (Fig. 36). Their location is a foreland setting approximately 100 km northwest of the boundary with the Philippine plate, a convergent boundary where the Eurasian plate is subducting under the Philippine plate, and where, for Taiwan, active collision is occurring. Juang and Chen (1992) used the K-Ar method to date a hornblende and a phlogopite crystal from the southern Penghu sequence. The two samples yielded ages of about 13 and 11 Ma, respectively, which appear likely to be the

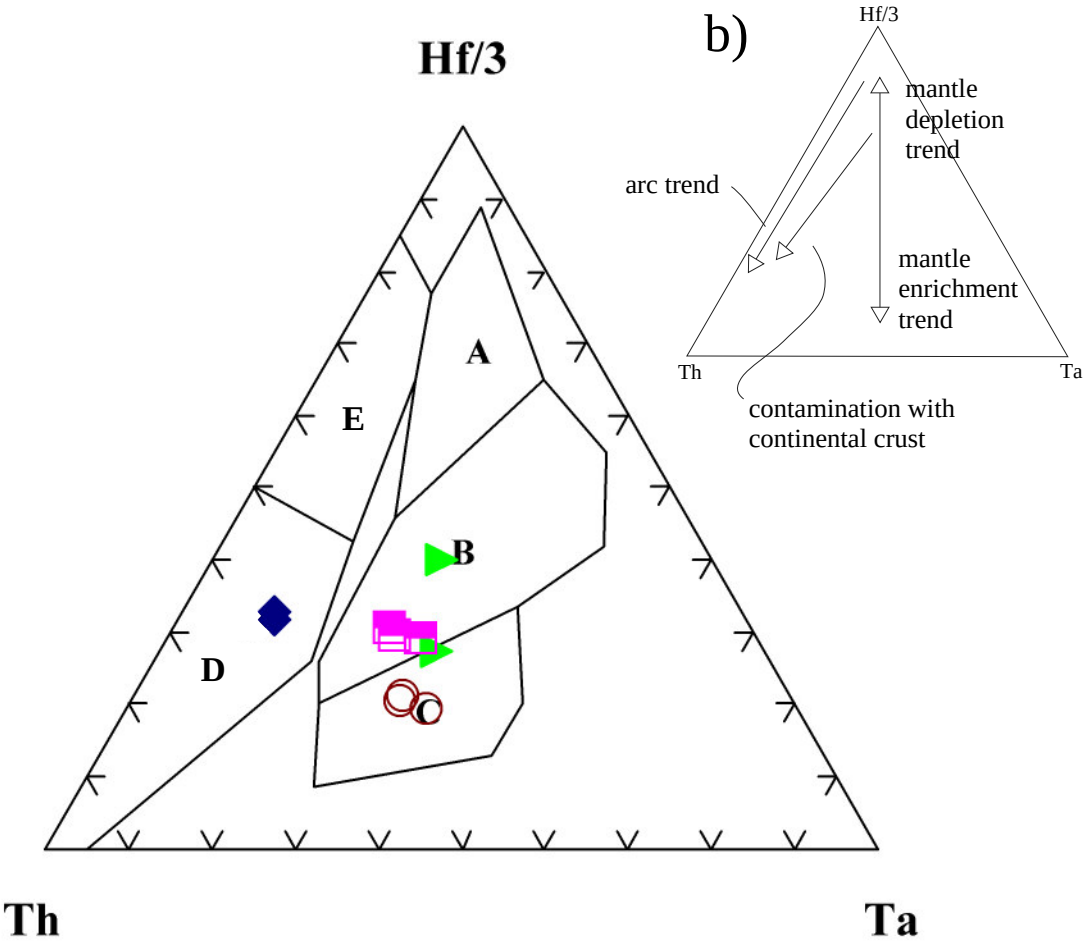


A Normal Mid-Ocean Ridge Basalt

B Enriched Mid Ocean Ridge Basalt and Tholeiitic Within Plate Basalt

C Within Plate Basalt

D Calc-Alkaline Basalt

E Island Arc Tholeiite

- Volcanic Rocks. This Study
- Hypabyssal Rocks. This Study.
- Karacalidag Basalt. Pearce, et al. (1990).
- Penghu Island Alkali Basalt. Greenough, et. al (1999).

Figure 33a. Hf-Th-Ta (Wood, 1980). Figure 33b. Schematic showing important trends on the Hf-Th-Ta diagram, from Pearce (1996).

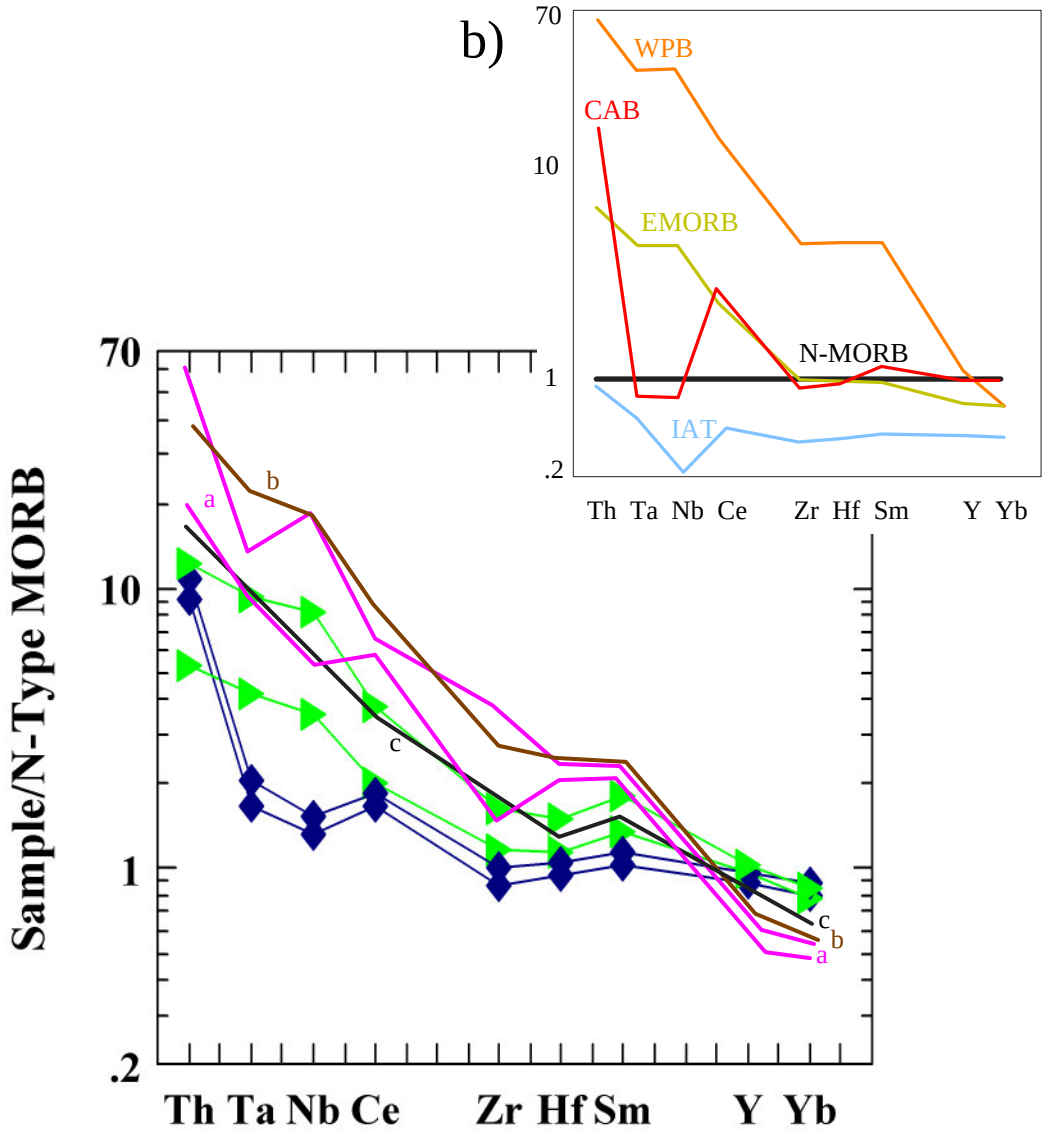


Volcanic Rocks. This Study

Hypabyssal Rocks. This Study.

a Maximum and Minimum Karacalidag Basalt Values. Pearce, et al. (1990).

b Average Penghu Island Alkali Basalt. Greenough, et. al (1999), Chen (1988).

c Average Penghu Island Tholeiite. Chen (1988).

Figure 34a. Mid-ocean ridge basalt normalized spider diagram for the Karacalidag basalts and the Penghu Island basalts. Element order is simplified from Pearce (1982). Figure 34b. Patterns of common basalt types shown for reference. Normalizing values for normal mid-ocean ridge basalt, enriched mid-ocean ridge basalt, and within-plate basalt are from Sun and McDonnough (1989). Normalizing values for calc-alkaline basalt and island arc tholeiite are from Pearce, et al. (1995).

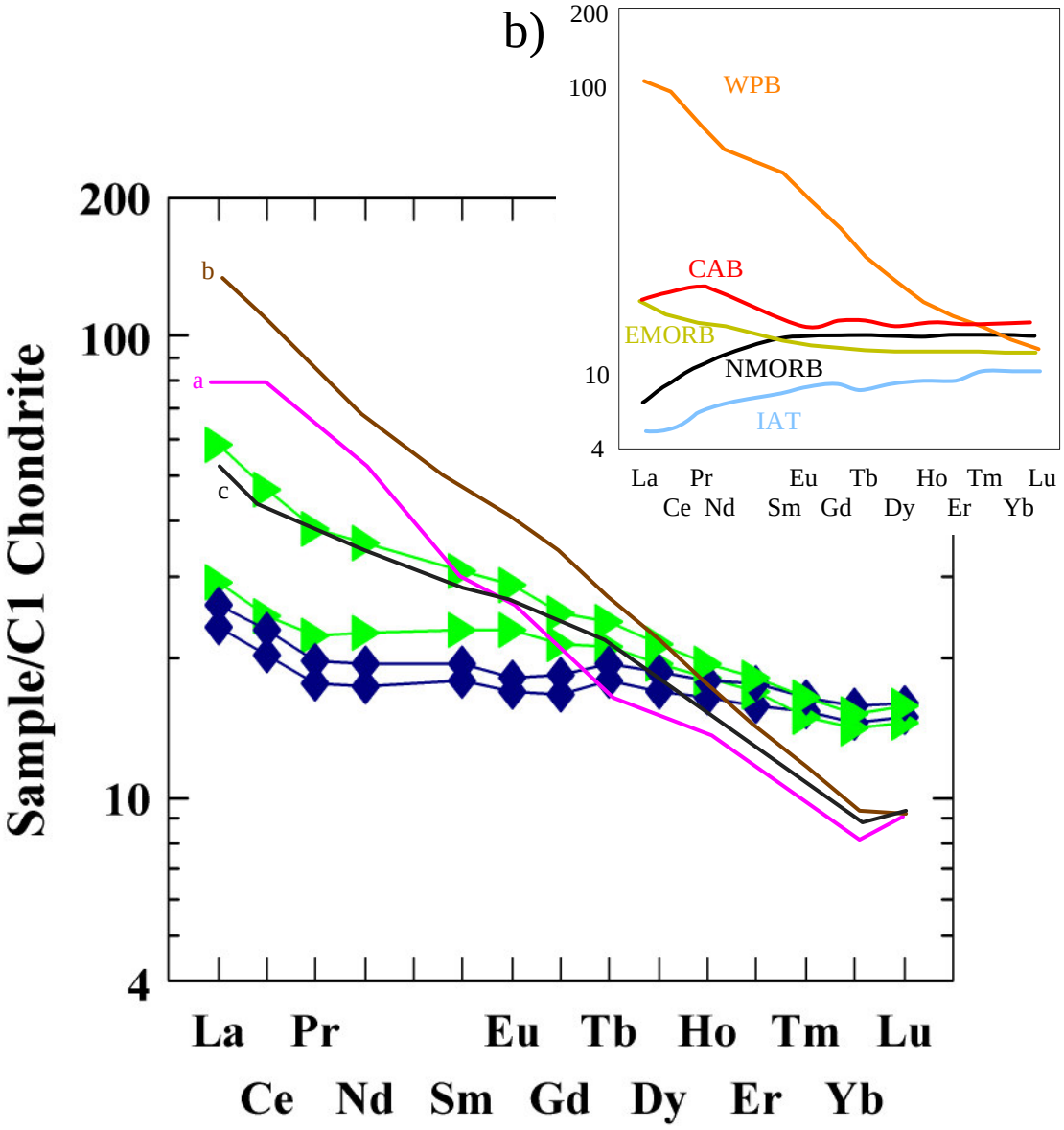


Volcanic Rocks. This Study

Hypabyssal Rocks. This Study.

a — Average Karacalidag Basa.t. Pearce, et al. (1990).

b — Average Penghu Island Alkali Basalt. Greenough, et al. (1999), Chen, (1988).

c — Average Penghu Island Tholeiite. Chen (1988).

Figure 35a. Rare earth elements normalized relative to C1 Chondrite (values from Sun and McDonough, 1989). Figure 35b. Patterns of common basalt types shown for reference. Normalizing values for normal mid-ocean ridge basalt, enriched mid-ocean ridge basalt, and within-plate basalt are from Sun and McDonnough (1989). Normalizing values for calc-alkaline basalt and island arc tholeiite are from Pearce, et al. (1995).

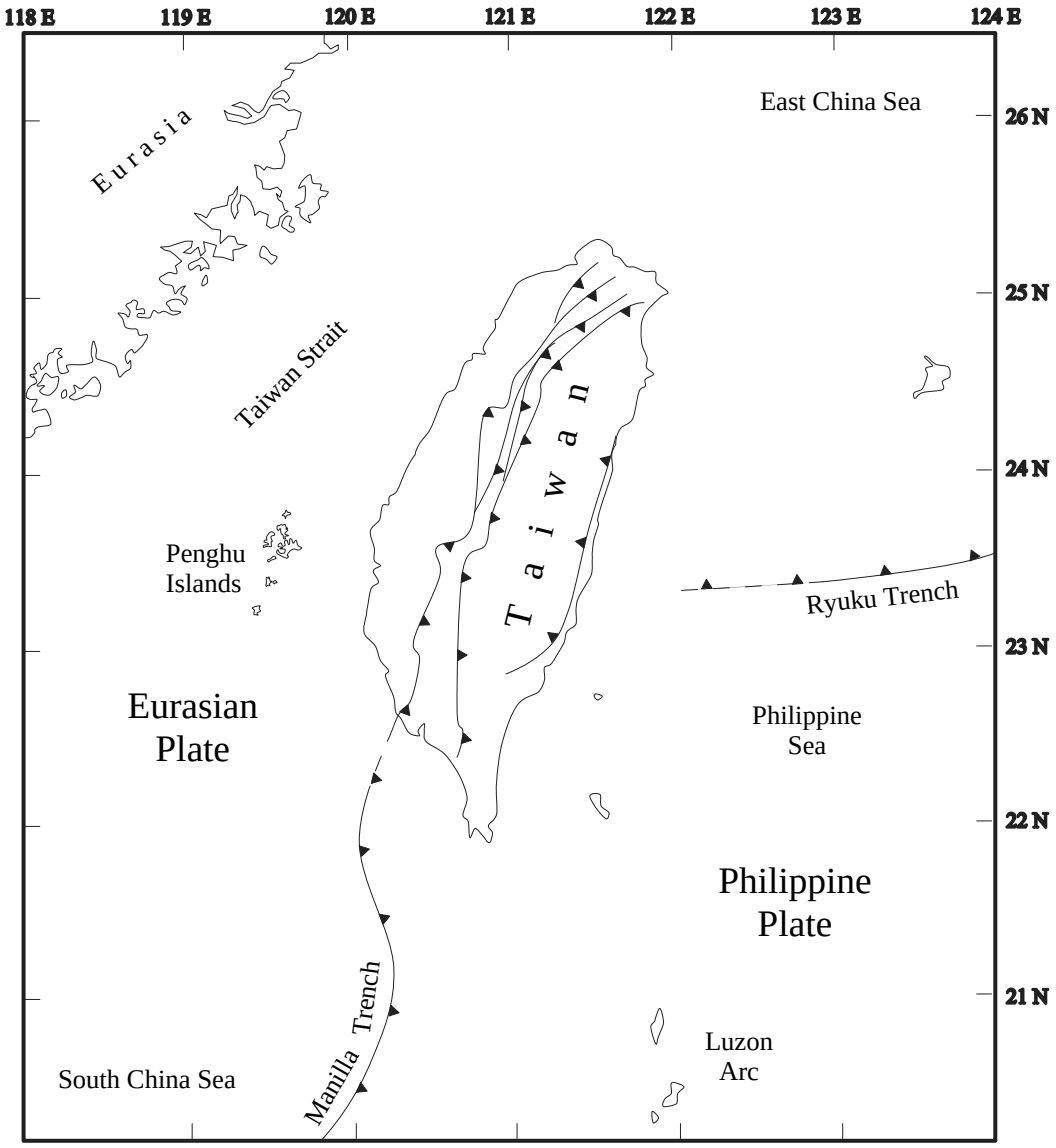


Figure 36. Map showing the location of the Penghu Islands and the present day tectonic setting of Taiwan. The Penghu Islands are in the Asian foreland, but are nearing the collisional zone in Taiwan. Map based on Angelier et al. (1990), location of trenches and thrust faults is from Suppe (1980). With respect to trenches or thrust faults, teeth are on overiding plate.

most reliable ages, because other dates are whole rock K-Ar ages. The latter ages range down to about 8 Ma.

Angelier, et. al, (1990), studied fracture, fault and slickenline data, and describe the current extensional stress oriented north-northeast to south-southwest. This is consistent with the direction of Eurasian plate- Philippine plate convergence. The previous tensional stress field was oriented north to south. According to Angelier, et al. (1990), the rotation from that field to the present orientation took place between 12 and 8 million years ago (Angelier, et al., 1990). They propose this tension is directly related to spreading in the South China Sea. However, sea floor spreading and opening of the South China Sea ceased by 17 Ma (Taylor and Hayes, 1983), ruling out the possibility that seafloor spreading that is closely relevant to the stress fields in the Penghu Islands.

The date of initiation of collision is not well constrained, although current arguments (Suppe, 1980) suggest that collision initiated only 4 million years ago. Suppe (1980) suggests that the convergence between the two plates is about 70 kilometers per million years. Mothereau, et. al. (2001), suggest a more conservative convergence rate of 30 to 40 kilometers per million years. Even the conservative estimate would place the trench 200 kilometers or more from the Penghu Islands at the time of volcanism. However, it is conceivable that the extensional fractures were related to far field stresses, or that collision was initiated earlier than currently thought, and that the collision and the basalts are closely related. These possibilities suggest this tension is analogous to the orogen normal rifting discussed in Sengor, et al. (1978). In any event, the environment, with extrusion of basalts, in a foreland setting, may be analogous to the Jonestown volcanics.

## Penghu Islands Geochemistry

Papers on the geochemistry of the Penghu Island basalts describe a variety of basalt types, from alkali to tholeiitic basalt, and suggest that they are within-plate basalts (Chen, 1988; Greenough, et al., 1999). The limited Ta data available on these basalts (Greenough, et al., 1999) is consistent with this classification (Fig. 33). Study of rare earth element patterns shows differences as well. The volatile influenced flows analyzed by Greenough, et al. (1989) and some alkali basalts analyzed by Chen (1988), show trace element versus MORB patterns (Fig. 34) and a rare earth element relative to chondrite patterns (Fig. 35) similar to within-plate basalt. Chen (1988) also analyzed tholeiites from the Penghu Islands, and the trace (Fig. 34) and rare earth (Fig. 35) elements in those rocks occur in abundances similar to enriched mid-ocean ridge basalt. Interestingly, the patterns exhibited by these rocks are quite similar to HK-43 (this study) of the Jonestown Volcanic Field.

## Belcher Islands Setting

The Belcher Islands are located in Hudson Bay, Canada, and expose Proterozoic rocks approximately 1.8 billion years old. The islands are mainly comprised of sedimentary rocks, but there are two separate volcanic sequences exposed there, the Eskimo Formation, and upsection, the Flaherty Formation. The Eskimo Formation is described as a sequence of massive flows and some dykes interbedded with arkosic sandstone, and fluvial conglomerate. It is underlain by platform carbonates and overlain by arkosic red beds, also interpreted as fluvial. This sequence suggests the rocks were erupted into a continental rift facies (Hoffman, 1987). The Flaherty Formation is mainly comprised of pillow basalt. It is underlain by a banded iron formation and is overlain by thick sequence of argillite and shale (Legault, et al., 1994). The argillite and shale are

interpreted to be flysch (Hoffman, 1987), and geological relations and their location in the circum-Superior belt (Hoffman, 1987) show that they were deposited in a foreland thrust and fold belt. Legault, et al., (1994) noted pumpellyite and prehnite in thin sections of both suites if igneous rocks, and interpreted that the rocks have undergone pumpellyite-prehnite facies metamorphism, but like the Jonestown igneous rocks (Zen, 1974) have not seen any higher degrees of metamorphism. The Flaherty Formation, therefore, may be a good analogue for the Jonestown volcanic rocks. The similar metamorphic grades of the two rock suites should allow meaningful comparisons of their whole rock geochemistry.

## Belcher Islands Geochemistry

Legault, et al., (1994), differentiate the Flaherty Formation into two groups of rocks based on the amount of Zr present in the rocks. It is these low Zr rocks that show some of the lower rare earth element data, especially with respect to the light rare earth element data. A plot of the two groups of rocks on the Hf-Th-Ta (Wood, 1980) diagram (Fig. 37) shows that both the low and high Zr Flaherty Formation samples plot in the enriched MORB and tholeiitic within plate basalt field, but cluster in slightly separate areas. The high Zr rocks are quite similar to HK-43 (this study). This is also the case on a C1 mantle normalized rare earth element diagram (Fig. 38), the low Zr Flaherty rocks have rare earth element abundances similar to HK-43. Overall, the Flaherty rocks range from enriched mid-ocean ridge basalt to within-plate basalt on that diagram.

A plot of the Flaherty Formation rocks on a spider diagram (Fig. 39) shows that the low Zr Flaherty rocks also have a minor Ta and Nb depletion relative to the high Zr flows. Legault, et al. (1994) attribute this depletion to marked interaction with continental lithosphere. Specifically, they refer to Devey and Cox (1987) and interpret

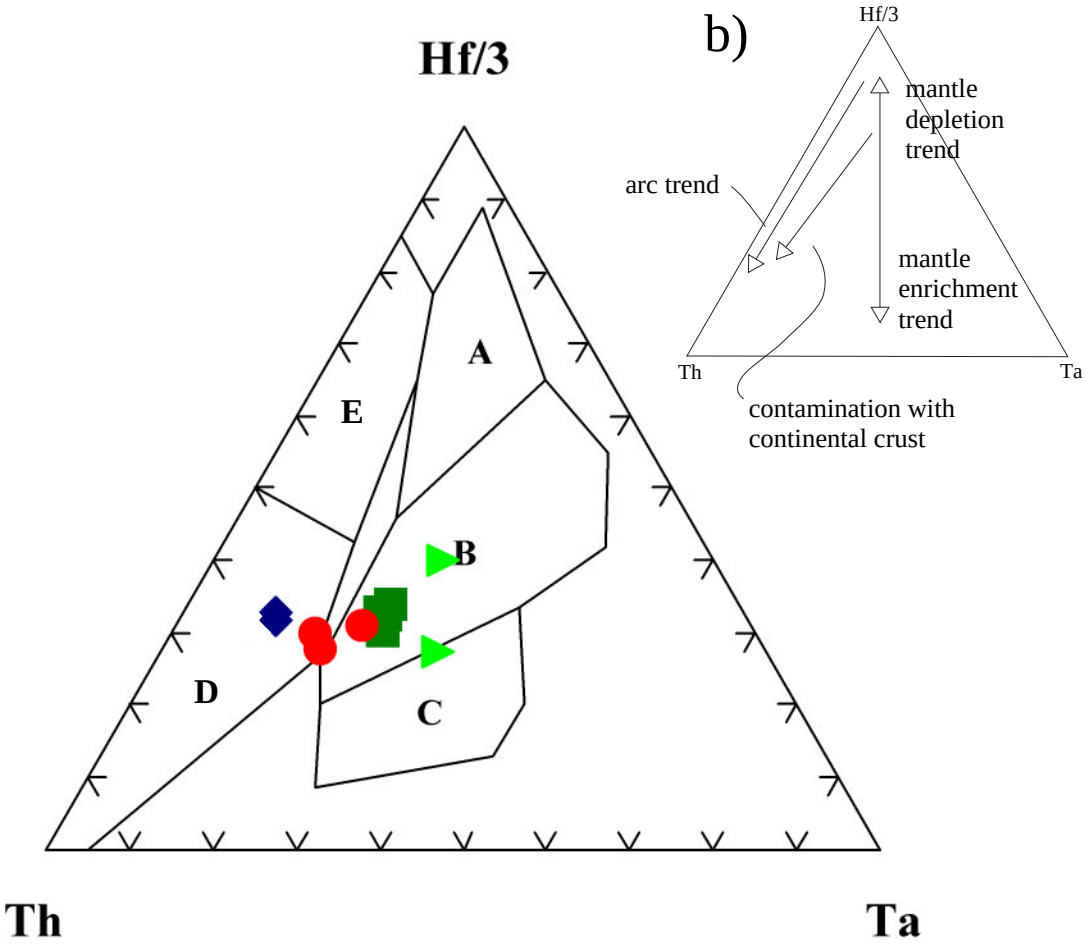


A Normal Mid-Ocean Ridge Basalt

B Enriched Mid Ocean Ridge Basalt and Tholeiitic Within Plate Basalt

C Within Plate Basalt

D Calc-Alkaline Basalt

E Island Arc Tholeiite

- Volcanic Rocks. This Study
- Hypabyssal Rocks. This Study.
- Flaherty Formation, High Zr Rock. Legault, et al. (1994).
- Flaherty Formation, Low Zr Rock. Legault, et al. (1994).

Figure 37a. Hf-Th-Ta (Wood, 1980). Figure 37b. Schematic showing important trends on the Hf-Th-Ta diagram, from Pearce (1996).

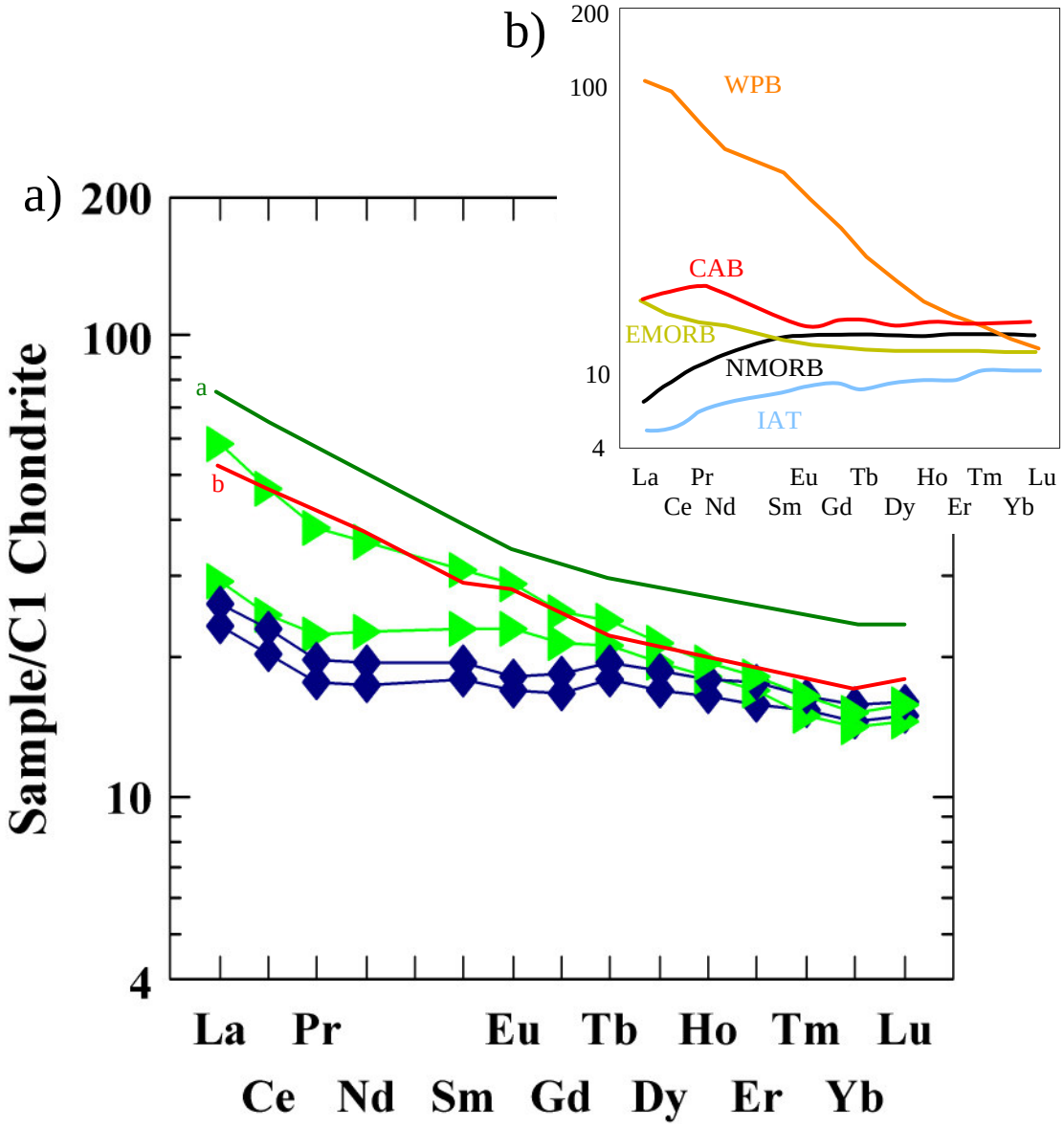


Volcanic Rocks. This Study

Hypabyssal Rocks. This Study.

a — Average Flaherty Formation Values, High Zr Rock. Legault, et al. (1994).

b — Average Flaherty Formation Values, Low Zr Rock. Legault, et al. (1994).

Figure 38a. Rare earth elements normalized relative to C1 Chondrite (values from Sun and McDonough, 1989). Figure 38b. Patterns of common basalt types shown for reference. Normalizing values for normal mid-ocean ridge basalt, enriched mid-ocean ridge basalt, and within-plate basalt are from Sun and McDonnough (1989). Normalizing values for calc-alkaline basalt and island arc tholeiite are from Pearce, et al. (1995).

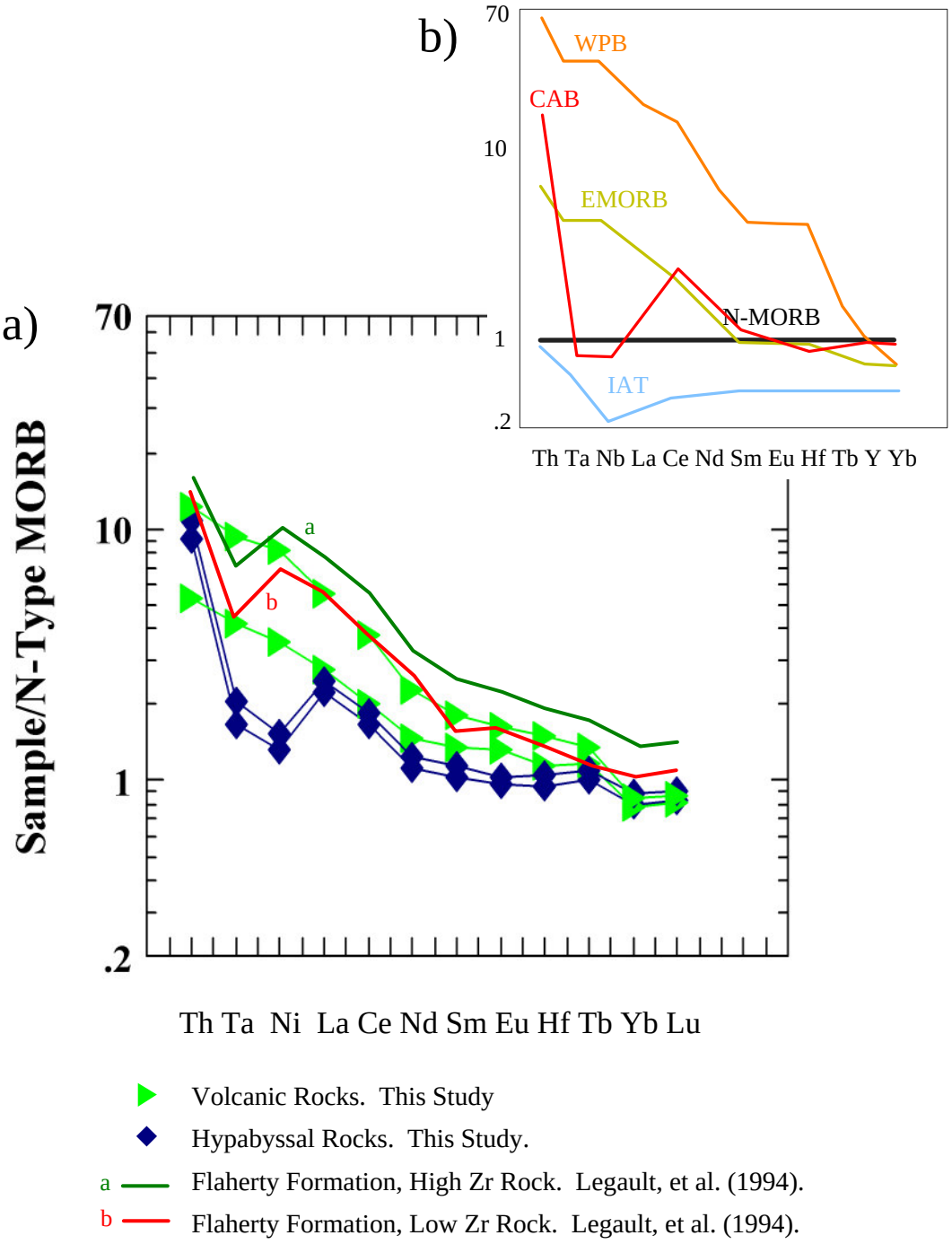


Figure 39a. Mid-ocean ridge basalt normalized spider diagram for the Flaherty Formation basalts. Element order is simplified from . Figure 39b. Patterns of common basalt types shown for reference. Normalizing values for normal mid-ocean ridge basalt, enriched mid-ocean ridge basalt, and within-plate basalt are from Sun and McDonnough (1989). Normalizing values for calc-alkaline basalt and island arc tholeiite are from Pearce, et al. (1995).

the Ta and Nb anomaly as caused by lower crustal granulites contaminating the source magmas through a process known as assimilation-fractional crystallization. Comparison of the Flaherty rocks with the Jonestown volcanic rocks (Fig. 39) shows that there is a significant Ta and Nb anomaly in the hypabyssal rocks of the Jonestown Volcanic Field.

This significant Ta and Nb anomaly in the coarse grained Jonestown rocks is similar in magnitude to the anomaly in the Eskimo Formation of the Belcher Islands (Fig. 40). Legault, et al. (1994) propose that the Eskimo Formation geochemistry is a result of incorporation of a significant component of continental lithosphere into the melt. This would help explain why rocks from a continental rift facies plot as calc-alkali basalt on a Hf-Th-Ta diagram (Fig. 41). Even though the Eskimo Formation likely represents a continental rift facies, which is likely not an analogous setting to the Jonestown volcanic rock setting, the rocks do show similar geochemical characteristics with respect to crustal contamination, and exhibit geochemical patterns similar to the Jonestown hypabyssal rocks.

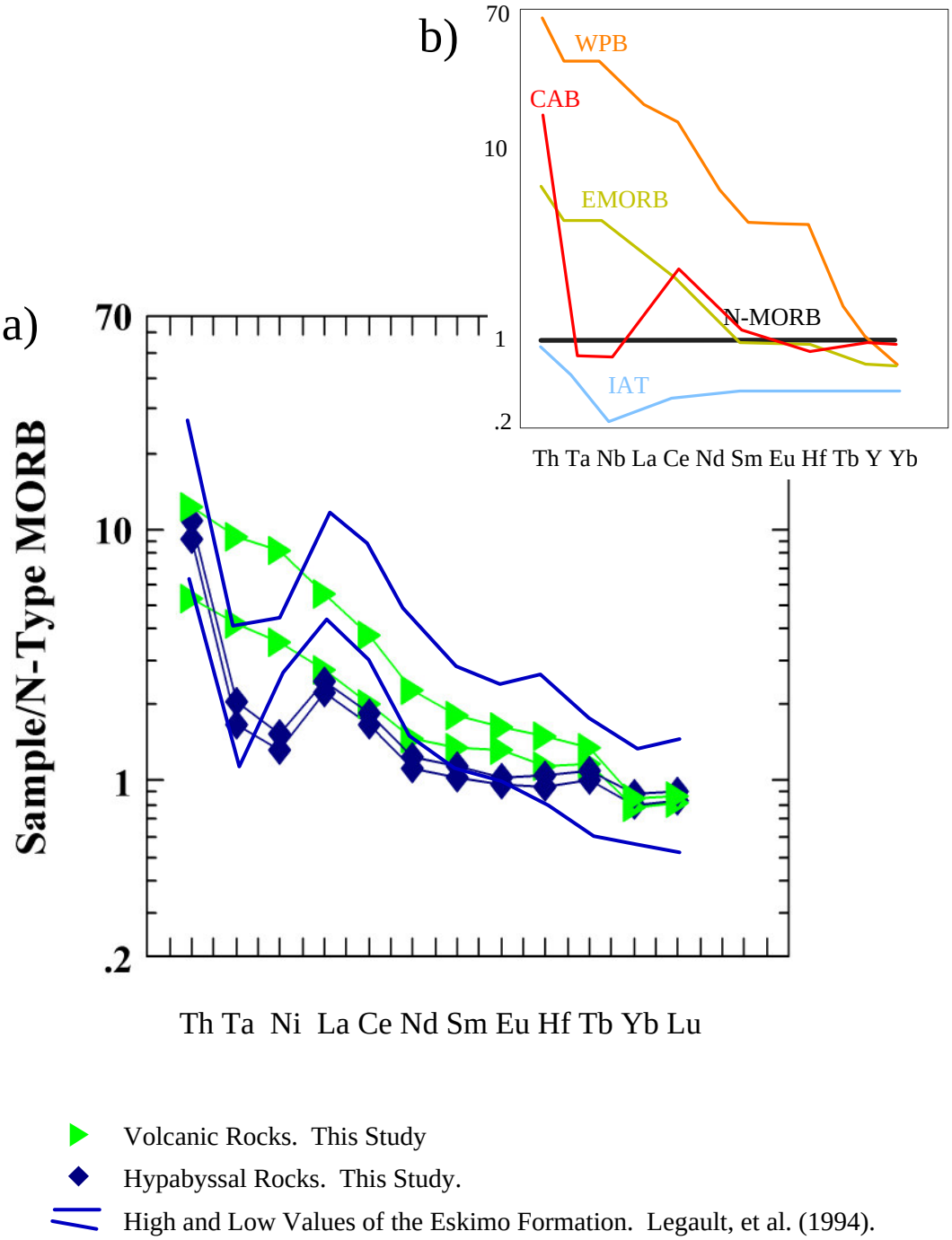


Figure 40a. Mid-ocean ridge basalt normalized spider diagram for the Eskimo Formation basalts. Element order is simplified from Legault, et al. (1994). Figure 40b. Patterns of common basalt types shown for reference. Normalizing values for normal mid-ocean ridge basalt, enriched mid-ocean ridge basalt, and within-plate basalt are from Sun and McDonnough (1989). Normalizing values for calc-alkaline basalt and island arc tholeiite are from Pearce, et al. (1995).

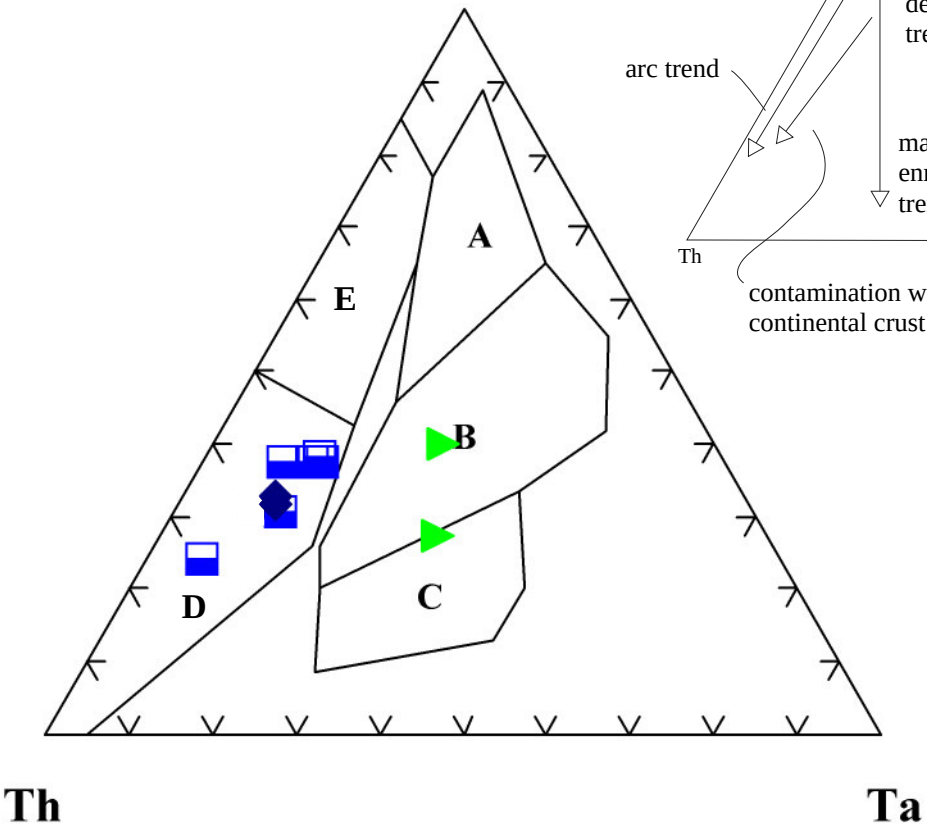


A Normal Mid-Ocean Ridge Basalt

B Enriched Mid Ocean Ridge Basalt and Tholeiitic Within Plate Basalt

C Within Plate Basalt

D Calc-Alkaline Basalt

E Island Arc Tholeiite

- Volcanic Rocks. This Study
- Hypabyssal Rocks. This Study.
- Eskimo Formation. Legault, et al. (1994).

Figure 41a. Hf-Th-Ta (Wood, 1980). Figure 41b. Schematic showing important trends on the Hf-Th-Ta diagram, from Pearce (1996).

# Chapter 6 Discussion

## Contacts Between Igneous and Sedimentary Rocks

A main point of this study was to determine the nature of the contacts between the igneous rocks and the clastic sedimentary rocks that occur in the bulk of the field area. Previous work (see Ganis, 1997 for summary) has assumed that the volcanic rocks in the Jonestown volcanic field are conformable to the clastic trench sedimentary rocks with which they presently occur. Lash (1986a) suggested that even though conformability had not been proved, there was little evidence of structural complication at those contacts. He suggested that this showed that the contacts were conformable, or that very little transport had been necessary to bring about the current juxtaposition of the flysch and the volcanics rocks.

This study has found no such conformable contacts, including no evidence of contact metamorphism and an absence of any indication of any intercalation of clastic sediments and the volcanics, between the igneous rocks and the trench sediments, and instead has found truncation of beds and intensified fracturing with slickensides near the contacts, suggesting there actually is significant structural complication. The structural effects at the contacts permit the idea that the igneous rocks could have been transported some distance relative to the trench sedimentary rocks.

The contacts between the basalt pillows and the massive limestone at Swatara Creek bridge show that the volcanics were extruded onto the limestone. Contacts between that limestone and the clastic trench sediments are not conformable. The massive limestone does not match descriptions of the thin-bedded limestones interbedded with the flysch, but rather fits the description of a shallow water carbonate deposited in an area with little to no clastic influence. Based on these findings, I

conclude that the Jonestown volcanic rocks were not emplaced into or on the sediments of the Hamburg Klippe, but were formed elsewhere, erupted on to the massive limestone, and volcanics and limestone were later juxtaposed with the flysch by thrusting.

It is important to note that the hypabyssal rocks are not associated with the massive limestone. Also, there are no known contacts between the hypabyssal rocks and the volcanic rocks. Therefore, not only is it possible that the igneous rocks have been transported a considerable distance relative to the sedimentary rocks, the coarse grained rocks could have been transported a considerable distance relative to the fine grained rocks. The relationship between the two sets of rocks is explored more in the discussion of the geochemistry.

## Structure and Deformation

The structure in the field area is complicated. Detailed mapping and stratigraphy in the eastern Hamburg Klippe (Lash and Drake, 1984) have shown that the red shale only occurs in a unit stratigraphically below the flysch (Fig. 8). These rock types are not interbedded. However, the red shale occurs throughout the field area, in the proximity of a variety of flysch rocks. Folding is not widespread in the field area, so it can not be invoked to explain the repetition of the shale. However, thrust fault horizons can preferentially propagate through mudstone or shale rather than sandstone. The pelagic red shale and mudstone could be one of these formations. The red shale could be a basal thrust horizon for the flysch rocks, and the repetition of the red shale suggests the thrust horizons could be repeated, and that the flysch rocks are imbricately thrust.

The igneous rocks are not associated with the red shale. Unlike the red shale, the igneous rocks occur in well defined belts up to one half of a kilometer wide. The rocks

in these belts are not intercalated with the flysch. The igneous rocks also do not occur repeatedly in the flysch like the red shale does. These observations suggest that the igneous rocks are not involved in the initial imbricate thrusting of the Hamburg Klippe sediments. If this is the case, then igneous rocks could not have been syndepositional with the flysch. The idea that the sedimentary rocks were initially deformed in an event that did not affect the igneous rocks, and that the Jonestown volcanic rocks could be an exotic lithology, implies that long distance transport was necessary to juxtapose the two rock types.

## Importance of the Bunker Hill Fault

The fault south of Bunker Hill is important, and warrants further discussion. The fault truncates the Bunker Hill sandstone. Since the Bunker Hill sandstone overlies the fine grained extrusive belt, the fault likely truncates those rocks as well. The Bunker Hill sandstone is interpreted to be an outlier of the Silurian Tuscarora Formation. The post-Taconic erosional unconformity lies below the Silurian Tuscarora Formation and its equivalent in eastern Pennsylvania, New Jersey, and New York, the Shawangunk Formation. Since the fault at Bunker Hills truncates this sandstone, it must be post Taconic.

There are three main post Taconic deformation events along the Appalachian orogen, the Acadian orogeny, the Alleghenian orogeny, and the rifting associated with the breakup of Pangea. There is no known Acadian deformation in this region of Pennsylvania, so the fault is not likely Acadian. The geometry of the Bunker Hills sandstone further constrains the age of faulting. The Bunker Hill sandstone is dipping south. If the fault were a normal fault, it is likely that a thrust fault or fold would repeat the sandstone somewhere in the Klippe. This is not the case, so the fault is not likely a

normal fault, and so is not likely caused by the Triassic rifting associated with the breakup of Pangea. Therefore, this fault must be Alleghenian, and therefore is likely a thrust. For this reason, it is shown as a thrust on the cross section (Plate 1).

## Note on the Origin of the Igneous Rocks

An important aspect of the idea that the igneous and sedimentary rocks did not form together is the fact that this allows the environment of formation of the igneous rocks to be outside the trench. This does not mean these rocks could have formed anywhere, for field study has shown the igneous rocks to be conformable to the limestone found at the base of the extrusive sequence. An understanding of the origin of the limestone could then lead to an understanding of the age and environment of formation of the igneous rocks.

## The Limestone

The age of the limestone at Swatara Creek bridge, therefore, needs to be understood in order to understand the history of the volcanic rocks. The only information concerning the age of that rock is in an abstract (Lash, 1984) stating that conodonts sampled from a block of limestone somewhere west of the railroad grade have been classified as North Atlantic province conodonts and dated as Late Tremadoc to Early Arenig, about 495 Ma (Lash, 1986c). The data used to make this conclusion has never been published in an article, however. Graptolite dates of the flysch sediments (Fig. 8) are upper Llandeilo to Lower Caradoc, about 476 to 471 Ma (Lash 1986c). This conodont date for the limestone is about twenty million years older than graptolite dates of the flysch (Fig. 8).

The preserved flysch sediments most likely record the timing of the collision between the Taconic arc and Laurentia. Bradley (1989) estimated the rate of

convergence between the Taconic arc and Laurentia to be 10 to 20 kilometers per million years. At this rate, the trench would have been 200 to 400 kilometers from Laurentia when the Jonestown volcanic rocks were forming. This distance is roughly equivalent to the distance between the trench and the Penghu islands when those basalts formed.

Outcrop characteristics of the limestone at the base of the pillow basalt sequence are visibly different than the characteristics of the other limestone found in the klippe. Given some uncertainty about the only known age discussed in published literature, it may be useful to compare these characteristics with other limestones in the region, those with well determined ages. The only known preserved Laurentian carbonate sequence from the time of Lash's (1984) date is the Beekmantown Group (Fig. 8), a Tremadoc to Llanvirn (Lash, 1986c) group in the Great Valley sequences. The Beekmantown group is described as comprised of dolostone throughout the section (Gray, et al., 1954). No dolostone, however, has been found in the limestones at the base of the pillow basalts. This would suggest, if Lash's (1984) date is correct, that the limestone at Swatara Creek Bridge was not deposited in the area of the Great Valley sequence Beekmantown Group.

The limestone in the Great Valley sequences with field descriptions most like the limestone at Swatara Creek bridge is the Annville Formation of the Lebanon Valley sequence (Fig. 8). The Annville Formation has an upper Llanvirn to Llandeilo age (Lash, 1986c). The Annville is a gray, massive, crystalline, high calcium (very little magnesian calcite or dolomite) limestone that weathers to smooth or fluted surfaces (Gray, et. al., 1954). The Lebanon Valley sequence, mainly carbonates, is interpreted as having formed on the Laurentian continental shelf inboard of the Taconic trench (Drake, et al., 1989).

Regardless of the age of the limestone at Swatara Creek bridge or which local unit it might correlate to, the field descriptions of it point to its environment of formation. It is a massive to thick bedded high calcium limestone, and there is no evidence of any clastic input. The limestone occurs in a belt of Ordovician rocks. Assuming this limestone is not remarkably exotic, two places where it could have formed are on the Laurentian carbonate shelf shortly before Taconic collision, or on a seamount in the Taconic (Iapetus) ocean at an earlier time.

## Whole Rock Geochemistry

The association between the limestone and the igneous rocks is informative, and helps constrain the probable environment of eruption to two possible environments, but it can not differentiate between the two. The results from the geochemical analysis can add some independent information.

The discrimination diagrams selected for this paper show that the two volcanic rocks plot in mid-ocean ridge basalt and within-plate basalt fields (Fig. 22- Fig. 28). The hypabyssal rocks are not as consistent as the fine grained rocks, but they mainly plot in or close to the boundaries of the mid-ocean ridge basalt and within-plate basalt fields (Fig. 22- Fig. 28). The Th-Ta-Hf diagram (Wood, 1980) (Fig. 25), while showing the volcanic rocks to be enriched MORB or within plate basalt, indicates that the hypabyssal rocks are island-arc tholeiite. However, the rocks also plot in an area that is consistent with continental contamination of mid-ocean ridge basalt. On the Nb-Zr-Y diagram (Meschede, 1986) (Fig. 26), the volcanic rocks plot in the Enriched MORB field. The hypabayssal rocks plot in the normal mid-ocean ridge basalt field. However, if the hypabyssal rocks had Nb levels similar to the volcanic rocks, they would also plot in the enriched mid-ocean ridge basalt field.

The plot of the samples on a mid-ocean ridge basalt normalized spider diagram (Fig. 27) highlights the different Ta and Nb values between the volcanic and hypabyssal rocks. The volcanic rocks have a pattern most like enriched mid-ocean ridge basalt. Aside from the significantly depleted Ta and Nb values, the hypabyssal rocks also are similar to enriched mid-ocean ridge basalt. The rare earth element abundances and ratios (Fig. 28) are similar for both the intrusive and the extrusive rocks, except for HK-43. HK-43 has slightly higher values of light rare earth elements than do the other three rocks. It should be pointed out that HK-43 was the freshest sample found in the project, so those values may be the closest to the values in the original fresh rock.

## Comparisons Between the Jonestown Rocks and the Analogues

### Karacalidag

The basalt discrimination diagrams show the basalts from Karacalidag are comparable to typical within plate basalts (Fig. 33-35). These results vary from the ones of the Jonestown volcanic rocks. Perhaps this is a result of the significant difference that Karacalidag is a convergent environment between continental lithosphere only, whereas the Jonestown environment is more likely one between a continental foreland and an island arc, presumably on oceanic crust.

### Penghu Islands

The Penghu Island basalts are not one uniform rock type. Specifically, discrimination diagrams (Fig. 33-35) show two suites, alkali within plate basalts quite similar to the Karacalidag basalts, and tholeiitic basalts that are similar to enriched mid-ocean ridge basalt. The mid-ocean ridge basalt normalized spider digram and rare earth element pattern of the tholeiites is quite similar to that of sample HK-43 from this study, and somewhat similar to the other samples from this study. The inferred distances

between the trench and the continental platform are similar. The environments could therefore be analogous. The Jonestown volcanics could have formed in a tensional environment on the foreland similar to the one in which the Penghu basalts were generated.

## Belcher Islands

Comparison of the Jonestown rocks to the Belcher Island basalts on a mid-ocean ridge basalt normalized spider diagram shows there are differences between the volcanic rocks and the hypabyssal rocks. The fine grained rocks compare favorably with the Flaherty formation (Fig. 39), both in element abundances and ratios. This is in accordance with field relations suggesting that the Jonestown volcanic rocks formed on a continental foreland. The hypabyssal rocks, however, have Ta and Nb depletions similar to the Ta and Nb depletions in the Eskimo formation (Fig. 41). Legault, et al. (1994) attribute the Ta and Nb depletion in the Eskimo Formation to significant interaction between the magma and continental lithosphere. This potential continental influence suggests the hypabyssal Jonestown rocks also formed on a continental foreland. The suggestion that these rocks formed on a foreland largely precludes the possibility that these rocks formed on a distant seamount in the Taconic (Iapetus) ocean.

## Differences Between Coarse Grained Rocks and Fine Grained Rocks

The consensus of previous work (Herting and Wright, 1977; Lash, 1986a) has been that the volcanic and hypabyssal rocks in the Jonestown volcanic field have a common history from genesis to emplacement to deformation and current juxtaposition. The fact that the two suites of rocks currently occur adjacent to each other can not be ignored. It is true that the hypabyssal rocks have not been shown to be associated with the limestone, and into exactly what they intruded is unclear. However, the difference

between them for Ta and Nb may be most significant. It shows that the magma for the two rock types either was not generated in the exactly the same place or that it did not share the same history after it was generated. Given their current proximity and location in the Taconic belt, the fact that both suites are exotic to the Hamburg Klippe, and the similarities in major element and many minor element abundances, it is unlikely that the differences between the volcanic rocks and the hypabyssal rocks were caused by great spatial differences. More likely, the rocks, and the magmas that generated them, are probably only separated by a either a reasonably small distance, perhaps on the order of a few tens of kilometers or less, or a reasonably small amount of time, perhaps a few million years or less. The volcanic rocks could have been erupted when the magma was formed, while the magma that produced the hypabyssal rocks could have spent some amount of time interacting with continental lithosphere before being emplaced.

## Chapter 7 Synthesis and Conclusions

This study makes the following conclusions about the geological relations and history of the igneous rocks in the Jonestown volcanic field.

Detailed analysis of the contacts between the igneous rocks and the sedimentary rocks has revealed: 1) The volcanic rocks, specifically the pillow basalts, can be shown to be conformable to the massive limestone that occurs stratigraphically below them. However, this massive limestone is not conformable to the sedimentary rocks of the Hamburg Klippe. The association between the massive limestone and the pillow basalts suggests the pillow basalts were extruded onto a carbonate bank. 2) The hypabyssal rocks can not be shown to be conformable to any other rocks in the field area. There are no known contacts between the hypabyssal rocks and the massive limestone or the hypabyssal rocks and the volcanic rocks. It is unclear what lithology was originally intruded by the hypabyssal rocks.

A study of the whole rock geochemistry of the igneous rocks shows: 1) The rare earth element patterns of the volcanic rocks are similar to the patterns of basalts extruded in extensional environments in foreland settings of collisional belts. The rare earth element pattern of HK-43, the fresher of the two extrusive rock samples is nearly identical to these foreland basalts. 2) The trace elements Ta and Nb show that the source magma for the coarse grained rocks probably had some significant continental contamination. 3) While the coarse grained and fine grained rocks differ significantly in their Ta and Nb patterns, they have similar abundances of major elements and many trace elements, and could have formed in the same magmatic province.

These conclusions suggest that the igneous rocks of the Jonestown volcanic field originated on the Laurentian carbonate shelf around the time the Laurentian margin

evolved from a passive margin (deposition of carbonates) to a continental foreland basin coincident with the arrival of the Taconic trench (deposition of flysch). Magma genesis could have been related to tensional stresses normal to the approaching Taconic allochthon. The timing of the igneous activity (Fig. 42) is intimately related to the uncertain age of the Limestone at Swatara Creek bridge (Lash, 1984). If the late Tremadoc to Early Arenig date suggested by Lash (1984) is correct, then the pure carbonate limestone represents a lithology not previously known on the Laurentian margin at that time, and suggests that the volcanics erupted on a seamount. If the date is wrong, then it is quite likely that the pure carbonate limestone is the upper Llanvirn to Llandeilo Annville Formation, and magmatism would have roughly been coeval with the Llandeilo to Caradoc deposition of the preserved flysch of the Hamburg Klippe. In this scenario, the limestone and volcanics are erosional remnants resting on a low angle thrust above the flysch sediments of the Hamburg Klippe (Fig. 43).

The structural geology of the field area is complex. The initial imbricate thrusting of the flysch likely occurred during the Taconic Orogeny, during emplacement of the flysch on the Laurentian margin. Continued thrusting could have led to the juxtaposition of the flysch and the igneous rocks. Thrusting during the Alleghanian orogeny truncated the southern margin of the fine grained rocks, and placed the coarse grained rocks structurally above them.

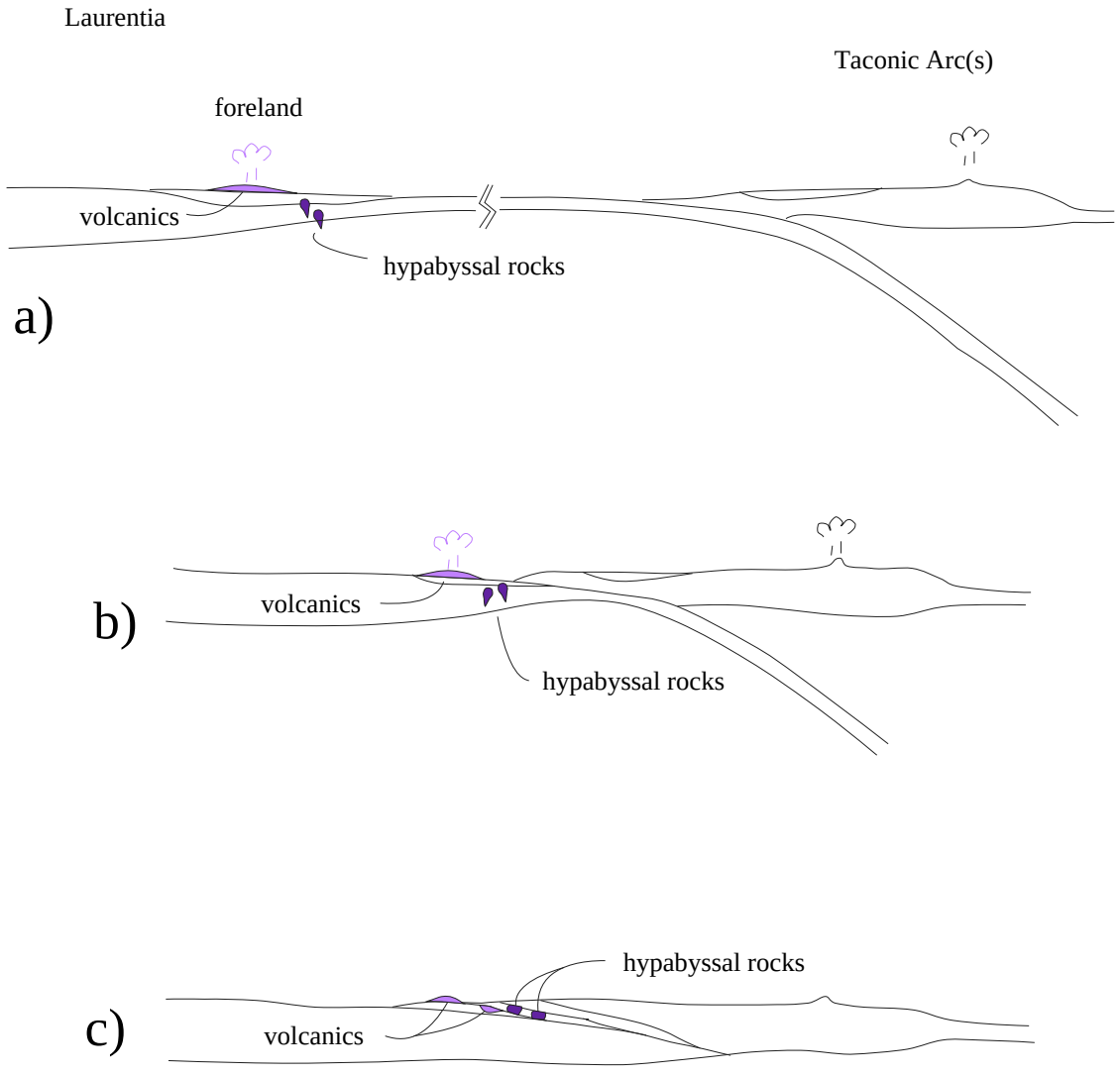


Figure 42. Series of simple sketches suggesting a history of emplacement and subsequent juxtaposition of the Jonestown igneous rocks. Timing of the volcanism on the Laurentian foreland is not precisely constrained, and the volcanic rocks and the hypabyssal rocks may have formed either during the time represented in Figure 42a or the time represented in Figure 42b. The subsequent juxtaposition of the hypabyssal and the volcanic rocks is shown in Figure 42c. Overall geometry of the Taconic convergence based on Bradley and Kidd (1991). Not to scale.

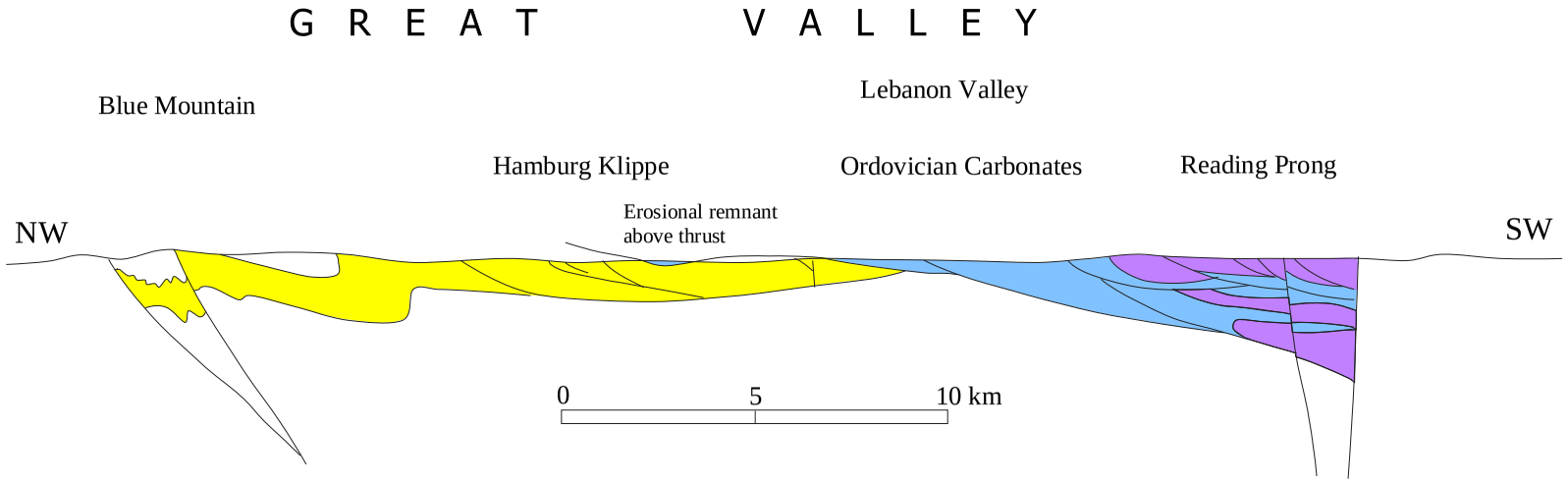


Figure 43. Generalized cross section (from Berg, 1980) of the Great Valley- Hamburg Klippe (in Yellow), Ordovician carbonates (in Blue) and Reading Prong (in purple). The section shows a scenario where the limestones (and associated volcanic rocks) are an erosional remnant of one of the thrust sheets ofOrdovician carbonate in the Lebanon valley. In this scenario, the limestones would rest in the only true klippe in the field area. No vertical exageration.

## References Cited


Alterman, I. B., 1972, Structure and history of the Taconic allochthon and surrounding a autochthon, east-central Pennsylvania (Ph.D. thesis): New York, Columbia University, 287p.

Angelier, J., Bergerat, F., Chu, H. T., Juang, W. S., and Lu, C. Y., 1990, Paleostress analysis as a key to margin extension: The Penghu Islands, South China Sea: Tectonophysics, v. 183, p. 161-176.

Ballard, R. D. and Moore, J. G., 1977, Photographic Atlas of the Mid-Atlantic Ridge Rift Valley: New York, Sringer-Verlag, 114p.

Berg, T. M., Edmunds, W. E., Geyer, A. R., Glover, A. D., Hoskins, D. M., MacLachlan, D. B., Root, S. I., Sevon, W. D., Socolow, A. A., 1980, Geologic map of Pennsylvania, 1980: Pennsylvania Topographical and Geological Survey, Harrisburg, PA, United States.

Bradley, D. C., 1989, Taconic plate kinematics as revealed by foredeep stratigraphy, Appalachian orogen: Tectonics, v. 8, p. 1037-1049.

Bradley, D. C. and Kidd, W. S. F., 1991, Flexural extension of the upper continental crust in collisional foredeeps: Geological Society of America Bulletin, v. 103, p. 1416-1438.

Bricker, O., 1960, Ordovician volcanics of the Bunker Hills, Lebanon County, Pennsylvania, *in:* Wise, D. U., and Kauffman, M. E., eds., Some tectonic and structural problems of the Appalachian piedmont along the Susquehanna River: 25th Field Conference of Pennsylvania Geologists, p.92-99.

Chapple, W. M., 1973, Taconican Orogeny: Abortive subduction of the North American continental plate?: Geological Society of America Abstracts with Programs, v. 11, p. 7.

Chen, J. C., 1988, Geochemistry of Basalts from the Niu-Hsin Shan area, Penghu Islands: Proceedings of the Geological Society of China, v. 31, p. 53-66.

Cotter, E., 1983, Shelf, paralic, and fluvial environments and eustatic sea-level fluctuations and the origin of the Tuscarora Formation (Lower Silurian) of central Pennsylvania: Journal of Sedimentary Petrology, v. 53, p. 25-49.

Devey, C. W., and Cox, K. G., 1987, Relationships between crustal contamination and crystallization in continental flood basalt magmas with special reference to the Deccan Traps of the Western Ghats, India: Earth and Planetary Science Letters, v. 84, p. 59-68.

Drake, A. A., Jr., Sinha, A. K, Laird, J., and Guy, R. E., 1989, The Taconic Orogen, *in* Hatcher, R. D., Jr., Thomas, W. A., and Viele, G. W., eds., The Appalachian Ouachita Orogen in the United States, The Geology of North America, v. F-2: Boulder, Colorado, Geological Society of America, , 767p.

Francheteau, J., Needham, D., Juteau, T., and Rangin, C., 1980, Naissance d'un Ocean Sur la Dorsale du Pacifique Est: Paris, Centre National pour l'Exploitation des Oceans, 87p.

Ganis, G. R., 1997, ed., Notes on the Hamburg klippe: Biostratigraphy, ash layers, olistostromes and "exotics": 16th Annual Harrisburg Area Geological Society Field Trip, 52 p.

Ganis, G. R., Williams, S. H., and Repetski, J. E., 2001, New biostratigraphic Information from the western part of the Hamburg klippe, Pennsylvania, and its Significance for interpreting the depositional and tectonic history of the klippe: Geological Society of America Bulletin, v. 113, p. 109-128.

Greenough, J. D., Lee, C.-Y., and Fryer, B. J., 1999, Evidence for volatile-influenced differentiation in a layered alkali basalt flow, Penghu Islands, Taiwan: Bulletin of Volcanology, v. 60, p. 412-424.

Gordon, S. G., 1920, Ordovician basalts and quartz diabases in Lebanon County, Pennsylvania: Proceedings of the Academy of Natural Sciences of Philadelphia, v. 72, p. 354-357.

Gray, C., Moseley, J. R., and McLaughlan, D. B., 1954, Summary of the regional geology, *in* Author Unknown, Guidebook: 20th Annual Field Conference of Pennsylvania Geologists: Pennsylvania Geological Survey, p. 1-13.

Hack J, T., 1989, Geomorphology of the Appalachian highlands, *in* Hatcher, R. D., Jr., Thomas, W. A., and Viele, G. W., eds., The Geology of North America, Volume F-2, The Appalachian-Ouachita Orogen in the United States, Boulder, Colorado, Geological Society of America, 767p.

Herting, D. A., and Wright, T. O., 1977, Geochemistry and tectonic implications of the Jonestown volcanic rocks: Proceedings of the Pennsylvania Academy of Science, v. 51, p. 150-152.

Hoffman, P. F., 1987, Early Proterozoic foredeeps, foredeep magmatism, and Superior-type iron formations of the Canadian Shield, *in* Kroner, A., ed., Proterozoic lithosphere evolution: Geodynamics Series, American Geophysical Union, v. 17, p. 85-98.

Holzer, 1977, D. B., Soil Survey of Lebanon County, Pennsylvania: US Department of Agriculture, 155p.

Johnson, D. M., Hooper, P. R., and Conrey, R. M., 1999, XRF analysis of rocks and minerals for major and trace elements on a single low dilution Li-tetraborate fused bead: Advances in X-ray Analysis, v. 41, p. 843-867.

Juang, W. S., and Chen, J. C., 1992, Geochronology and geochemistry of Penghu basalts, Taiwan Strait and their tectonic significance: Journal of Southeast Asian Earth Sciences, v. 7, p. 185-193.

Kidd, W. S. F., Plesch, A., and Vollmer, F. W., 1995, Lithofacies and structure of the Taconic flysch, melange, and allochthon, in the New York capital district, *in:* Garver, J. I. and Smith, J. A., eds., Field Trips for the 67th annual meeting of the New York State Geological Association, p. 57-80

Lash, G. G., 1984, The Jonestown volcanic rocks, eastern Pennsylvania, near-trench volcanism in the central Appalachians: Geological Society of America (abstracts with Programs), v. 16, p. 46.

Lash, G. G., 1985, Accretion-related deformation of an ancient (early Paleozoic) trench fill deposit, central Appalachian orogen: Geological Society of America Bulletin, v. 96, p.1167-1178.

Lash, G. G., 1986a, Sedimentologic and geochemical evidence for middle Ordovician near-trench volcanism in the central Appalachian orogen: Journal of Geology, v. 94, p. 91-107.

Lash, G. G., 1986b, Sedimentology of channelized turbidite deposits in an ancient (early Paleozoic) subduction complex, central Appalachians: Geological Society of America Bulletin, v. 79, p. 703-710.

Lash, G. G., 1986c, Anatomy of an early Paleozoic subduction complex in the central Appalachian orogen: Sedimentary Geology, v. 51, p.75-95.

Lash, G. G. and Drake, A. A., Jr., 1984, The Richmond and Greenwhich slices of the Hamburg klippe in eastern Pennsylvania- Stratigraphy, structure and plate tectonic implications: U. S. Geological Survey Professional Paper 1312, 40 p.

Legault, F., Francis, D., Hynes, A., and Budkewitsch, 1994, Proterozoic continental volcanism in the Belcher Islands: implications for the evolution of the Circum Ungava Fold Belt: Canadian Journal of Earth Sciences, v. 31, p. 1536-1549.

Meschede, M. 1986, A method of discriminating between different types of mid-ocean ridge basalts and continental tholeiites with the Nb-Zr-Y diagram: Chemical Geology, v. 56, p. 207-218.

Mouthereau, F., Lacombe, O., Deffontaines, B., Angelier, J., and Brusset, S., 2001, Deformation history of the southwestern Taiwan foreland thrust belt: insights from tectono-sedimentary analyses and balanced cross-sections: Tectonophysics, v. 333, p. 293-322.

NURE map JGM-261,1978, NOAA.

Pearce, J. A., 1980, Geochemical evidence for the genesis and eruptive setting of lavas from Tethyan ophiolite, *in* Panayiotou, A., ed, Ophiolites: Proceedings of the International Ophiolite Symposium, Nicosa, Cyprus, p. 261-282.

Pearce, J. A., 1982, Trace Element characteristics of lavas from destructive plate boundaries, *in*: Thorpe, R. S., ed., Andesites: John Wiley and Sons, Chichester, p. 525-547.

Pearce, J. A., 1996, A user's guide to basalt discrimination diagrams, *in:* Wyman, D. A., ed., Trace Element Geochemistry of Volcanic Rocks: Applications for Massive Sulfide Exploration: Geological Association of Canada, Short Course Notes, v. 12, p. 79-113.

Pearce, J. A. and Cann, J. R., 1973, Tectonic setting of basic volcanic rocks determined using trace element analysis: Earth and Planetary Science Letters, v. 19, p. 290-300.

Pearce, J. A., Bender, J. F., DeLong, S. E., Kidd, W. S. F., Low, P. J., Guner, Y., Saroglu, F., Yilmaz, Y., Moorbath, S., and Mitchell, J. G., 1990, Genesis of Collision volcanism in Eastern Anatolia, Turkey: Journal of Volcanology and Geothermal Research, v. 44, p. 189-229.

Pearce, J. A., Baker, P. E., Harvey, P. K., and Luff, I. W., 1995, Geochemical evidence for subduction fluxes, mantle melting and fractional crystallization between the South Sandwich island arc: Journal of Petrography, v. 36, p. 1073-1109.

Root and MacLachlan, 1978, Western limit of Taconic allochthons in Pennsylvania: Geological Society of America Bulletin, v. 89, p. 1515-1528.

Rowley, D. B. and Kidd., W. S. F., 1981, Stratigraphic relationships and detrital composition of the Middle Ordovician flysch of western New England: Implications for the tectonic evolution of the Taconian Orogeny: Journal of Geology, v. 89, p. 199-218.

Sengor, A. M. C., Burke, K, and Dewey, J., 1978, Rifts at high angles to orogenic belts: tests for their origin and the upper Rhine graben as an example: American Journal of Science, v. 278, p. 24-40.

Shervais, J. W., 1982, Ti-V plots and the petrogenesis of modern and ophiolitic lavas: Earth and Planetary Science Letters, v. 59, p.101-118.

Smith, R. C. II, and Barnes, J. H., 1994, Geochemistry and geology of metabasalt in southeastern Pennsylvania and adjacent Maryland, *in:* Faill, R. T. and Sevon., W. D., eds., Various aspects on Piedmont Geology in Lancaster and Chester counties, Pennsylvania: 59th Field Conference of Pennsylvania Geologists, p. 45-72.

Stanley, R. and Ratcliffe, N., 1985, Tectonic synthesis of the Taconian Orogeny in western New England: Geological Society of America Bulletin, v. 96, p. 1227-1250.

Stose, G. W., 1946, The Taconic sequence in Pennsylvania: American Journal of Science, v. 244, p. 665-696.

Stose, G. W., and Jonas, A. I., 1927, Ordovician shale and associated lava in Southeastern Pennsylvania: Geological Society of America Bulletin, v. 38, p. 505-536.

Sun, S. S., and McDonough, W.F., 1989, Chemical and isotopic systematics of oceanic basalts, implications for mantle composition and processes, *in:* Saunders, A. D., and Norry, M. J., eds., Magmatism in Ocean Basins, Geological Society Special Publication No. 42, p. 313-345.

Suppe, J. 1980, A retrodeformable cross section of northern Taiwan: Proceedings of the Geological Society of China, n. 23, p. 46-55.

Taylor, B, and Hayes, D. E., 1983, Origin and History of the South China Sea Basin, *in* Hayes, D. E., ed., The Tectonic Evolution of Southeast Asian Seas and Islands: Part 2, Geophysical Monograph Series, American Geophysical Union, v. 27, p. 23-56.

Urry, W. D., 1936, Ages by the Helium method: II. Post-Keweenawan: Geological Society of America Bulletin, v. 47, p. 1217-1234.

Vollmer, F. W., and Bosworth, W., 1984, Formation of melange in a foreland basin overthrust setting: example from the Taconic Orogen, *in:* Raymond, L. A., ed., Melanges: their nature, origin and Significance, Geological Society of America Special Paper 198, p. 53-70.

Winchester, J. A. and Floyd, P. A., 1976, Geochemical magma type discrimination; application to altered and metamorphosed basic igneous rocks: Earth and Planetary Science Letters, v.28, p. 459-469.

Wood, D. A., 1980, The application of a Th-Hf-Ta diagram to problems of tectonomagmatic classification and to establishing the nature of crustal contamination of basaltic lavas of the British Tertiary volcanic province: Earth and Planetary Science Letters, v. 50, p. 11-30.

Yardley, B. W., 1989, An Introduction to Metamorphic Petrology, Pearson Education Ltd., Harlow, England, 248 p.

Zen, E., 1974, Prehnite- and pumpellyite bearing mineral assemblages, west side of the Appalachian metamorphic belt, Pennsylvania to Newfoundland: Journal of Petrology, v. 15, p. 197-242.

# Appendix A

## Whole Rock Geochemical Data From Other Studies of the Jonestown Volcanic Field.

Table II
Whole Rock Geochemical Data from Herting and Wright (1977)

| | Hypabyssal Rocks | | | | | | | | | | Volcanics | |
|---|---|---|---|---|---|---|---|---|---|---|---|---|
| | HW-1 | HW-4 | HW-7 | HW-8 | HW-15 | HW-23 | HW-25 | HW-35 | HW-36 | HW-37 | HW-16 | HW-22 |
| $SiO_2$ | 47.06 | 45.50 | 47.05 | 45.90 | 47.01 | 48.77 | 46.88 | 45.11 | 47.38 | 45.8 | 48.85 | 49.79 |
| $Al_2O_3$ | 12.72 | 13.24 | 12.86 | 13.15 | 12.50 | 13.33 | 12.94 | 12.94 | 13.00 | 13.39 | 12.30 | 11.83 |
| $Ti0_2$ | 1.00 | 1.17 | 1.11 | 0.75 | 1.27 | 0.94 | 0.79 | 0.84 | 1.03 | 1.23 | 1.69 | 1.19 |
| $Fe_2O_3$* | 10.87 | 10.92 | 10.62 | 9.81 | 10.77 | 9.51 | 9.74 | 9.15 | 9.68 | 8.83 | 9.71 | 10.97 |
| MnO | 0.19 | 0.20 | 0.21 | 0.18 | 0.23 | 0.21 | 0.20 | 0.21 | 0.22 | 0.19 | 0.24 | 0.24 |
| MgO | 6.84 | 6.88 | 6.36 | 7.85 | 5.89 | 7.19 | 7.95 | 7.56 | 6.36 | 7.35 | 6.47 | 5.13 |
| CaO | 12.66 | 9.85 | 9.20 | 10.39 | 8.29 | 10.53 | 9.98 | 10.04 | 10.04 | 10.90 | 6.24 | 7.78 |
| $Na_2O$ | 1.52 | 1.73 | 1.75 | 1.82 | 1.70 | 1.53 | 1.50 | 1.63 | 1.81 | 1.92 | 2.92 | 2.12 |
| $K_2O$ | 0.71 | 0.85 | 0.83 | 0.71 | 0.75 | 0.58 | 0.76 | 0.61 | 0.81 | 0.67 | 0.43 | 0.47 |
| $P_2O_5$ | 0.33 | 0.33 | 0.31 | 0.31 | 0.26 | 0.38 | 0.36 | 0.34 | 0.34 | 0.39 | 0.23 | 0.28 |
| | | | | | | | | | | | | |
| Zr | 106 | 103 | 185 | 208 | 181 | 140 | 136 | 127 | 122 | 132 | 219 | 152 |
| V | 113 | 132 | 130 | 91 | 151 | 141 | 123 | 129 | 149 | 166 | 197 | 172 |
| Sr | 326 | 290 | 363 | 272 | 235 | 144 | 308 | 290 | 235 | 490 | 308 | 272 |
| Cr | 179 | 69 | 121 | 329 | 29 | 129 | 240 | 277 | 130 | 173 | 212 | 44 |
| Ni | 108 | 110 | 90 | 140 | 93 | 104 | 158 | 116 | 84 | 105 | 160 | 60 |

Table II. Whole rock major and trace element data of Herting and Wright (1977). Sample numbers HW-16 and HW-22 are volcanic, while the rest of the samples are hypabyssal.

Table III
Whole Rock Geochemical data from Lash (1986a).

| | Hypabyssal Rocks | | | | | | | | | | | | Volcanic Rocks | | | | |
|---|---|---|---|---|---|---|---|---|---|---|---|---|---|---|---|---|---|
| | GL-3 | GL-9 | GL-11 | GL-12 | GL-14 | GL-17 | GL-21 | GL-23 | GL-29 | GL-31 | GL-33 | GL-37 | GL-40 | GL-10b | GL-22b | GL-27b | GL-43b |
| $SiO_2$ | 51.78 | 50.32 | 51.89 | 51.48 | 51.49 | 51.55 | 50.46 | 50.84 | 50.15 | 51.32 | 51.60 | 51.59 | 47.71 | 51.22 | 50.15 | 51.52 | 51.92 |
| $Al_2O_3$ | 13.75 | 15.54 | 13.80 | 14.01 | 14.31 | 13.89 | 13.22 | 13.41 | 16.11 | 14.41 | 14.66 | 14.29 | 15.84 | 13.34 | 13.78 | 13.87 | 14.35 |
| $Fe_2O_3$* | 14.00 | 10.34 | 13.18 | 12.83 | 11.71 | 11.57 | 16.66 | 16.33 | 10.43 | 13.17 | 11.92 | 13.02 | 10.15 | 14.32 | 15.41 | 14.22 | 13.24 |
| MgO | 5.86 | 8.27 | 6.65 | 7.00 | 7.65 | 7.45 | 6.04 | 6.36 | 8.53 | 7.05 | 7.70 | 7.13 | 7.29 | 5.99 | 7.13 | 5.92 | 6.79 |
| CaO | 10.08 | 12.18 | 10.31 | 10.76 | 10.42 | 11.14 | 9.49 | 8.47 | 11.76 | 10.09 | 10.20 | 10.41 | 13.85 | 9.94 | 9.93 | 10.32 | 9.83 |
| $Na_2O$ | 1.99 | 1.72 | 1.98 | 1.85 | 2.33 | 2.35 | 1.45 | 1.72 | 1.30 | 1.72 | 1.72 | 1.50 | 2.44 | 2.58 | 1.29 | 2.16 | 1.66 |
| $K_2O$ | 0.78 | 0.60 | 0.69 | 0.57 | 0.89 | 0.75 | 0.86 | 1.04 | 0.81 | 0.84 | 1.03 | 0.71 | 0.88 | 0.83 | 0.74 | 0.44 | 0.83 |
| $TiO_2$ | 1.43 | 0.79 | 1.20 | 1.19 | 1.01 | 1.04 | 1.36 | 1.45 | 0.70 | 1.10 | 0.91 | 1.07 | 1.52 | 1.41 | 1.18 | 1.23 | 1.08 |
| MnO | 0.21 | 0.17 | 0.20 | 0.20 | 0.19 | 0.18 | 0.23 | 0.25 | 0.16 | 0.20 | 0.19 | 0.19 | 0.14 | 0.23 | 0.22 | 0.22 | 0.21 |
| $P_2O_5$ | 0.12 | 0.07 | 0.10 | 0.11 | 0.09 | 0.08 | 0.23 | 0.13 | 0.05 | 0.10 | 0.07 | 0.09 | 0.18 | 0.14 | 0.17 | 0.10 | 0.09 |
| | | | | | | | | | | | | | | | | | |
| Cr | 150 | 251 | 150 | 73 | 100 | 121 | 107 | 215 | 537 | 199 | 443 | 213 | 355 | 173 | 118 | 89 | 214 |
| V | 277 | 224 | 303 | 275 | 249 | 274 | 308 | 282 | 198 | 299 | 260 | 288 | 222 | 263 | 343 | 328 | 279 |
| Rb | 10 | 16 | 15 | 23 | 21 | 17 | 22 | 17 | 15 | 14 | 15 | 13 | 4 | 21 | 20 | 3 | 15 |
| Sr | 262 | 204 | 401 | 191 | 250 | 233 | 181 | 224 | 496 | 193 | 234 | 202 | 222 | 351 | 312 | 279 | 208 |
| Y | 25 | 30 | 29 | 23 | 22 | 20 | 25 | 22 | 21 | 27 | 23 | 22 | 24 | 26 | 30 | 25 | 23 |
| Zr | 115 | 131 | 110 | 119 | 116 | 114 | 90 | 76 | 73 | 87 | 75 | 77 | 105 | 122 | 101 | 95 | 84 |
| Ba | 153 | 225 | 34 | 181 | 91 | 102 | 243 | 109 | 132 | 52 | 201 | 141 | 79 | 170 | 220 | 271 | 181 |
| Nb | 8 | 10 | 8 | 4 | 6 | 7 | 5 | 4 | 8 | 6 | 7 | 5 | 12 | 9 | 8 | 7 | 6 |
| Ce | 13 | 6 | 10 | 17 | 21 | 9 | 14 | 13 | 4 | 11 | 10 | 2 | 3 | 14 | 19 | 32 | 12 |

Table III. Whole rock geochemical data collected by Lash (1986a). Major elements are in weight percent, minor elements are in ppm. Samples with the suffix b are volcanic, the rest are hypabyssal.

Table IV.
Whole Rock Geochemical Data from Smith and Barnes (1994).

| | SB-1 | SB-2 | SB-3 |
|---|---|---|---|
| $TiO_2$ | 1.90 | 1.48 | 1.10 |
| V | 300 | 270 | 310 |
| Y | 36 | 24 | 22 |
| Zr | 150 | 95 | 66 |
| Nb | 12 | 14 | 5 |
| Ce | 19 | 16 | 11 |
| Hf | 2.7 | 2 | 1.6 |
| Ta | 0.4 | 0.5 | <0.1 |
| Th | 0.6 | 0.6 | 0.8 |
| U | <0.5 | <0.5 | <0.5 |
| Ni | 220 | 190 | 95 |
| La | 7.4 | 6.9 | 4.4 |

Table IV. Whole rock geochemical data gathered by Smith and Barnes (1994) on the Jonestown rocks. $TiO_2$ reported in weight percent and all other elements reported in ppm. SB-1 and SB-2 are pillow fragments. SB-3 is a hypabyssal rock.

# Appendix B

Thin Section Descriptions of Selected Rocks.

HK-11b2

Primary Minerals:

Plagioclase ($An_{55}$-$An_{60}$)- 30%, Clinopyroxene- 25%,
Phenocrysts replaced with serpentine, likely originally Olivine- 10%.
Quartz and untwinned Feldspar in Graphitic Texture- 15%.

Secondary Minerals:

Opaque mineral, 5%, Amphibole replacing Clinopyroxene, <5%,
Pumpellyite in groundmass, <5%.

Crystallization Order:

Olivine (or Orthopyroxene), Plagioclase, Clinopyroxene.

Rock Texture:

Intergranular.

Grain Size:

Groundmass: Medium Grained.
Phenocrysts: Medium to Coarse Grained.

Classification of Original Igneous Rock:

Diabase

Notes: Plagioclase shows minor alteration. Two phenocrysts have aligned serpentine, suggesting relict cleavage planes, perhaps they are Orthopyroxene and not olivine? The Myrmekite is presumed secondary based on the assumed presence of igneous olivine in the rock. Opaque mineral is significantly altered.

HK-23

Primary Minerals:

Plagioclase ($An_{30}$)- 50%, Clinopyroxene, 20%,
Phenocrysts replaced with Serpentine, likely originally Olivine- 20%

Secondary Minerals:

Chlorite- 5%, minor Pumpellyite, Prehnite.

Crystallization Order:

Olivine (or Orthopyroxene), Plagioclase, Clinopyroxene.

Rock Texture:

Sub-ophitic.

Grain Size:

Groundmass: Aphanitic to Fine Grained
Phenocrysts: Fine Grained

Classification of Original Igneous Rock:

Basalt.

Notes: Phenocrysts are presumed to be olivine based on shape and the fact that they altered to serpentine.

HK-31

Primary Minerals:

Clinopyroxene- 35%, Plagioclase- 10%,
Phenocrysts replaced with Serpentine, likely originally Olivine- 15%.
Quartz and untwinned Feldspar in Graphitic Texture- 10%.

Secondary Minerals:

Opaque- 5%, Chlorite- 5%, Prehnite(?)- 10% minor Amphibole- < 5%, minor Pumpellyite- <5%, minor Calcite- <5%.

Crystallization Order:

Olivine, Clinopyroxene/Plagioclase (order uncertain).

Rock Texture:

Intergranular.

Grain Size:

Groundmass: Fine to Medium Grained.
Phenocrysts: Medium Grained.

Classification of Original Igneous Rock:

Diabase.

Notes: The Graphitic Quarz and Feldspar, Opaque mineral (likely magnetite) and Chlorite are associated, perhaps this is as a result of a secondary process. The grains thought to be Pumpellyite are unusually large (up to 300 μm) for this suite, but they are third order blue. The amount of Plagioclase may be low due to alteration. The Opaque mineral is significantly altered.

HK-43

Primary Minerals:

Plagioclase- 35%.

Secondary Minerals:

amygdaloidal Calcite- 15%, Chlorite- 10%, Actinolite- 10%,
minor Pumpellyite- < 5%, minor quartz- <5%, minor Opaques- <5%.

Crystallization Order:

Olivine, Plagioclase.

Rock Texture:

Ophitic.

Grain Size:

Groundmass: Aphanitic
Phenocrysts: Fine Grained

Classification of Original Igneous Rock:

Basalt

Notes: 15% is vesicles filled with a blue mineral.

SN-4

Primary Minerals:

Plagioclase- 40%, Phenocrysts- 15%.

Secondary Minerals:

Calcite- 15%, minor Pumpellyite- <5%, minor Prehnite -<5%.

Crystallization Order:

Olivine, Plagioclase.

Rock Texture:

Ophitic.

Grain Size:

Groundmass: Aphanitic.
Phenocrysts: Fine Grained.

Classification of Original Igneous Rock:

Basalt.

Notes: 20 % of the rock is aphanitic groundmass. Some (perhaps one-quarter) phenocrysts are likely relict olivines. The rest are comprised of quartz- 40%, Opaques- 30%, calcite- 20%, and Chlorite- 10%. Calcite in the rest of the rock is primarily in veins. Plagioclase often occurs in 6 fold stars made of three crossed elongate crystals. The rock contains a xenolithic fragment comprised of quartz, opaque grains, and altered feldspar. It likely originated in continental crust.

# Appendix C

## Analyses of Standards and Calculations of Accuracy for the Washington State University ICP-MS.

Table V
Estimate of Accuracy

| | BCR-1 Basalt | | W-2 Diabase | | G-2 Granite | | DNC-1 Diabase | |
|---|---|---|---|---|---|---|---|---|
| | | WSU | | WSU | | WSU | | WSU |
| | 94GOV | 94Kn | 94GOV | 94Kn | 94GOV | 94Kn | 94GOV | 94Kn |
| Ba | 681 | 672 | 182 | 162 | 1882 | 1870 | 114 | 102 |
| La | 24.9 | 25.86 | 11.4 | 10.50 | 89.0 | 89.22 | 3.8 | 3.88 |
| Ce | 53.7 | 53.05 | 24.0 | 22.21 | 160.0 | 159.64 | 10.6 | 8.08 |
| Pr | 6.8 | 7.05 | 5.9 | 3.01 | 18.0 | 16.95 | 1.3 | 1.20 |
| Nd | 28.8 | 28.87 | 14.0 | 12.65 | 55.0 | 53.63 | 4.9 | 5.08 |
| Sm | 6.59 | 6.86 | 3.25 | 3.26 | 7.20 | 7.28 | 1.38 | 1.47 |
| Eu | 1.95 | 2.00 | 1.10 | 1.09 | 1.40 | 1.37 | 0.59 | 0.62 |
| Gd | 6.68 | 6.90 | 3.60 | 3.70 | 4.30 | 4.00 | 2.00 | 2.09 |
| Tb | 1.05 | 1.09 | 0.63 | 0.63 | 0.48 | 0.48 | 0.41 | 0.41 |
| Dy | 6.34 | 6.34 | 3.80 | 3.66 | 2.40 | 2.15 | 2.70 | 2.72 |
| Ho | 1.26 | 1.26 | 0.76 | 0.74 | 0.40 | 0.35 | 0.62 | 0.60 |
| Er | 3.63 | 3.62 | 2.50 | 2.12 | 0.92 | 0.81 | 2.00 | 1.90 |
| Tm | 0.56 | 0.53 | 0.38 | 0.32 | 0.18 | 0.12 | 0.33 | 0.30 |
| Yb | 3.38 | 3.33 | 2.05 | 2.00 | 0.80 | 0.75 | 2.01 | 1.96 |
| Lu | 0.51 | 0.50 | 0.33 | 0.30 | 0.11 | 0.11 | 0.32 | 0.31 |
| Rb | 47.2 | 48.1 | 20.0 | 19.0 | 170.0 | 171.9 | 4.5 | 4.1 |
| Y | 38 | 37.78 | 24 | 22.07 | 11 | 10.90 | 18 | 18.59 |
| Nb | 14.0 | 11.88 | 7.9 | 6.68 | 12.0 | 12.12 | 3.0 | 1.51 |
| Cs | 0.96 | 1.08 | 0.99 | 0.93 | 1.34 | 1.65 | 0.34 | 0.23 |
| Hf | 4.95 | 4.93 | 2.56 | 2.38 | 7.90 | 8.09 | 1.01 | 1.01 |
| Ta | 0.81 | 0.85 | 0.50 | 0.50 | 0.88 | 1.01 | 0.10 | 0.10 |
| Th | 5.98 | 6.26 | 2.20 | 2.04 | 24.70 | 24.89 | 0.20 | 0.30 |
| U | 1.75 | 1.63 | 0.53 | 0.43 | 2.07 | 1.84 | 0.10 | 0.07 |
| Sr | 330 | 332 | 194 | 189 | 478 | 483 | 145 | 147 |

Table V. Estimate of Accuracy for WSU values compared to recommended values for four international rock standards.

## Table VI Precision

BCR-P (N=50) run as unknown 1992-1994

| | La ppm | Ce ppm | Pr ppm | Nd ppm | Sm ppm | Eu ppm | Gd ppm | Tb ppm | Dy ppm | Ho ppm | Er ppm | Tm ppm |
|---|---|---|---|---|---|---|---|---|---|---|---|---|
| Average | 26.26 | 51.67 | 6.32 | 27.36 | 7.03 | 2.14 | 6.75 | 1.17 | 7.14 | 1.44 | 4.05 | 0.55 |
| Std. Dev. | 0.49 | 0.62 | 0.06 | 0.48 | 0.15 | 0.04 | 0.08 | 0.01 | 0.10 | 0.02 | 0.06 | 0.01 |
| Minimum | 25.22 | 50.05 | 6.16 | 26.23 | 6.70 | 2.00 | 6.62 | 1.15 | 6.96 | 1.39 | 3.92 | 0.53 |
| Maximum | 27.43 | 52.9 | 46.41 | 28.42 | 7.29 | 2.21 | 6.86 | 1.21 | 7.33 | 1.48 | 4.18 | 0.56 |
| Coeff. var.% (stdev/avg) | 1.86 | 1.20 | 0.98 | 1.75 | 2.07 | 1.92 | 1.13 | 1.12 | 1.33 | 1.53 | 1.37 | 1.23 |

| | Yb ppm | Lu ppm | Ba ppm | Th ppm | Nb ppm | Y ppm | Hf ppm | Ta ppm | U ppm | Pb ppm | Rb ppm | Cs ppm |
|---|---|---|---|---|---|---|---|---|---|---|---|---|
| Average | 3.36 | 0.52 | 670.50 | 5.13 | 13.31 | 38.11 | 4.67 | 0.82 | 1.15 | 9.11 | 48.06 | 0.96 |
| Std. Dev | 0.03 | 0.01 | 12.68 | 0.49 | 0.29 | 0.29 | 0.07 | 0.02 | 0.11 | 0.29 | 0.67 | 0.03 |
| Minimum | 3.30 | 0.50 | 646.30 | 3.93 | 12.62 | 37.57 | 4.56 | 0.78 | 0.84 | 8.45 | 46.95 | 0.91 |
| Maximum | 3.40 | 0.54 | 692.68 | 5.85 | 13.73 | 38.72 | 4.82 | 0.86 | 1.28 | 9.58 | 49.57 | 1.02 |
| Coeff. var.% (stdev/avg) | 0.94 | 1.90 | 1.89 | 9.50 | 2.16 | 0.77 | 1.47 | 2.70 | 9.34 | 3.23 | 1.39 | 3.06 |

Table VI. Precision of theWashington State University ICP-MS, determined by multiple analyses of BCR-P over a two year period.

## Table VII Detection Limits

| Sample ID | La ppm | Ce ppm | Pr ppm | Nd ppm | Sm ppm | Eu ppm | Gd ppm | Tb ppm | Dy ppm | Ho ppm | Er ppm | Tm ppm | Yb ppm |
|---|---|---|---|---|---|---|---|---|---|---|---|---|---|
| Calc'd Det Lim | 0.007 | 0.012 | 0.009 | 0.045 | 0.014 | 0.010 | 0.026 | 0.007 | 0.024 | 0.006 | 0.021 | 0.006 | 0.023 |

| Sample ID | Lu ppm | Ba ppm | Th ppm | Nb ppm | Y ppm | Hf ppm | Ta ppm | U ppm | Pb ppm | Rb ppm | Cs ppm | Sr ppm |
|---|---|---|---|---|---|---|---|---|---|---|---|---|
| Calc'd Det Lim | 0.007 | 0.258 | 0.009 | 0.018 | 0.015 | 0.032 | 0.014 | 0.014 | 0.204 | 0.057 | 0.014 | 0.115 |

Table VII. Detection limits of the Washington State University ICP-MS. Detection limits are derived from the counts on the blank plus 3 times the standard deviation of the blank calculated as an unknown. According to Charles Knack (personal communication) of the Washington State University geoanalytical laboratory, these calculated detection limits, like most published LLDs, are unrealistically low. Precision at these levels is usually +/- 100%. He usually quotes lower limits of reliable quantification that are 2-10 times higher than these, eg. 0.1 x chondrite for the REEs.